

**ESTIMATION OF SATURATED HYDRAULIC
CONDUCTIVITY IN SPATIALLY VARIABLE
FIELDS USING VARIOUS SOFT COMPUTING
TECHNIQUES.**

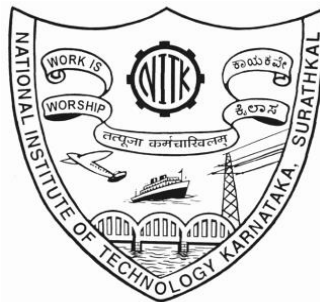
Thesis

Submitted in partial fulfillment of the requirements for the degree of

DOCTOR OF PHILOSOPHY

By

SATISH BHURAO MORE



DEPARTMENT OF APPLIED MECHANICS AND HYDRAULICS

NATIONAL INSTITUTE OF TECHNOLOGY KARNATAKA,

SURATHKAL, MANGALORE - 575025

APRIL, 2019

**ESTIMATION OF SATURATED HYDRAULIC
CONDUCTIVITY IN SPATIALLY VARIABLE
FIELDS USING VARIOUS SOFT COMPUTING
TECHNIQUES.**

Thesis

Submitted in partial fulfillment of the requirements for the degree of

DOCTOR OF PHILOSOPHY

By

SATISH BHAURAO MORE



DEPARTMENT OF APPLIED MECHANICS AND HYDRAULICS

NATIONAL INSTITUTE OF TECHNOLOGY KARNATAKA,

SURATHKAL, MANGALORE - 575025

APRIL, 2019

DECLARATION

I hereby *declare* that the Research Thesis entitled **Estimation of saturated hydraulic conductivity in spatially variable fields using various soft computing techniques.**

Which is being submitted to the National Institute of Technology Karnataka, Surathkal in partial fulfilment of the requirements for the award of the Degree of Doctor of Philosophy in the Department of Applied Mechanics and Hydraulics is a *bonafide report of the research work carried out by me.* The material contained in this Research Thesis has not been submitted to any University or Institution for the award of any degree.

Register Number: - AM13P03

Name: - SATISH BHAURAO MORE

(Signature)

Department of Applied Mechanics and Hydraulic

National Institute of Technology Karnataka, Surathkal

Place: NITK-Surathkal

Date:

C E R T I F I C A T E

This is to *certify* that the Research Thesis entitled **Estimation of saturated hydraulic conductivity in spatially variable fields using various soft computing techniques** submitted by SATISH BHAURAO MORE (Register Number: AM13P03) as the record of the research work carried out by him, is *accepted as the Research Thesis submission* in partial fulfilment of the requirements for the award of degree of Doctor of Philosophy.

Prof. Paresh Chandra Deka

(Research Guide)

Department of Applied Mechanics and Hydraulics

National Institute of Technology Karnataka, Surathkal

Prof. Amba shetty

(Chairman - DRPC)

Department of Applied Mechanics and Hydraulics

National Institute of Technology Karnataka, Surathkal

ACKNOWLEDGEMENT

This thesis is an outcome of work carried out by me in last couple of years. Whereby I have been accompanied and supported by many people. It is an honor and pleasant opportunity to be able to express my gratitude to all of them.

It is my pleasure to express profound gratitude and indebtedness towards my research supervisor **Dr. Paresh Chandra Deka**, for his continued inspiration, motivation, support, discussions and great patience throughout this research. I admire among his other qualities, kindness and balanced approach towards success and failure. His scientific foresight and excellent knowledge have been crucial for the accomplishment of this work. I consider myself privileged for having had the opportunity to study under his able supervision.

I am greatly thankful to Research Progress Appraisal Committee members, Dr. Nagraj M.K. and Dr. B. Manu for their critical evaluation during the progress of the work.

I also extend my heartfelt thanks to Prof. A. Mahesha, Head, Department of Applied Mechanics and Hydraulics, and Chairman DRPC for providing me all the necessary facilities during my research period.

I gratefully acknowledge all the faculty members of Applied Mechanics and Hydraulics Department, for their continuous support, care and good wishes during the course of my work.

I sincerely acknowledge Mr. Jagdish, Mr. Anil, Mr. Balakrishna, Mrs. Prathima, Mr. Harish and all the other non-teaching staff of Applied Mechanics and Hydraulics department.

I am very much thankful to my college management and Principal who have supported me and encouraged me as and when needed. I would like to offer special thanks to my colleague Mr. Amit Patil who extended his support and encouragement during my stay in the NITK.

I wish to express my gratitude to Sujay, Parthsarthy, Bhuvanmitra, Rohit and Ganesh for the help they extended to me as and when needed.

Finally, I wish to express my love and affection to my family members, thank you for being with me during good and bad times.

Last but not the least; I am grateful to everyone who has helped and me during this research work.

SATISH BHAURAO MORE.

ABSTRACT

Saturated hydraulic conductivity (Kfs) is one of the dominant and most essential soil hydrology characteristics, for understanding and duplicating various hydrological processes having environmental importance. Its estimation by (laboratory / field) method is cumbersome, time consuming and costly. In addition, the results may not be representative due to spatial variability of Kfs. This attracted researcher to address this problem by developing pedotransfer function (PTF), which estimate saturated hydraulic conductivity by using routinely measured soil properties.

Objective of this study is to investigate the spatial variability of saturated hydraulic conductivity under different land use land cover by using Guelph permeameter, and to develop PTF for estimating Kfs, from soil index properties, by using soft computing techniques and thus evaluate the performance of these techniques by using statistical tests.

Study is carried out at Solapur, India. Three sites (0.76ha) were identified which are having different land use land cover. The site is divided in to small grids of 10m X 10m, and observations were taken at corner of each such grid, at 15cm, 30cm and 45cm depth. In situ and laboratory tests were carried out to estimate Kfs and other basic index properties of soil.

Observed data (In situ as well as laboratory) were preprocessed and then used for modeling purpose.

Total dataset (Three sites, three depth with 100 sampling points; so overall 900 sample data) is segregated into six sub dataset (college, Mulegaon, Punanaka, 15cm, 30cm and 45cm).

Each subset consisting of 300 observations is further split into two parts in six different ways (90% + 10%, 85% + 15%, 80% +20%, 75% + 25%, 70% + 30%, and 67% + 33%) to train the models and validate it, the combination which gives good results during training and validation is selected. For checking performance of model, various statistical parameters such as correlation coefficient (R), mean relative error

(MRE), root mean square error (RMSE), normalized root mean square error (NRMSE) and Nash Sutcliffe efficiency (NSE) has been made. Scatter plots were used to evaluate the accuracies of the models. For deciding best model these checks are used, Value of $R \sim 1$, value and NSE ~ 1 , MRE close to zero, and NRMSE is close to zero. Scatter plot point distribution should be around and close to 1:1 line.

Maximum value of log saturated hydraulic conductivity was observed at Punanaka (3.842 m yr^{-1}) and minimum value at college site (0.002 myr^{-1}). Standard deviation for Kfs was least at Punanaka (0.598 m yr^{-1}) and was maximum at college site (0.804 myr^{-1}). Porosity has strong positive Correlation coefficient 0.9 whereas bulk density has strong negative correlation of 0.9. The performance of ELM model at all six subsets was found performing better than SVM and ANFIS model. NRMSE values of ELM model (training: testing) were found [0.02:0.06, 0.07:0.09, 0.02:0.07, 0.03:0.08, 0.07:0.10 and 0.008:0.04] at college site, Mulegaon site, Punanaka site, 15cm depth, 30cm depth and 45cm depth respectively.

Saturated hydraulic conductivity was found varying spatially, land use land cover has influence on Kfs and it found declining with depth. College station has shown more variability in Kfs also variation of Kfs was found more at 45cm depth. Maximum Standard deviation was found in college site and minimum standard deviation was found at Punanaka site. Variability of porosity, bulk density and particle density was found insignificant in logarithmic scale. Soil particle size was found declining with depth. Porosity has shown strong positive correlation with Kfs, whereas bulk density has shown strong negative correlation. Performance of ELM model was found excellent in all six sub data set both during training and testing. Performance of SVM and ANFIS was not found satisfactory during testing although they are within acceptable accuracy.

Saturated hydraulic conductivity has shown spatial variation; it was varying along depth as well as lateral and longitudinal direction, generally Kfs was found decreasing with depth. Kfs was found decreasing down the slope. ELM model outperformed other two models tried in this study (ANFIS and SVM). Texture of soil was found

declining from coarse to fine with depth at majority of sampling location. Mean value of Kfs was found more at Punanaka site (15cm depth) as compared to other two sites.

Key words: Saturated hydraulic conductivity, Guelph permeameter, ANFIS, SVM, ELM

TABLE OF CONTENTS

Sr.No.	Topic	Page No.
	Declaration	
	Certificate	
	Acknowledgement	
	Abstract	
	Table of Contents	i
	List of Figures	iv
	List of Tables	viii
	CHAPTER 1- INTRODUCTION	1-9
1.1	Introduction	1
1.2	Problem identification/need of study	7
1.3	Organization of the thesis	8
	CHAPTER 2 -LITERATURE REVIEW	10-27
2.1	Introduction	10
2.2	Hydraulic conductivity	10
2.2.1	Summary	11
2.3	In situ methods	11
2.3.1	Summary	15
2.4	Factors affecting hydraulic conductivity	16
2.4.1	Scaling	16
2.4.2	Land use land cover	18
2.4.3	Terrain and soil structure	20
2.4.4	Summary	21
2.5	Pedotransfer function	21
2.5.1	PTF by using MLR and ANN	22
2.5.2	PTF by using ANFIS	25
2.5.3	PTF by using SVM	26
2.5.4	PTF by using ELM	27
2.5.5	Summary	27
2.5.6	Objectives of the study	27
	CHAPTER 3- MATERIAL AND METHOD	28-55
3.1	Study area	28
3.2	Field measurement of saturated hydraulic conductivity by GUELLPH PERMEAMETER	30
3.2.1	Introduction	30
3.2.2	Description of method	30
3.3	Laboratory measurement of soil properties	34
3.3.1	Particle density (specific gravity)	34
3.3.2	Organic content	34
3.3.3	Bulk dry density	35
3.3.4	Porosity	36

3.3.5	Grain size analysis	36
3.4	Soft computing modeling	37
3.4.1	Artificial neural network	38
3.4.1.1	Feed-forward back propagation network (FFBP)	38
3.4.1.2	Training neural network	38
3.4.2	Fuzzy logic	40
3.4.3	Adaptive neuro-fuzzy influence system (ANFIS)	41
3.4.4	Support vector machine	43
3.4.4.1	Support vector regression	44
3.4.5	Extreme learning machine	47
3.5	Soil data collection	48
3.6	Data preprocessing	49
3.7	Selection of input parameters	52
3.8	Model performance criteria	53
3.8.1	Coefficient of correlation (R)	54
3.8.2	Root mean square error (RMSE)	54
3.8.3	Mean relative error (MRE)	54
3.8.4	Normalized root mean Square error (NRMSE)	55
3.8.5	Nash-Sutcliff model efficiency coefficient (NSE)	55
	CHAPTER 4 -RESULT AND DISCUSSION	56-107
4.1	Statistical analysis	56
4.1.1	College site	57
4.1.2	Mulegaon site	59
4.1.3	Puna naka site	60
4.1.4	At 15 cm depth	61
4.1.5	At 30 cm depth	62
4.1.6	At 45 cm depth	63
4.2	Variability of soil parameters	65
4.3	Textural analysis of soil	100
4.4	Land use and land cover	102
4.5	Modeling	103
4.5.1	Training/testing data set	103
4.5.2	Development of model	104
4.5.3	Performance evaluation of model	107
	CHAPTER 5-CONCLUSION AND SUMMARY	119-122
5.1	Summary	119
5.2	Conclusion	120
5.2.1	Main finding of the work	120
5.2.2	Conclusion drawn from the study	120
5.2.3	Limitation of study	121
5.2.4	Suggested direction for future work	121
5.2.5	Contribution from the thesis	122
	REFERENCES	123-137

LIST OF PUBLICATIONS	138
BIO-DATA	139

LIST OF FIGURES

Fig. No	CAPTION	Page No.
3.1	Location Of Study Area	29
3.2	Sampling Scheme Grid At College, Mulegaon And Puna Naka Site	30
3.3	Schematic Diagram Of Mariotte System For Use In GUELPH Permeameter	31
3.4	Cylindrical Sampler (Container) Being Driven Into Soil To Collect The Soil Sample After The In Situ Test	35
3.5	Architecture Of FFBP Neural Network	39
3.6	Sipmle Architecture Fuzzy Logic Model	40
3.7	Architecture Of ANFIS Model	42
3.8	Nonlinear Support Vector Regression With ε -Insensitive Loss Function	46
3.9	Architecture Of ELM Model	47
3.10	QQ Plot For Saturated Hydraulic Conductivity. (A) Before Transformation And (B) After Transformation	51
3.11	Flow Chart Of The Methodology Used In The Study	53
4.1	Coefficient Of Variation In % Of Various Soil Parameters Sampled At Three Sites	65
4.2	Variation Of Coefficient Of Variation Of Soil Parameters Sampled And Tested At (15cm Depth) All Three Sampling Location	66
4.3	Variation Of Coefficient Of Variation Of Soil Parameters Sampled And Tested At (30cm Depth) All Three Sampling Location	67
4.4	Variation Of Coefficient Of Variation Of Soil Parameters Sampled And Tested At (45cm Depth) All Three Sampling Location	67
4.5	Variation Of Soil Parameters Along Lateral Direction At Lateral 1 In College, Mulegaon And Puna Naka Site, At 15cm Depth, 30cm Depth And 45cm Depth	68
4.6	Variation Of Soil Parameters Along Lateral Direction At Lateral 2 In College, Mulegaon And Puna Naka Site, At 15cm Depth, 30cm Depth And 45cm Depth	70
4.7	Variation Of Soil Parameters Along Lateral Direction At Lateral 3 In College, Mulegaon And Puna Naka Site, At 15cm Depth, 30cm Depth And 45cm Depth	71
4.8	Variation Of Soil Parameters Along Lateral Direction At Lateral 4 In College, Mulegaon And Puna Naka Site, At 15cm Depth, 30cm Depth And 45cm Depth	72
4.9	Variation Of Soil Parameters Along Lateral Direction At Lateral 5 In College, Mulegaon And Puna Naka Site, At 15cm Depth, 30cm Depth And 45cm Depth	73
4.10	Variation Of Soil Parameters Along Lateral Direction At Lateral 6 In College, Mulegaon And Puna Naka Site, At 15cm Depth, 30cm Depth And	75

	45cm Depth	
4.11	Variation Of Soil Parameters Along Lateral Direction At Lateral 7 In College, Mulegaon And Puna Naka Site, At 15cm Depth, 30cm Depth And 45cm Depth	76
4.12	Variation Of Soil Parameters Along Lateral Direction At Lateral 8 In College, Mulegaon And Puna Naka Site, At 15cm Depth, 30cm Depth And 45cm Depth	77
4.13	Variation Of Soil Parameters Along Lateral Direction At Lateral 9 In College, Mulegaon And Puna Naka Site, At 15cm Depth, 30cm Depth And 45cm Depth	79
4.14	Variation Of Soil Parameters Along Lateral Direction At Lateral 10 In College, Mulegaon And Puna Naka Site, At 15cm Depth, 30cm Depth And 45cm Depth	80
4.15	Variation Of Soil Parameters Along Lateral Direction At Lateral 11 In College, Mulegaon And Puna Naka Site, At 15cm Depth, 30cm Depth And 45cm Depth	81
4.16	Variation Of Soil Parameters Along Lateral Direction At Lateral 12 In College, Mulegaon And Puna Naka Site, At 15cm Depth, 30cm Depth And 45cm Depth	82
4.17	Variation Of Soil Parameters Along Lateral Direction At Lateral 13 In College, Mulegaon And Puna Naka Site, At 15cm Depth, 30cm Depth And 45cm Depth	83
4.18	Variation Of Soil Parameters Along Lateral Direction At Lateral 14 In College, Mulegaon And Puna Naka Site, At 15cm Depth, 30cm Depth And 45cm Depth	85
4.19	Variation Of Soil Parameters Along Lateral Direction At Lateral 15 In College, Mulegaon And Puna Naka Site, At 15cm Depth, 30cm Depth And 45cm Depth	86
4.20	Variation Of Soil Parameters Along Lateral Direction At Lateral 16 In College, Mulegaon And Puna Naka Site, At 15cm Depth, 30cm Depth And 45cm Depth	87
4.21	Variation Of Soil Parameters Along Lateral Direction At Lateral 17 In College, Mulegaon And Puna Naka Site, At 15cm Depth, 30cm Depth And 45cm Depth	89
4.22	Variation Of Soil Parameters Along Lateral Direction At Lateral 18 In College, Mulegaon And Puna Naka Site, At 15cm Depth, 30cm Depth And 45cm Depth	90
4.23	Variation Of Soil Parameters Along Lateral Direction At Lateral 19 In College, Mulegaon And Puna Naka Site, At 15cm Depth, 30cm Depth And 45cm Depth	91
4.24	Variation Of Soil Parameters Along Lateral Direction At Lateral 20 In	92

	College, Mulegaon And Puna Naka Site, At 15cm Depth, 30cm Depth And 45cm Depth	
4.25	Variation Of Saturated Hydraulic Conductivity Along The Longitudinal L At 15cm, 30cm And 45cm Depth In College, Mulegaon And Puna Naka	94
4.26	Variation Of Saturated Hydraulic Conductivity Along The Longitudinal 2 At 15cm, 30cm And 45cm Depth In College, Mulegaon And Puna Naka	95
4.27	Variation Of Saturated Hydraulic Conductivity Along The Longitudinal 3 At 15cm, 30cm And 45cm Depth In College, Mulegaon And Puna Naka	97
4.28	Variation Of Saturated Hydraulic Conductivity Along The Longitudinal 4 At 15cm, 30cm And 45cm Depth In College, Mulegaon And Puna Naka	98
4.29	Variation Of Saturated Hydraulic Conductivity Along The Longitudinal 5 At 15cm, 30cm And 45cm Depth In College, Mulegaon And Puna Naka	99
4.30	Textural Distribution Soilacross All Three Sites (College, Mulegaon And Puna Naka)	100
4.31	Textural Distribution Soilacross All Three Sites (College, Mulegaon And Puna Naka) At 15cm Depth	100
4.32	Textural Distribution Soilacross All Three Sites (College, Mulegaon And Puna Naka) At 30cm Depth	101
4.33	Textural Distribution Soilacross All Three Sites (College, Mulegaon And Puna Naka) At 45cm Depth	101
4.34	Scatter Plot Of Predicted Kfs V/S Observed Kfs For College Station During Training (A) And Testing (B)	108
4.35	Box Plot Of Kfs For Observed And Predicted Values By ELM, SVM And ANFIS (A) During Training And (B) During Testing At College Station.	109
4.36	Scatter Plot Of Predicted Kfs V/S Observed Kfs For Mulegaon Station During Training (A) And Testing (B)	110
4.37	Box Plot Of Kfs For Observed And Predicted Values By ELM, SVM And ANFIS (A) During Training And (B) During Testing At Mulegaon Station.	110
4.38	Scatter Plot Of Predicted Kfs V/S Observed Kfs For Puna Naka Station During Training (A) And Testing (B)	112
4..39	Box Plot Of Kfs For Observed And Predicted Values By ELM, SVM And ANFIS (A) During Training And (B) During Testing At Puna Naka Station.	112
4.40	Scatter Plot Of Predicted Kfs V/S Observed Kfs For 15cm Station During Training (A) And Testing (B)	113
4.41	Box Plot Of Kfs For Observed And Predicted Values By ELM, SVM And ANFIS (A) During Training And (B) During Testing At 15cm Station.	114
4.42	Scatter Plot Of Predicted Kfs V/S Observed Kfs For 30cm Station During Training (A) And Testing (B)	115
4.43	Box Plot Of Kfs For Observed And Predicted Values By ELM, SVM And ANFIS (A) During Training And (B) During Testing At 30cm Station.	115
4.44	Scatter Plot Of Predicted Kfs V/S Observed Kfs For 45cm Station During Training (A) And Testing (B)	117

4.45	Box Plot Of Kfs For Observed And Predicted Values By ELM, SVM And ANFIS (A) During Training And (B) During Testing At 45cm Station	117
4.46	Bar Chart Showing The Variation Of R At Various Sampling Station (A) During Training And (B) Testing	118
4.47	Bar Chart Showing The Variation Of R At Various Sampling Depth (A) During Training And (B) Testing	118

LIST OF TABLES

TABLE No.	CAPTION	Page No.
3.1	Texture-Structure Categories For Usual Estimation Of α^*	33
3.2	Various Models Proposed In This Study	49
3.3	Input Parameters Selected Based On Stepwise Regression For Various Data Set	52
4.1	Summary Statistics Of Soil Parameter Samples At All Three Sites And All Three Depths (15cm, 30cm And 45cm)	57
4.2	Correlation Coefficient Of Various Soil Parameter With Saturated Hydraulic Conductivity Of Sampled At College (CO), Mulegaon(MU) And Puna Naka(PN)	57
4.3	Summary Statistics Of Soil Parameters Sampled At College Site, (15cm, 30cm And 45cm Depth)	58
4.4	Correlation Coefficient Of Various Soil Parameter Sampled At College (15cm, 30cm And 45cm Depth)	58
4.5	Summary Statistics Of Soil Parameters Sampled At Mulegon Site, (15cm, 30cm And 45cm Depth)	59
4.6	Correlation Coefficient Of Various Soil Parameter Sampled At Mulegaon(15cm, 30cm And 45cm Depth)	60
4.7	Summary Statistics Of Soil Parameters Sampled At Puna Naka Site, (15cm, 30cm And 45cm Depth)	60
4.8	Correlation Coefficient Of Various Soil Parameter Sampled At Puna Naka (15cm, 30cm And 45cm Depth)	61
4.9	Correlation Coefficient Of Various Soil Parameter Sampled At 15cm Depth In College Site, Mulegaon Site And Puna Naka Site With Saturated Hydraulic Conductivity	61
4.10	Summary Statistics Of Soil Parameters At 15cm Depth Sampled At College Site, Mulegaon Site And Puna Naka Site	62
4.11	Summary Statistics Of Soil Parameters Sampled At 30cm Depth Sampled At College Site, Mulegaon Site And Puna Naka Site	63
4.12	Correlation Coefficient Of Various Soil Parameter Sampled At 30cm Depth In College Site, Mulegaon Site And Puna Naka Site With Saturated Hydraulic Conductivity	63
4.13	Summary Statistics Of Soil Parameters 45cm Sampled At College Site,	64

	Mulegaon Site And Puna Naka Site	
4.14	Correlation Coefficient Of Various Soil Parameter Sampled At 45cm Depth In College Site, Mulegaon Site And Puna Naka Site With Saturated Hydraulic Conductivity	65
4.15	Sample Distribution For Training And Validating Model	104
4.16	ELM Model Parameters	104
4.17	SVM Model Parameters	105
4.18	ANFIS Model Parameters	106
4.19	Performance Comparison Of Model For College (90% Training And 10% Testing)	107
4.20	Performance Comparison Of Model For Mulegaon (70% Training Data And 30% Testing)	109
4.21	Performance Comparison Of Model For Puna Naka (67% Training Data And 33% Testing Data)	111
4.22	Performance Comparison Of Model For 15cm Depth (75% Training And 25% Testing)	113
4.23	Performance Comparison Of Model For 30 Depth (75% Training Data And 25% Testing Data)	114
4.24	Performance Comparison Of Model For 45cm Depth (80% Training Data And 20% Testing Data)	116

CHAPTER 1

INTRODUCTION

1.1 INTRODUCTION

Soils are heterogeneous, and this characteristic property of soil alters their hydraulic properties even in a small scale (Parasuraman et al., 2006). Therefore, researchers are keen in developing the method to estimate hydraulic properties of the soil with less effort, less costly and less time requirement irrespective of the scale of the research area. Also Quantification of the hydraulic properties of porous media is a concern shared by soil scientists, hydrologists, agricultural engineers, and petroleum engineers (Jauhiainen. 2004). Accurate knowledge about soil hydraulic properties (water retention characteristic and conductivity functions) is very much required to efficiently administer (Stumpp et al., 2009) soil related problems in forest ecology such as protection and remediation techniques.

Hydraulic conductivity is one of the dominant and most essential soil hydrology characteristics, for understanding and duplicating various hydrological processes having environmental importance, such as rainfall partition into infiltration and runoff or water and solute transport in the soil profile drainage, design of waste containment system, and movement of solutes in soils (Braud et al., 1995; Mallants et al., 1997; Zeleke and Si. 2005; Ghanbarian et al., 2010; Khodaverdiloo et al., 2017;). Proper knowledge of soil Hydraulic conductivity is essential in various geotechnical designs such as estimation of bearing capacity, consolidation settlement of foundation, earth dam design (seepage loss), drainage filter design, ground improvement etc. (Hausman., 2012, Raj., 2008). It is also used as a matching point to determine the unsaturated soil hydraulic conductivity function and also as a soil physical quality parameter (Lee et al., 1985; Reynolds et al., 2000, Alagna et al., 2016; Iovino et al., 2013;).

Hydraulic conductivity, that affects the retention and movement of water and dissolved substances through soils has being one of the major requirements in engineering and soil management applications dealing with forestry, agriculture, terrestrial ecosystem management and land reclamation (Balland et al. 2008). The

value of hydraulic conductivity is one of the most important parameters for design and realization of all type measures for mitigation of negative impact of hydrological extremes as are floods and enduring droughts. Thus, it can be said that a proper knowledge of the hydraulic conductivity is a prerequisite for most projects involving earthen materials (Mbonimpa et al., 2002).

Soils as a porous media are highly heterogeneous and hydraulic conductivity of soil is an interaction between soil and fluid, thus is affected by intrinsic properties of both materials such as particle size, porosity, pore connectivity, texture of soil, structure of soil, organic matter (Jarvis et al., 2013) viscosity of fluid, physical and chemical composition of fluid (Sepaksha and Karizi., 2011), rock fragment content (RFC) (Fu et al., 2015); ESP (Exchangeable sodium percentage), SAR sodium absorption ratio, (Candemir and Gulser., 2012), WSA water stable aggregate stability (Jiang and shaoa., 2014), SSWC saturated soil water content (Wanga., 2013) ; as well as extrinsic factors which such as tillage (Khaledian et al., 2013; Kargas and Londra ., 2014), topographical location, land use type, slope gradient, slope exposure, and elevation. (Fu et al., 2015), anthropogenic activities, cattle grazing, root holes, worm holes etc. (Hua et al., 2013).

Hydraulic conductivity can be estimated by the correlation method or by the hydraulic method (Shukla, 2013). The indirect method (correlation method) involves estimation of hydraulic conductivity; by using empirical equation or model developed relating hydraulic conductivity and the possible influencing factors based on correlation analysis (Jabro., 1992; Cosby et al., 1984; Saxton et al., 1986; Vereecken et al., 1990; Wosten et al., 1999; Rawls and Brakensiek., 1985; Campbell and Shiozawa., 1994; Mbonimpa et al., 2002., Twarakavi et al., 2009; Merdum., 2010; Stumpp et al., 2009; Lamorski et al., 2008).

The direct method (hydraulic method) involves actual measurement of hydraulic conductivity either in the laboratory or/and in the field. In laboratory, test can be performed by using constant head or falling head method (IS 2720-17., (1986); Das ., 2002; Klute and Dirksen., 1986) whereas in field it can be determined by using Auger hole method, Tension infiltrometer (Raouf et al., 2011), Poned infiltrometer, single ring Infiltrimeter, double ring infiltrometer (Kohne et al., 2011;), double tube test

method (Bouwer., 1964), Gas pressure permeameter, Air entry permeameter (Stephens.,1988; Lee et al., 1985),constant head well permeameter (Reynold at al., 1983; Lee et al., 1985; Reynold et al., 1985;Talsma., 1987; Ammozegar., 1989; Gallichand et al., 1990; Salverda and Dane., 1993;Lilly., 1994;; Bagarello and Giordano., 1999; Hayashi and Quinton., 2008)Borehole Permeameter and Pressure Infiltrimeter (Deb and Shukla 2012), panda light penetrometer, geoendoscope technique (Bouteldja et al., 2011). For a detailed review of different laboratory and field measurements of soil hydraulic data, refer Klute and Dirksen (1986).

Most of the in - situ equipment such as double ring infiltrimeter has inherent drawbacks such as bulky, time consuming, need flat surface etc. On the contrary, Guelph permeameter is easy to use, handy, requires less time for measurement and needs less amount of water for the test, the minimal disturbance of the soil and the replicability of the measurements. Also it can be used in all type of soil and terrain. Most of the researchers (Mohanty et al., 1994; Lee et al., 1985; Bagarello and Giordano., 1999; Bagarello., 1997; Campbell and Fritton., 1994; Elrick and Reynolds., 1992; Elrick et al., 1989; Reynolds et al., 1985; Reynolds et al., 1992; Zang et al.,1997; Archer et al., 2014; Talsma., 1987; Gallichand et al., 1990; Lilly ., 1994; Salverda and Dane., 1993) used it successfully to measure the hydraulic conductivity in the field.

Hydraulic conductivity in case of hydraulic method is computed by using Darcy law; which is applied to the flow through the soil and by measuring the head responsible for flow and outflow from the soil after imposing boundary condition to the soil.

In the laboratory methods, the liquid is made to flow through a soil sample enclosed in a cylindrical container representing a one dimensional soil configuration through which the circulating liquid is forced to flow based on the variation of head with respect to the time during the flow the test can be called as constant head test and falling head test. Constant head test is commonly used for coarse-grained soil and falling head is used for fine-grained soil. The advantage of laboratory method is simple equipment, better control condition and results are reliable if the soil sample is undisturbed which is difficult to procure in case of granular soil. The major

disadvantage of this method is boundary conditions and size of the sample being tested is very small and is not representative of the soil in the field in terms of solid phase and void volume (representative elementary volume. REV) along with the interconnectivity of the voids. (Anderson and Bouma., 1973; Dirksen., 1999).

The methods in which the soil is tested in the field at its natural condition are called in situ test. These tests usually give most appropriate value of hydraulic conductivity as compared to any other methods. Although lot of methods are there to determine hydraulic conductivity particularly in surface soils where variability is more, all of them have limitations and most appropriate method must be chosen based on the project requirements, time available, soil type, and budget . No single method is ideal for all circumstances.

Again distribution and variability of saturated hydraulic conductivity is scale dependent (Seyfried and Wilcox., 1995), thus to characterize given site, large amount of observations are required. Both field and laboratory procedures are difficult, cumbersome, time-consuming and expensive. In addition, the results may not be accurate due to spatial and temporal variability in soil physical and hydraulic properties. This has led to the development and widespread use of indirect methods that estimated K_s from more easily, widely available, routinely or cheaply measured basic soil properties such as sand, silt, clay, bulk density, and organic matter.(Hamedi et al., 2015; Das and Basudhar., 2007; Kakhajeh et al., 2012; Elbisy., 2015; Twarakavi et al., 2009).

In addition to above scenario, anthropogenic factors influenced the soil physical chemical and biological properties in a significant way since long back. These influences are identified as land use land cover change. Land-use and land cover are the most dynamic phenomenon as they change frequently. It is controlled by the potential value of the land for agricultural, forest, urban, or nature protection use and is governed by multilevel economic and socio-cultural interactions. Land-cover refers to the surface appearance of the landscape, which is mainly affected by its use, its cultivation and the seasonal phenology. Changes of land-use are caused by modified biophysical or human demands that arise from changed natural, economic or political conditions (O'Callaghan, 1996). The consequences are either modification or

conversion: modification implies a change of condition within a type, caused by different cultivation techniques or management strategies; conversions include a transition from one land-use type to another. Alterations in land-use exert an influence on the ecosystem as a whole because they affect the water cycle, biodiversity, radiation budgets and many other processes (Riebsame et al., 1994). Land use has strong influence on the hydraulic conductivity as it is responsible to alter the pore structure within the soil as well as their interconnectivity. Saturated hydraulic conductivity found to be less in bare land than in case of land covered with vegetation and type of vegetation's (Jarvis et al., 2013). Due to urbanization of land hydraulic conductivity was found responsible for flooding (Suriya and Mugdal.,2012), Ksat at shallow depth (12.5 cm depth) in case of various land cover were related as follows: {forest, banana, capoeira} > {teak} > {pasture} (Zimmermann et al.,2006).

Soil horizons or terrain is another phenomena which also influences soil properties significantly. Sloping lands are commonly seen in Indian subcontinent. Researchers have reported that slope influences hydraulic properties such as moisture distribution, infiltration rate, cumulative infiltration and hydraulic conductivity of soil. Hydraulic conductivity in hill slope is a deciding factor for slope stability. Hence, knowledge of hydraulic conductivity becomes essential for landslide analysis (Malaya &Sreedeeep 2013). Hydraulic conductivity along the slope was found declining down the slope (Hu et al.,2008; Raoof et al .,2011).

Regardless of the equipment used, in situ Kfs is the point representation of the result due to inherent heterogeneity of the soil mass i.e. Kfs was found to vary significantly both in space and in time (Bhattacharyya et al., 2006; Alletto and Coquet, 2009).

Saturated hydraulic conductivity is one of the most important physical properties of soil for environmental site characterization such as rate of flow to wells from aquifer, movement of contaminant through soil, performance of landfills, drainage design, irrigation, and in the design of geotechnical engineering projects such as design of slopes, earth dams etc. It is essential to estimate it accurately, so that management and design of various facilities related to flow of fluid can be tackled easily. This property of soil depends on variety of factors related to soil, terrain, land use land cover, pores

and their interconnectivity, biological changes that take place under below ground, chemical composition of soil. The methods used for measurement (Laboratory / field), representative elementary volume (REV) of soil being sampled in the test. Number of tests conducted to account for spatial variability of soil etc. All these factors affecting saturated hydraulic conductivity will lead to a laborious and costly affair to measure it, so alternative technique is emerged out suggested by Bouma (1989), to estimate it indirectly by using basic soil properties which are available easily in the database or can be measured; which is called Pedotransfer function (PTF). It is just a functional relation between saturated hydraulic conductivity and basic soil properties. The PTF were developed by various researchers by using linear or nonlinear regression, artificial neural network, fuzzy logic, genetic algorithm, support vector machine and hybrid techniques.

The main advantage of the ANN approach over traditional methods is that it does not require information about the complex nature of the underlying process under consideration to be explicitly described in mathematical form. Whilst ANN models implement the empirical risk minimization principle. SVM implements the structural risk minimization principle. The solution of the SVM may be globally optimal, while ANN models may tend to fall into a local optimal solution. At the same time, overfitting is unlikely to occur with the SVM, if the parameters are properly selected. So the SVM seems to be a powerful alternative, which makes it possible to overcome some of the basic weaknesses related to the application of ANNs, while retaining all the strengths of an ANN. The main characteristics of the SVM are as follows: (a) a global optimal solution is found by the quadratic programming method; (b) the result is a general solution, which avoids overtraining as it implements the structural risk minimization principle; (c) according to the Karush-Kuhn-Tucker (KKT) conditions, the solution is sparse and only a limited set of training points contribute to this solution; and (d) nonlinear solutions can be calculated efficiently due to the usage of kernel function. A disadvantage of the SVM is that the training time scales may be somewhere between quadratic and cubic with respect to the number of training samples. So a large amount of computation time will be involved when an SVM is applied for solving large-size problems.

ANFIS combine fuzzy systems and neural networks. i.e. to design architecture that uses a fuzzy system to represent knowledge in an interpretable manner, in addition to possessing the learning ability of a neural network to optimize its parameters. The drawbacks of both of the individual approaches - the black box behaviour of neural networks, and the problems of finding suitable membership values for fuzzy systems - could thus be avoided.

Extreme learning machine is one of the best algorithms attracting the attention of researchers towards it due to following features.(1) faster learning speed than conventional methods; (2) learns without iteration; (3) better generalization performance; (4) automatically determines all the network parameters analytically; (5) suitable for many non-linear activation function and kernel functions; (6) efficient for online and real-time applications; and (7) viable alternative technique for large-scale computing and machine learning.

Considering the above scenario, this study proposed to identify the influencing factors for Spatial in – situ variability of saturated hydraulic conductivity by using Guelph Permeameter at various depths. Also, the study is further extended to correlation of various soil index properties and saturated hydraulic conductivity encompassing various categories of land use and land cover in Deccan plateau of India and to develop model by using soft computing techniques.

In this part of study, Laboratory analysis of the 900 samples collected during field observation of saturated hydraulic conductivity was carried out. The laboratory results of soil properties such as bulk density, particle density, grain size distribution and organic matter, were used for development of models to estimate saturated hydraulic conductivity of the study area by using soft computing approach such as ANFIS,SVM and ELM approach ; to determine the dominant parameters influencing the saturated hydraulic conductivity.

1.2 PROBLEM IDENTIFICATION / NEED OF STUDY

This study proposes a soft computing model for estimating saturated hydraulic conductivity by using easily measurable soil physical properties such as bulk density, porosity, soil texture etc. ELM model, SVM model and ANFIS model are developed

for estimating saturated hydraulic conductivity (for various data sets) . Further, performances of these models are compared to select the best model for estimating saturated hydraulic conductivity.

In semiarid area like Solapur, precipitation is highly variable, sporadic and unpredictable. Primary occupation of the people in these areas is agriculture. Yield from agricultural areas depend on proper water management. One of the major factors which is essential for proper water management and effective distribution is the proper knowledge of saturated hydraulic conductivity. This is the motivating force for us to develop an efficient model to determine saturated hydraulic conductivity of the soils in these areas. The knowledge of the saturated conductivity helps in proper management of the water and thus resolves the water crisis problem in such areas. Further to increase the yield of crop from agriculture (to avoid farmers suicide and make them self sustained), proper understanding of water flow, and nutrient/chemical transport in the rooting zones is essential. Knowledge of Kfs is required in modeling of water transport and waste contaminant migration through soil, management of soil organic matter and management of water resources.

1.3 ORGANIZATION OF THE THESIS

This thesis comprises of five chapters as follows:

- Chapter 1 (Introduction) presents the relevant information pertaining to saturated hydraulic conductivity and further deals with an overview of the conceptual basis for the research.
- Chapter 2 (Literature Review) deals with a brief discussion about the work carried out by researchers for estimating saturated hydraulic conductivity and other hydrological parameters.
- Chapter 3 (Material and Method) describes the in - situ method of estimating saturated hydraulic conductivity, Laboratory methods of estimating various physical properties of soil, basics of ANFIS, SVM and ELM. The procedure used for selecting relevant inputs is discussed in this chapter. Further, a brief discussion about the study area is also included.

- Chapter 4 (Results and Discussion) describes the method of evaluation and goes on to present the analysis of the results obtained from the developed models. Statistical analysis of field data, correlation. Model results and their performance evaluation.
- Chapter 5 (Conclusions) presents a summary and conclusions of the research work. Limitations and future scope of the study is included towards the end.

CHAPTER 2

LITERATURE REVIEW

2.1 INTRODUCTION

In this section, literatures relevant to soil hydraulic conductivity, techniques for determining soil hydraulic conductivity based on unidirectional and spatial infiltration, factors affecting surface soil hydraulic properties and modeling techniques for development of pedotransfer functions (PTF) are presented.

2.2 HYDRAULIC CONDUCTIVITY:

The infiltration of water in soils is an important facet of agriculture. The ingress of water into the soil, water movement in the soil profile, flow of water to drains, and its loss (evaporation) from soil surface are some of the examples in which the rate of water movement plays a major role. The soil characteristics that control the nature of such soil water movements are hydraulic conductivity that is ability of soil to allow water to percolate through it and water retention, which is ability of soil to store water (Edoga, 2010). These are collectively referred to as soil hydraulic properties (Klute and Dirksen, 1986). These properties are essential to address problems of water balance, irrigation, drainage and solute movement.

Li Yan et al. (2002) investigated the spatial and temporal change of root water uptake under in - situ conditions. They found that when existing soil water is plenty the contiguous root density control the water extraction by roots, with the dominance of the roots near plant. However when the soil water is insufficient then the spatial distribution of roots depends on the variation of hydraulic conductivity function $K(\theta)$ from critical value (higher or lower). The limiting value of hydraulic conductivity obtained was 0.002 times the relative hydraulic conductivity. They concluded that the decreased value of $K(\theta)$ of the soil mass is responsible for spatial propagation of the roots.

J. Jadczyzyn, J. NiedŹwiecki (2005) carried out research in Poland on small size plot on different texture soils to understand the factors influencing the soil losses due to

erosion caused by natural rainfall. They found that the lower sand content and lower values of log Ks increase soil losses. Pedotransfer function obtained by them based on the regression analysis $\text{Soil losses} = 8.86385 - 0.132241(\text{sand}) - 2.07151 \log K_s$ with $R^2 = 0.82$

Hydraulic conductivity of clay liners used in America was tested in order to know the factors controlling hydraulic conductivity by Benson' and Trast (1995). Authors have collected samples from thirteen liners at various sites in the United States. The Specimens were tested in the laboratory under controlled conditions to assess the hydraulic conductivity. The soils were compacted and permeated in the laboratory. The results implies that hydraulic conductivity has negative relationship with liquid limit, plasticity index and percentage fines.

2.2.1 Summary: Saturated hydraulic conductivity is one of the important parameter in the analysis and understanding of all the processes related to flow of fluid through porous media such as agriculture, ecology, hydrogeology, environmental issues, various models have this as an important input parameter

2.3 IN SITU METHODS:

Measurement of soil hydraulic properties in situ is quite difficult. However, infiltration-based methods are recognized as promising tools to investigate hydraulic and transport properties of soil. In particular, three complimentary methods have become popular in the study of saturated and near-saturated soil behavior. They are the confined one-dimensional pressure double-ring infiltrometer, the unconfined three-dimensional single-ring pressure infiltrometer, and the unconfined three-dimensional tension disc infiltrometer methods.

A research was done by Fernuik and Haug (1990) in order to assess the trustworthiness and efficiency of field permeability testing equipment. Measurements were carried out by using the sealed single-ring infiltrometer, sealed double-ring infiltrometer, and air-entry permeameter on a residual soil-liner test pad installed at a site near Jamestown, California. prototype liner made of uniform Ottawa sand and sodium bentonite was tested in the laboratory. The field permeability test results were

compared with triaxial permeameter (low gradient, backpressure saturated) tests carried out on undisturbed 101.4 mm cored and remolded samples. They found that results obtained by in situ tests and laboratory test were in good agreement. In addition, temporal changes in hydraulic conductivity of hydrating sand-bentonite in field tests, was at par with the results obtained in the triaxial permeability tests.

Bagarello et al (2009) carried out experimental investigation on sandy loam soil in Italy to determine field saturated hydraulic conductivity (K_{fs}) and α^* parameter. They used the transient WU method (developed by Wu et al (1999)) and the TPD (two-ponding depth) method. The values of K_{fs} and α^* obtained by WU method were positive as well as reasonable for all infiltration tests. Use of average soil water content for all observations rather than locally measured soil water content did not deviate the values of K_{fs} and α^* too much (~22%). In few cases, the TPD method gave negative results or excessively low α^* values. The average results of the both these methods were identical for both K_{fs} and α^* (K_{fs} : 175.1–214.1 mm h⁻¹; α^* : 3.32–3.94 m⁻¹). The differences between these two methods were reduced, also in terms of relative variability of the data (coefficient of variation=76.9–81.3% for K_{fs} and 126.1–149.4% for α^*). They concluded that the WU method is best alternative to the TPD method. When there is time constraint transient method (WU) should be preferred.

Investigation of variation in field saturated hydraulic conductivity of a fine textured soil was carried out by Bagarello and Sgroi (2004); by using single ring infiltrometer with different procedure of application (ring equipped permanently and ring equipped immediately prior to beginning of infiltrometer measurements.) They found that at permanent sampling sites (PSs) average K_{fs} were higher than (1.0 to 3.5 times) than the non-permanent sites (NPSs). The large difference between the PSs and the NPSs was found in relatively moist soil. Ratio of maximum and minimum values of K_{fs} during the study period was (~6) in NPSs and in PSs it was around 2.6. They concluded that smearing effect of ring insertion is responsible for smaller values of K_{fs} in the volume of soil sampled in case of NPSs than of the PSs.

Three techniques of measurement of saturated hydraulic conductivity i.e. Philip – Dunne field permeameter, Guelph permeameter and constant head laboratory permeameter were used in a volcanic soil off greenhouse banana plantation by Regalado and Carpena (2003) to understand and quantify spatial variability of the saturated hydraulic conductivity (Ks). Measurements by all three methods were carried out at 15cm depth at the corner points of rectangular array (2.5m X 5m). They found result by all three methods were different which they have attributed to volume of soil explored and dimensionality of flow, spatial variation of the Ks was found sinusoidal which was due to soil structural disturbance caused by tillage and allied works for alignment of banana plants on the field.

Mohanty et al (1994) investigated performance of the four methods (Guelph permeameter GP, velocity permeameter VP, disc permeameter DP and double tube DT method) of measurement of in situ saturated hydraulic conductivity. They measured Ks at five locations on a glacial till soil at depths of 15cm, 30cm, 60cm and 90cm. They found that results of GP method were lower than that obtained by other methods, Ks by DP and DT methods were maximum with least variability. Variability in Ks was more at shallow depth. The possible reasons for the lower values in case of GP method and larger values was due to sample size (smaller in case of GP and larger in case of DP and DT) and that more variability at shallow depth was more due to influence of macropores.

Research was conducted by Lee et al (1985) to compare the methods of measurement of hydraulic conductivity. Air entry permeameter AEP, Guelph permeameter GP and Falling head soil core permeameter SC method was used to measure hydraulic conductivity on four different soil type (loamy sand, fine sandy loam, silty loam and clayey soil). Results obtained by them reveals that Ks values follow log – normal distribution rather than normal frequency distribution. Measured Ks values vary by order of magnitude in case of sand (one order) in case of loams (one or two order) and in clays (three order). All three methods were able to discriminate between different types of soil. The method to be used will depend on the accuracy desired, sample size, soil type, and other site constraints.

Guelph Permeameter (GP) and Compact Constant Head Permeameter (CCHP) are the compact and handy instruments to determine field saturated hydraulic conductivity for calculating Kfs. Both these methods are identical in all aspects however they differ in the solution they use to determine the Kfs. CCHP uses Grovers solution whereas GP uses Richards and Laplace equation. Comparative analysis to calculate Kfs using all three kinds of solution was carried out by Jabro and Ivans 2006. In order to compare the results constant head of 20cm is maintained in the borehole assuring steady state of flow and then these flow data were used to calculate Kfs by using all three solutions; the values of geometric mean of Kfs computed using Richards was 0.112 cmh^{-1} , that by using Laplace was 0.185 cm h^{-1} and finally by Grovers solution it was 0.224 cmh^{-1} . the effect of unsaturated capillary flow was not accounted by both Glover's and Laplace's solutions, The Kfs obtained by both these solutions were (1.5 – 2 times) more than that obtained by Richards solution. Ratio of Kfs obtained by Glover's solution and that obtained by using the Laplace's solution was ~ 1.4 .

Saturated hydraulic conductivity of vadose zone can be estimated by using constant head well permeameter in which Glover solution and Richards simultaneous equation approach is used to compute Kfs. Amoozgar (1989) investigated comparison of these approaches. Based on the study he concluded that The Glover solution is applicable to both homogeneous and heterogeneous soils and does not yield a negative value, whereas the simultaneous-equations approach can only yield reliable results for homogeneous and isotropic media.

Prima (2016) devised automated single ring infiltrometer, which consist of electronic gazzetes to exercise various controls and data acquisition system Arduino (microcontroller platform). It consists of a demarcation ring with a small pseudo-constant head of water (2 – 3 mm) which is controlled by a Mariotte reservoir. The infiltrometer was tested for sandy loam soil in a citrus orchard and found to yield reliable results. The device is cost effective and best alternative to the existing methods of measurements having allied advantages such as speed, high precision, efficient handling and analysis of data, factual hydraulic characterization. Effort reduction and free from human error.

Experimental investigation was carried out in western Sicily, Italy, by Bagarello et al (2013) to assess the reliability of TPD procedure in evaluating the single-ring infiltrometer data of various soil types. They found invalid results amounting 40% in clay loam soil, 25% in sandy loam soil. Soil non-homogeneity and observational errors were major factors leading to invalidity of results. They concluded that in case of fine textured soil such as clay risk of getting invalid results is high so in order to characterize such soil one need to do repetitive measurements and to encompass soil heterogeneity large rings need to be used. Macro pores effect needs to be accounted while doing numerical simulations.

Lai and Ren (2007) to investigate the effect of diameter of double-ring infiltrometer on measured values of hydraulic conductivity did research. They measured hydraulic conductivity at seven sites using four different diameter (20cm, 40cm, 80cm and 120cm) double ring infiltrometer. Subsequent numerical investigation results and field results shown large variability was in inverse proportion to the size of ring, more variability being for smaller size and less for larger. They suggested minimum size of 80 cm should be used to get more realistic values of hydraulic conductivity in case of soil having large spatial variability.

2.3.1 Summary Accurate determination of saturated hydraulic conductivity is important for various water management related issues; Hydraulic properties may be measured or estimated either by measurements on undisturbed samples in the laboratory or by in situ (field) measurements. While laboratory measurements are more controlled and generally more convenient than field methods, a large area of measurements and preservation of field structure are the inherent advantages of field methods over laboratory methods. Therefore, development of in situ techniques to determine both the saturated and unsaturated hydraulic properties of the surface soil has received much attention of soil scientists and engineers dealing with water and solute flow in the soil. Researchers have explored the use of variety of field methods to estimate hydraulic properties of soil in variety of soil type to assess the reliability of the instrument and method and to understand the possible limitation of the method

in terms of time required, labour and accuracy and tried to switch over towards automated system requiring less labour, time, cost, water and giving more accurate results.

2.4 FACTORS AFFECTING HYDRAULIC CONDUCTIVITY

Flow through porous saturated media is defined by Darcy's law (Hillel, D.,1980) which states that flow is directly proportional to the hydraulic gradient and constant of proportionality is the saturated hydraulic conductivity. Saturated hydraulic conductivity (K_s) is essentially constant for the saturated porous media. The K_s is affected by the properties of a porous media (structure, pore connectivity) and fluid properties (viscosity).

Factors affecting infiltration and hydraulic properties can be grouped into soil, soil surface and agricultural management categories. Soil factors include texture, structure (bulk density, porosity, pore-size distribution and pore continuity), structural stability and soil layering. Surface factors are mainly topography or slope gradient, the presence or absence of cover materials and soil crust. Agricultural management systems involve type of land use or vegetation, tillage, residue management and type of grazing practices in grasslands (Rawls et al., 1993). Topography or slope gradient and type of land use are among the main soil and management factors that greatly influence surface soil hydraulic properties. Among different soil hydrological properties, saturated hydraulic conductivity is reported to have the greatest statistical variability, which is associated with sample support, soil types, land use land covers, depths, skill of investigator, scale, accuracy of tools and equipment, instruments and methods of measurement and experimental errors. (Deb and Shukla., 2012).

2.4.1 Scaling :

Makuch et al (1999) conducted research with an objective of developing the relationship of hydraulic conductivity to the scale of measurement for which they have collected aquifer data from different location; tested by using various techniques (permeameter test, piezometer test, packer tests, single and multiple well pumping tests. Tracer tests etc) to find hydraulic conductivity and chosen volume of the sample tested as measure of the scale. They found no variation of K with scale for

homogeneous medium but in case of heterogeneous medium it followed power law defined by $K = c V^n$ where c is parameter related to intrinsic property of geologic strata relating geologic variables such as average pore size and pore interconnectivity, V is the volume of material tested and n is the exponent (slope of log log plot) which is function of the type of flow through medium and is usually taken as 0.5, for multiple flow media its value ranged from 0.5 to 1.0

Fuentes and Flury (2005) investigated the effect of length of sample on the saturated and near-saturated hydraulic conductivity (K). They extracted soil core of diameter 9 cm and 25 cm length from the A horizon of a no-till, silt loam soil, and determined K at different hydraulic heads (matric potential heads) under steady-state flow conditions and they found that core length has considerable effect on the measured hydraulic conductivity, the effect of core length is predominant in case of saturated condition than in unsaturated condition. They inferred that small sample would not be representative of large sample volume in the field.

To investigate the effect of macropores on the hydraulic conductivity, study was carried out by Mallants et al (1997) for carrying out this study they have prepared three columns of different size (5cm, 20cm and 100cm length). All these columns being collected from same soil (sandy loam) along a transect with macropore. The geometric mean of K_s obtained shown a declining trend with increase in column size. Geostatistical analysis of K_s data revealed small range spatial structure or micro heterogeneity for 5cm size column whereas bigger spatial structures were discovered in 20cm and 100cm columns. Spatial correlation existed between type-II K , and depth-averaged macropore area

Hu et al (2013) measured saturated hydraulic conductivity (K_s); using soil core (SC), tension infiltrometer (TI) and Guelph permeameter (GP). To quantify variability of K_s in terms of measurement method, landscape features (sloped surfaces and gullies), and scale (sampling spacing and extent). Measurements were carried out in an area of 0.2km² in China. To encompass sloping surface, gullies. They found the spatial dependence decreased with a decrease in sampling extent. Structured variability was not seen at the 10-m space between sampling points. When this space

decreased from 10 to 2 m, the nugget variance decreased, whereas the structured variance, sill variance, and spatial dependence increased. When sampling space changed from 2 to 0.2 m, the changes in spatial pattern of K_s was not significant; thus in order to capture spatial variability sampling space should not be more than 2m. K_s in the sloped portion were found more than that in case of gullies.

2.4.2 Land use land cover

Tekin and sabit (2006) conducted study to understand the effect of land cover on the saturated hydraulic conductivity. They have tested 36 samples from natural uncultivated field and adjacent cultivated field and measured saturated hydraulic conductivity in the laboratory on samples of size 100cm^3 . The variability found in cultivated land was more than that in the virgin field by almost 2.5.

Effect of vegetation on hydraulic conductivity was studied by Chen et al (2009) on the hill slope at experimental station Taoyuan in Hunan province of China. Measurements were carried out by using permeameter in red loam soil having different vegetation covers. The result has shown that there is one order difference in the values of K_s at 25cm depth is lesser than that at surface soil for soil without vegetation. However, for soil with vegetation cover, roots of plants increased the value of K_s in lower layer soil but it is insignificant in the surface layer soil. However, variability of K_s depends on the species and age of the vegetation cover.

Zimmermann et al (2006) conducted research at Rancho Grande (108180S, 628520W, 143 m a.s.l.), in the northwestern Brazilian state of Rondonia to assess the effect of land use on saturated hydraulic conductivity and they found K_{sat} at the 12.5 cm depth varies as follows: {forest, banana, capoeira} > {teak} > {pasture}, At the 20 cm depth, the differences in K_{sat} among the land uses are minor compared to prevailing rainfall intensities, i.e., the vertical flow of water is impeded regardless of land use.

Suriya and Mugdal (2012) carried out research study to assess the impact of land use change on flooding in Thirusoolam sub watershed combination of both rural and urban watersheds Land use changes from 1976 to 2005 were studied for this watershed. The land use pattern of the watershed has been classified into a built up

area, tanks, scrub land, plantation, forest, agricultural land and barren land. The results from the study indicate that due to urbanization land use was changed and thus for the same extent of rainfall and different land use conditions between 1976 and 2005, the flooded area and the water depth has increased for the 2005 conditions.

The effect of the land use change of a Typic Hapludand on some soil properties which depends on the structure of soil was studied at two sites : a native forest (NF) and a prairie used for permanent pasture for over 50 years (P50) by Dorner et al (2010). They found that change in the land use from native forest to P50 wherein the soil structure alters to considerable extent, the saturated hydraulic conductivity decreased.

Jarvis et al. (2013) used global database to assess the effect of various parameters on the hydraulic conductivity of soil and they found that in the surface soil (0 to 30cm) saturated hydraulic conductivity was not affected by the soil texture but it was strongly influenced by the bulk density and organic matter and land use. Ks at bare ground (arable land) was found smaller than that under vegetation, forests and perennial agriculture. Clay soil had less Ks as compared to other type of soil

Chen et al (2009) conducted research in small catchment of Chenqi in Guizhou Province of China to understand the consequence of land use and land cover (LULC) on Soil moisture content (SMC) and hydraulic conductivity of various kinds of soil in a karst area. In their study, they measured hydraulic conductivities(K) and soil moisture contents by using Guelph permeameter and time domain reflectometry along four karst hillslopes respectively, each plot has a different land surface slope, vegetative cover, landform, rock fragment content and soil property. The results revealed that changes in land cover affect the distribution of soil moisture and hydraulic properties considerably. In bare soil SMC was found less as compared to that in the grass area, shrub area and forest area. Measured K values were least for bare soil area (0.01cm/min), medium for agriculture area (0.6cm/min) and highest for the forest area (0.8cm/min).

2.4.3 Terrain and soil structure:

Investigation was done by Wang et al (2007) In the Nebraska Sand Hills (NSH) to understand the spatial 3D patterns of Kfs by using constant head permeameter. The results reveals that Kfs showed increasing trend with depth up to the lower boundary of the root zone (up to 2 m). Highlands had more Kfs values than lowlands, and they found a strong correlation between Kfs and absolute elevation. At intermediate depths (50cm –150 cm), Kfs shows the greatest variability, and systematic change of Kfs is less predictable. At near-surface depths (~20 cm), Kfs at both lowlands and highlands converged to lower values. Near the surface (20 cm depth), Kfs ranged from 300 to 700 cm/day, and its values increased with depth, averaging 1400 cm/day at 200 cm depth. It is found that the effect of short-term vegetation disturbance on Kfs was minimal that may not hold in the long run.

Veronika Jirků (2013) carried out research study, to assess the temporal variability of the soil structure, aggregate stability and hydraulic properties; due to variation in the climatic conditions, soil management activity, physical and chemical properties of soil. For this study, they measured soil properties in surface horizon of three soil types for three years. Undisturbed soil samples were used to estimate (representative) soil water content, bulk density, porosity and soil hydraulic properties. Soil samples of relatively larger volume were also collected every month to evaluate aggregate stability using the water stable aggregates, unsaturated hydraulic conductivity were measured by using mini disk tension infiltrometer. Similar trend was observed in soil intrinsic properties in different soils whereas variability was very high in case of hydraulic properties and it was different for different soils. No strong correlation was observed between hydraulic properties of soil and other properties of soil.

Variability of Ks and soil water retention properties ($\theta(h)$) across a soil-slope transition in a glacial till material in Iowa was carried out by Mohanty (2000). In his study he tested around 400 samples along two orthogonal transect of slope and measured at 15cm and 30 cm depth saturated hydraulic conductivity and water retention. Results indicated that most of these parameters are significantly different across the soil-slope transition except water holding capacity ($\theta_{(333-15000)}$). A

lower nugget effect at the 30-cm depth in comparison with the 15-cm depth implies surface disturbances due to farm related activities.

Raouf et al (2011) investigated effect of sloping terrain on hydraulic conductivity of loamy soil. Experiment were carried out in Gonbad research station Iran in homogeneous loamy soil with slope angle ranging from 10 to 40 degrees with step of 10 degree and measurements were carried out by using double ring and tension infiltrometer at different tensions varying from 0 to 15 cm. They found that hydraulic conductivity has shown declining trend with increase in tension and slope in both steady state and transient state of flow

A research study was carried out by Yao et al (2013) in Niaman Desertification Research Station in the Horqin Sand Land China. In order to understand and quantify relation between Ks with type of sand and soil depths, Guelph permeameter was used to measure Ks at all six typical lands (mobile dune, fixed dune, pine woodland, poplar woodland, grassland, and cropland). The results showed that mean value of Ks was shown a decreasing trend with higher value for mobile dune and lower value for the cropland. Bulk density, coarse sand and organic matter were dominant factors affecting the Ks as compared to clay and silt content proportions. Strong positive correlation was observed for sand in the study area.

Effect of topography, land use, slope aspect on soil properties is studied by many researchers (Mahler et al., 1979; Luk et al., 1993 ;)

2.4.4 Summary: Topography, landscape position, land use, and sloping aspect influence the Hydraulic conductivity of soil. Fine-textured soils are often found in the lower parts of slopes and have small water intake rates and large runoff potential. For gentle slopes, there is inverse relationship between slope gradient and infiltration under non-crusted conditions, may be reversed under crusted conditions.

2.5 PEDOTRANSFER FUNCTION.

Pedotransfer functions are predictor functions that relate soil hydraulic characteristics to the basic soil properties. The main reason for developing pedotransfer functions arises from the fact that soil hydraulic characteristics like saturated hydraulic

conductivity are difficult to measure accurately and are also tedious and time consuming and expensive to measure.

2.5.1 PTF by using MLR and ANN

Stumpp et al (2009) evaluated two types of pedotransfer functions (PTFs) for their accuracy and applicability to a wider range of Alpine soils in the Halbammer area (Germany). The PTF were assessed based on the difference between predicted and measured values of water retention values and statistical parameters such as mean error (ME) correlation coefficient (R) and root mean square deviation (RMSD) were used to check the accuracy. They suggested following things while using these PTFs. In case of SOILPROP for soil with more organic content (> 10%) there is overestimation of water content , thus while using this PTF in a soil with lower bulk density a correction factor for organic matter need to be used. They found performance of PTF was good for silty and clayey soil. In ROSETTA, the user has freedom to select model hierarchies depending on amount of input data more the number of input parameters more will be the accuracy. Though huge database was used in case of ROSETTA but water content predicted by it were on lower side.

Mbonimpa et al (2002) developed pedotransfer function to estimate saturated hydraulic conductivity (Kfs) by using pedologic properties. PTF developed by them was extension of established Kozeny–Carman equation and can be used for estimating value of Kfs of granular and plastic/cohesive soil. PTF for granular soil and that for plastic soil developed by them was $K_G = C_G \frac{\gamma_w}{\mu_w} \frac{e^{3+x}}{1+e} C_U^{1/3} D_{10}^2$ for granular soil and $K_P = C_P \frac{\gamma_w}{\mu_w} \frac{e^{3+x}}{1+e} \frac{1}{\rho_s^2 w_L^{2\chi}}$ for plastic soil where C is constant, C_U – coefficient of uniformity, D_{10} - effective size, e – void ratio, γ_w – density of fluid, μ_w – viscosity of flowing fluid, ρ_s – density of soil solid and w_L - liquid limit of soil, x and χ are constants. Developed model was tested and found to yield reliable results in wide spectrum of materials

Salchow et al (1996) developed simple pedotransfer function using sand, silt, clay, OM and BD by separating data into four texture class (silty clay loam, silt loam, loam

and sandy loam). They found that prediction capability of the PTF for log of saturated hydraulic conductivity, permanent wilting point, field capacity, available water capacity, and percentage of water stable aggregates, was better for each textural class.

Minasny et al (1999) developed pedotransfer function for Australian soil for predicting water retention from bulk density and particle size using different approaches: Extended nonlinear regression (ENR), Multiple linear regression(MLR) and artificial neural network(ANN).They developed both parametric and point estimation PTF. Performance of each of these was checked by taking 733 samples for training and 109 samples for testing. Performance of ENR was adequate for parametric PTF, MLR did not predicted Van Genuchten parameters due to nonlinearity between curve shape parameters and soil properties. ANN and ENR was performed in similar way for training dataset whereas ENR was good for testing dataset. In case of point estimation MLR performance was good as compared to other PTF.

Pedotransfer function using Artificial Neural network was developed by Nemes et al (2003). They used HYPRES database to continental scale PTFs , data set from Hungary were used to derive national scale PTFs and database of American and European continent were used to develop intercontinental scale PTFs. For every database they developed 11 PTFs differing in their input data. Hungarian database was used to check Predictive accuracy of each PTF. Performance of PTF using Hungarian dataset was better than continental and intercontinental PTF.

Merdun et al (2006) developed point and parametric PTF for predicting hydraulic properties of soil using regression method and ANN. They have used basic soil properties such as bulk density, particle size distribution and pore sizes. For model development, they used 195 samples segregated into training data 130 samples and testing data 65 samples. Predictive capability of models was checked by using coefficient of determination (R^2) and the root mean square error (RMSE). They found that regression model performance was good as compared to that of ANN model; both model performance was good for point prediction than parametric prediction.

Jana et al (2007) have developed a Multiscale Pedotransfer Functions using ANN based PTFs trained on SSURGO soil textural data with scale of 1: 24000; to determine soil water content at field capacity, residual and saturation, as well as Van Genuchten soil water retention function at local scale (1:1). The output was corrected using Van Genuchten equation prior to constructing the soil water characteristic curve. The results revealed better agreement between field observations and soil water retention curve developed using ANN based PTFs. Model was tested further to check its robustness for different dataset from Washita watershed and was found suitable.

Parasuraman and Si (2007) developed PTFs to estimate saturated hydraulic conductivity by using the soil index properties such as bulk density, sand, silt and clay content, using Genetic programming (GP). They used data from the UNSODA for developing the model and its performance they compared with NN model. The performance of GP model was good in predicting saturated conductivity as revealed by their study; the reason for its better performance was due to ability of GP to optimize both the model structure as well as parameters. Also PTF had relatively less uncertainty for model parameters as compared to model structure.

Zacharias and Wessolek (2007) developed a PTF for predicting water retention characteristics (WRC) without considering only bulk density and soil texture. They used 676 measured WRCc for calibration purpose; which is good blend of topsoil (353) and subsoil (323) to account for heterogeneity. Validation of PTF was done by using 147 dataset (topsoil + subsoil) the performance of the model was good ($R^2 = 0.94$). They concluded that bulk density indirectly account for the effect of organic matter on water retention.

Multiple linear regression based PTF was developed (Aimrun and Amin; 2009) adopting stepwise regression to determine robust model based on coefficient of determination (R^2). They used randomly collected 408 samples from a 2300 ha rice cultivation area. They used Dry density (Db), percentage of sand (S), percentage of silt (Si) , percentage of clay (C), organic matter (OM) and geometric mean diameter (GMD) as input parameter for regression and they found for the best model for predicting Ks sand content and silt content has least correlation.

Khodaverdiloo et al (2011) conducted study to assess whether soil water retention characteristic of cancerous soil is affected by calcium carbonate and developed a PTF for this soil. In order to develop model, 220 sample were used for calibration and separate dataset of 55 samples were used for testing purpose for multiple regression. They found that there is no change in the prediction of water retention value (van Genuchten) by using calcium carbonate and by not using it as input parameter. The results of point and parametric PTF were in good agreement with that obtained by using ROSETTA PTFs of Schaap et al. (2001). with average RMSE values of 0.028 and $0.107 \text{ cm}^3 \text{ cm}^{-3}$, respectively.

Han et al (2012) developed a PTF for estimating field capacity, saturated soil water content and saturated hydraulic conductivity in the Loess Plateau of China. They used 252 dataset to derive PTF by using multiple linear regressions (MLR). Predictive capability of the model was evaluated by using independent 130 dataset for validation. Performance of the model was good for saturated soil water content ($R_{\text{adj}} = 0.78$), they used particle composition and organic content as input parameters. Performance of model was improved for Log Ks.

Zhao et al (2016) developed PTF model using MLR and ANN to predict Ks for which they have selected 243 across Loess Plateau of China ($430,000 \text{ km}^2$), undisturbed and remolded samples were collected samples from ground level up to a depth of 40cm and measured Ks along with the soil parameters which influence Ks such as bulk density, clay content, silt content, saturated soil water content. Performance of both PTF (MLR and ANN) was similar however PTF developed by ANN was not good from stability point of view.

2.5.2 PTF by using ANFIS

Kalkhajeh et al (2012) developed PTF for predicting soil Ks by using multiple linear regressions (MLR), adaptive neuro-fuzzy inference system (ANFIS) and artificial neural network (ANN) including Multi-Layer Perceptron (MLP) and Radial basis function (RBF) models using available soil data in Khuzestan province, southwest Iran. Accuracy of these PTF were evaluated by using statistical parameters such as

coefficient of determination (R^2) and mean square error (MSE). The obtained results indicated that the performance of ANN was better than other models with R^2 value of ~ 0.8 , performance of ANFIS ($R^2 = 0.71$) was better than MLR ($R^2 = 0.53$).

Use of ANFIS are available in other field (Mukerji et al., 2009; Terzi et al., 2006; Wang et al., 2009; Shiri and Kisi., 2011; Chang 2006., Sarmadian and Mehrjardi ., 2010))

2.5.3 PTF by using SVM

Very few literatures are available using SVM as PTF for estimating saturated hydraulic conductivity.

Pedotransfer function by using support vector machine was developed by Twarakavi et al (2009) to estimate soil hydraulic properties by using database which was used for ROSETTA. By using all or some of these parameters sand, silt, and clay percentage, bulk density and retention data. Predictive capability of the PTF was evaluated by using Mean error (ME), root mean square error (RMSE) and coefficient of determination (R^2). They found that performance of model was good in estimating all hydraulic parameters as compared to that of ROSETTA.

An ANN and SVM model for estimation of field hydraulic conductivity of clay liners was developed by Das et al (2011). For these models input parameters used were liquid limit, Plastic limit, percentage fine content (F), moisture content (MC), dry density (DD), maximum dry density (MDD), optimum moisture content (OMC), percentage of field compaction (Po), weight of compactor(W), lift thickness (LT), number of lifts (LN) and height of lift (HL). They found performance of SVM model was better than ANN model.

Pedotransfer function (PTF) by using Support vector machine (SVM) was developed by Elbisy (2015) for estimating saturated hydraulic conductivity using following input parameter such as calcium carbonate, hydro carbonate ions, chloride ions, liquid limit and clay / silt ratio. Linear, radial basis and sigmoid kernel function were tried and optimal free parameter of SVM model was determined by using genetic algorithm.

They found that RBF model has shown better accuracy (modelling efficiency = 0.972 and correlation coefficient = 0.976) as compared to other kernel functions.

2.5.4 PTF by using ELM

Very few attempts have been made by researchers to develop ELM model to estimate hydraulic conductivity. It is used in other fields (Tian et al., 2015; Deo and Sahin, 2015; Yaseen et al., 2016; Patil and Deka., 2016; Atiquzzaman and Kandasamy (2016)

2.5.5 Summary: Actual measurement of saturated hydraulic in the field is laborious, costly, however due to inherent variability (temporal and spatial) of this parameter, large number of samples are required to characterize the area under consideration. To overcome this limitation researchers have developed an indirect method of estimation of saturated hydraulic conductivity by using the simple basic parameters of the soil, which can be measured and available easily such method is called pedotransfer function (PTF). Though this method does not give most accurate results but the results will be useful to characterize the area under consideration.

2.5.6 Objectives of the study

Based on literature survey, following objectives are finalized for this study.

- 1) To investigate the spatial variability of vadose zone saturated hydraulic conductivity of sloping terrain using Guelph permeameter in semi - arid region, under different LU / LC
- 2) To establish a relationship between saturated hydraulic conductivity and index properties of soil.
 - a) To develop the Pedotransfer function for estimating saturated hydraulic conductivity using ANFIS, ELM and SVM models.
 - b) Performance evaluation of ANFIS, ELM and SVM models.

CHAPTER 3

MATERIAL AND METHOD

To achieve the objectives, field in – situ data has been collected by using sampling and Guelph Permeameter method. Statistical analysis is carried out for field variability at spatial scale. Field saturated hydraulic conductivity was measured by using Guelph permeameter. Laboratory analysis was done on the soil, sampled from field to determine its index properties for developing various PTF (Pedotransfer function) models. In this study an attempt is made to develop PTF by using soft computing approach like Adaptive Neuro – fuzzy system (ANFIS), support vector machine (SVM) and Extreme Learning Machine (ELM), for saturated hydraulic conductivity of soil in Solapur, India. Study area, field method of measuring saturated hydraulic conductivity, various laboratory methods for finding basic soil properties, the basics of various modeling techniques used in this study are discussed in this chapter.

3.1 STUDY AREA

Study area selected for the work is Solapur as shown in Fig 3.1, which is geographically located at 17° 39' 35.7120" N and 75° 54' 22.9932" E. Its elevation is 483 m above mean sea level. The mean annual rainfall at Solapur is 723 mm (highest 1292 mm and lowest 270 mm). The rainfall is scanty, erratic and ill distributed. Due to scanty and non-uniform rain, scarcity conditions prevail in the district. This has adversely affected the socio economic condition of peoples. May is the hottest and December is the coldest month, in general, climate is “semi – arid”. The soil in this area is derived from basic igneous rock namely basalt and underlain by partially disintegrated rock locally called “murum”.

Three sites have been selected for the experimental work, which are Hipparga site (close to college), Mulegaon site and Punanaka site. Hipparga site is having mild downslope followed by undulated terrain with grass cover dominated by blend of silty and clayey soil. Mulegaon site is agricultural harvested land (no crops) with silty soil and Punanaka site is bare land having coarse size soil. These three stations are as

shown in Fig 3.1, distance between college and Punanaka is around 10km. that between College and Mulegaon is 15km and between Punanaka and Mulegaon is 20Km.

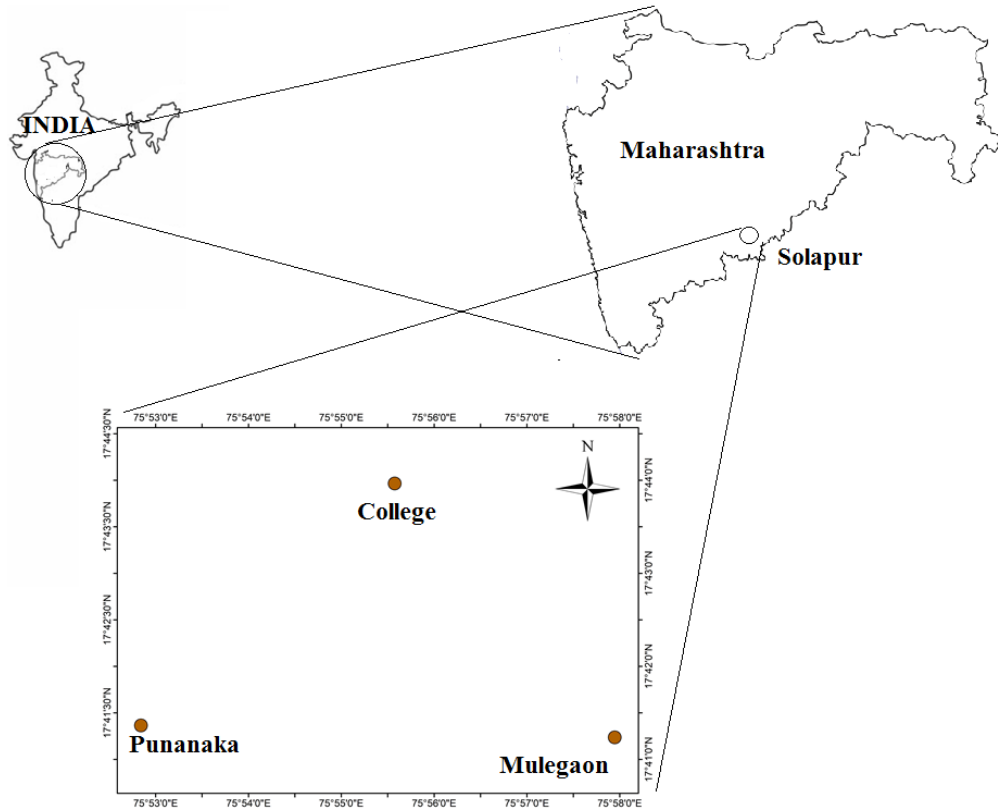


Fig 3.1 Location of Study area

Sampling at each site was done in an area of 0.76ha (190m X 40m). Area is divided in to small grids of 10m X 10m as shown in Fig 3.2. In-situ saturated hydraulic conductivity was determined by using Guelph permeameter, for which observations were taken at each corner of the grid at a depth of 15cm, 30cm and 45cm. The measurement consisted in estimating a quasi – steady discharge Q of water infiltrating into a vertical borehole of radius a (3cm) in which the water level is maintained at a height H (5cm / 10cm) above the bottom of borehole.

Soil sample were collected at all three depths after finishing the observations for permeameter to carry out laboratory analysis these samples are collected carefully in a cylindrical container two in number (100mm diameter and 125mm height). These samples were used for laboratory analysis of soil. Samples from first cylindrical core were used to determine dry bulk density, particle density (Das

2002), and organic matter, and then sample from second core was used to determine soil texture by using hydrometer analysis (Bowles 1992, Das 2002).

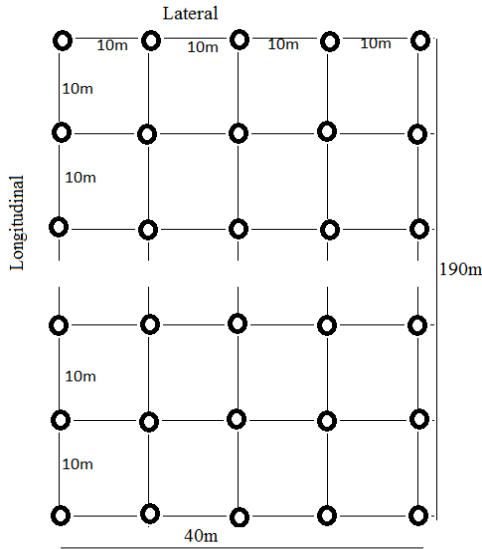


Fig 3.2 Sampling scheme grid at College, Mulegaon and Punanaka site

3.2 FIELD MEASUREMENT OF SATURATED HYDRAULIC CONDUCTIVITY BY GUELPH PERMEAMETER:

3.2.1 Introduction: Guelph permeameter is handy instrument used for measuring in situ saturated hydraulic conductivity (K_f), matrix flux potential, $\phi_m [L^2T^{-1}]$, sorptive number, $\alpha^*[L^{-1}]$, sorptivity number, $S, [LT^{-1/2}]$, the effective Green – Ampt wetting front pressure head. Guelph permeameter (well or borehole permeameter) method is well known method for in – situ measurement of saturated hydraulic conductivity. This method involves establishing constant head of water in an uncased well, and then measuring rate of outflow of water into unsaturated porous material. This instrument is equipped with an “in – hole Mariotte bottle” which maintain constant head and measure corresponding Q , Single head, two – head, and multiple head analysis are available for this method.

3.2.2 Description of method: Apparatus, detailed procedure and theory involved, are given in detail in soil moisture equipment corp.(2010), Reynold et al (1985) and Reynold and Elrick (1986). Brief description of Guelph permeameter and its use is given below; for detailed description, reader can refer above literature.

1. Mode of operation:

This method measures quasi steady state recharge, Q (L^3T^{-1}), necessary to maintain a constant head of water, H (L), in an uncased cylindrical well of radius a (L). Kfs , S and α^* for infiltration are calculated from known values of Q , a , and H using appropriate equations

2. Apparatus:

Guelph permeameter (GP) has a support tube, a reservoir assembly, and a system to control the ponded depth of water into the well.

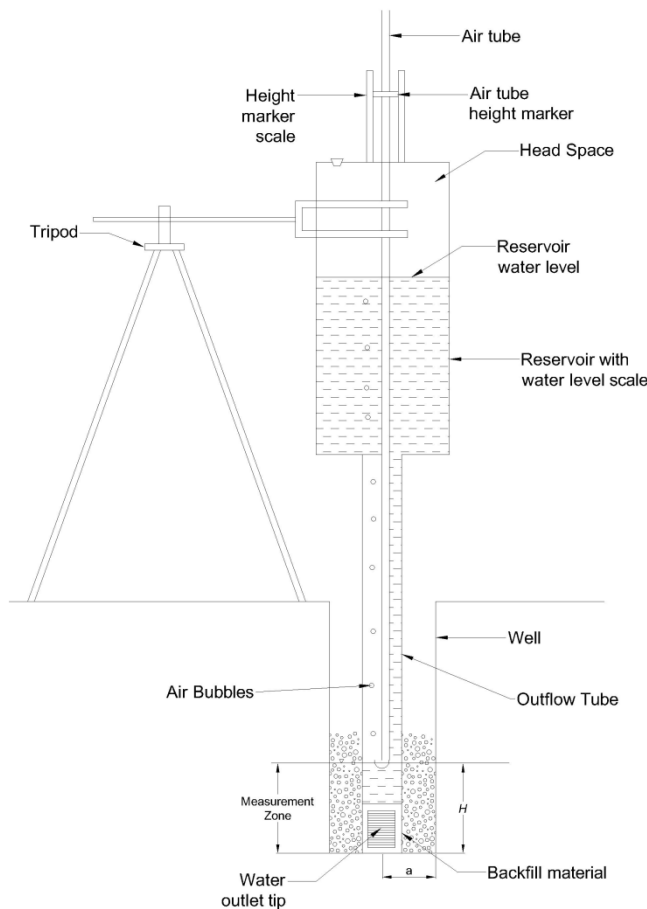


Fig 3.3 Schematic diagram of Mariotte system for use in Guelph permeameter (adapted from Reynolds, W.D., Soil sampling and methods of analysis, Canadian Society of soil science)

The reservoir assembly is supported on support tube and regulates water in the well. The outlet tip of the device has ribbed opening at the bottom end of tip, which helps in discharging flow of water uniformly without causing any flow concentration. Water

storage facility is provided in the reservoir assembly in the form of concentric cylinders with a scale engraved on inner reservoir cylinder. Knowing the cross sectional area of reservoir and drop in the level of water will give outflow rate from the reservoir. Valve fitted at the bottom of the concentric reservoir regulate the flow either through combined reservoir or through only inner reservoir based on nature of soil. The reservoirs are filled through a opening provided on the reservoir cap that remains sealed with a plug when the device is used to make a measurement. Air tube, which is open at both ends slide freely within the inner reservoir and the support tube along the vertical axis of the device; which will regulate the head of water in the well.

3. Procedure:

Ground surface where observations are to be taken cleaned and then well of diameter 4cm was excavated up to required depth (15cm/30cm/45cm). Necessary precautions were taken to see that bottom of well is flat and to minimize smearing and compaction of the well surfaces particularly in fine textured soil.

Permeameter was filled with water and is inserted into the well with its tip slightly above the bottom of well, a support is provided to the permeameter to give it good stability. Air tube was lifted out of the outlet end of to establish the desired head (5cm/10cm). Rate of flow of water out of Mariotte bottle and into soil is measured by observing the rate of fall of water level in the reservoir, rate of fall decrease with lapse of time and approach a constant value (steady). If two head analysis is to be used then repeat the procedure for second constant head H_2 by raising the air tube. Calculate the field saturated hydraulic conductivity (K_{fs}) by using appropriate formula for single head and two head method

4. Governing equations: Equation for calculating field saturated hydraulic conductivity (K_{fs}) are as given below

For one head analysis

$$K_{fs} = \frac{C_1 Q_1}{2\pi H_1^2 + \pi a^2 C_1 + 2\pi(H_1/\alpha^*)} \quad (3.1)$$

For two head analysis

$$K_{fs} = G_2 Q_2 - G_1 Q_1 \quad (3.2)$$

Where

$$G_1 = \frac{H_2 C_1}{\pi[2H_1 H_2 (H_2 - H_1) + a^2 (H_1 C_2 - H_2 C_1)]} \quad (3.3)$$

$$G_2 = \frac{H_1 C_2}{\pi[2H_1 H_2 (H_2 - H_1) + a^2 (H_1 C_2 - H_2 C_1)]} \quad (3.4)$$

$$Q_1 = XR_1 \text{ or } YR_1 \quad (3.5)$$

depending on whether combined reservoir is used or inner reservoir is used
 R_1 – steady state rate of flow, X – area of combined reservoir, Y – area of inner reservoir, H_1 – constant head at which steady state rate was measured, a – radius of well, C – shape factor which depends on the well radius (a) and head of water (H) and soil type and is given by following equation

$$\text{For sandy soil } C = \left[\frac{H/a}{2.074 + 0.093(H/a)} \right]^{0.754} \quad (3.6)$$

$$\text{For structured loam s and clays } C = \left[\frac{H/a}{1.992 + 0.091(H/a)} \right]^{0.683} \quad (3.7)$$

$$\text{For unstructured clays } C = \left[\frac{H/a}{2.081 + 0.121(H/a)} \right]^{0.672} \quad (3.8)$$

C_2 and Q_2 - are corresponding values for head H_2 ,

α^* - Sorptive number its value (cm^{-1}) is as given in Table 3.1 below

Table 3.1 Texture – structure categories for visual estimation of α^*

Texture – structure category	α^* (cm^{-1})
Compacted structure less clayey material such as landfill caps and liners; lacustrine or marine sediments	0.01
Soil which are both fine textured (clayey) and massive; include unstructured clayey and silty soils, as well as fine structure less sandy material	0.04
Most structured and medium texture materials; include structured clayey and loamy soils, as well as unstructured medium sands. This category is generally most appropriate for agricultural soils	0.12
Coarse and gravelly sands which also includes some highly structured soils with large cracks and bloopers	0.36

Source: Adapted from Elrick et al (1989)

3.3 LABORATORY MEASUREMENT OF SOIL PROPERTIES:

Soil samples were collected from each of the sampling point at desired depth below ground level by using two cylindrical containers (Fig 3.4) of size (100mm dia. and 125mm height). Sample from one cylinder was used to determine particle density and soil textural analysis and that from second cylinder was used for finding particle density and organic matter.

3.3.1 Particle density (specific gravity):

soil from cylindrical container is removed weighed (M_1) and kept it in oven for twenty-four hours; after twenty four hours sample is removed from oven and again it is weighed (M_2) this sample is used for finding particle density and organic content. For finding particle density; density bottle is cleaned and weighed (m_1) bottle is filled with 20 – 25 gm of oven dried soil and bottle is again weighed (m_2), water is added to the soil in density bottle until it fill completely; air from it is removed by shaking it vigorously and then it was weighed (m_3). Density bottle is again cleaned and then it was filled with only water and weighed again (m_4). Using these observations particle density can be determined by using (IS 2720 (Part. III) Sec I and Sec II, 1980)

$$G = \frac{m_2 - m_1}{(m_3 - m_4) - (m_2 - m_1)} \quad (3.9)$$

3.3.2 Organic content :

Loss on Ignition (LOI) analysis is used to determine the organic matter content (% OM) of a soil sample. LOI calculates %OM by comparing the weight of a sample before and after the soil has been ignited. Before ignition, the sample contains OM, but after ignition all that remains is the mineral portion of the soil. The difference in weight before and after ignition represents the amount of the OM that was present in the sample.

Porcelain crucible was heated for 1 hour at 375°C in a muffle furnace, cooled and weighed. Soil sample to be tested is hammered lightly with wooden mallet to break all the clods and then was sieved through 2mm sieve in a tray; and tray was placed in an oven for 24 hours at a temperature of 105°C . Sample tray was taken out from an oven and kept in desiccator for cooling. Five crucibles were taken, in each crucible around 5 – 10 gm. of soil from desiccator is placed, each crucible is weighed accurately, then it was placed in muffle furnace turned on the furnace, and temperature was gradually

increased to 375⁰c. Sample was kept in the furnace for heating for a period of 16hours to ensure that sample was heated sufficiently. Furnace was turned off and waited for a period of 2 – 3 hours to cool it down and then crucibles were taken out from the furnace and then kept in desiccator for further cooling for a period of half hour and then crucibles were removed and weighed again. Organic matter (%) is calculated by using an equation for each of the crucible sample and then was averaged to get mean value of it

$$.OM (\%) = \frac{\text{pre ignition weight (gm)} - \text{post ignition weight (gm)}}{\text{pre ignition weight (gm)}} \times 100 \quad (3.10)$$

3.3.3 Bulk dry density :

Empty Cylindrical container is weighed (m_5), cylindrical container with soil is weighed (m_6), empty moisture content crucible is weighed (m_7), small amount of soil (20 – 25gm) from cylindrical container is placed in the crucible and is weighed again(m_8), crucible is kept in oven for 24 hours and temperature of oven is adjusted to 105⁰c, after 24 hrs. crucible is taken out from oven cooled in desiccator and then again is weighed (m_9), the bulk density (ρ) dry bulk density (ρ_d),



Fig 3.4 Cylindrical sampler (container) being driven into soil to collect the soil sample after the in situ test

(IS 2720(Part 29):1975) is then determined by using following equation

$$\rho = \frac{m_6 - m_5}{v} \quad (3.11)$$

Where v – volume of the cylindrical container and is calculate by using

$$v = 0.25\pi d^2 h, \quad (3.12)$$

Where d is diameter and h is height of container

$$\rho_d = \frac{\rho}{(1+\omega)} \quad (3.13)$$

Where ω – moisture content of the soil and is calculated by using

$$\omega = \frac{m_8 - m_9}{m_9 - m_7} \quad (3.14)$$

3.3.4 Porosity :

Porosity of soil was calculated by using bulk density (ρ), dry bulk density (ρ_d), and particle density(ρ_s). (Punmia B.C. 2005) Particle density for the soil is equal to specific gravity times the density of water, if densities are expressed in gm cm^{-3} , then ρ_s will be equal to G. Porosity of soil is given by

$$n = \frac{\rho_s}{\rho_d} - 1 \quad (3.15)$$

3.3.5 Grain size analysis:

Soil from cylindrical container is removed, oven dried and then all clods present in it were broken by using wooden mallet. About 200 – 250 gm. of oven dried soil sample is taken and soaked with 2% calgon solution for proper mixing it was stirred thoroughly and left for soaking period of about an hour. Slurry of soil then sieved through 4.75mm sieve and washed with water jet, material retained on it will be gravel. Fraction which was dried in oven and weighed, material finer than 4.75mm was sieved again through 75 micron sieve, material was washed till water coming out through sieve is clean (colorless), soil slurry passing through 75micron is collected and dried in oven. Material retained on the 75 micron sieve is oven dried (IS 2720 part IV- 1985) and is then is sieved. Sieving (4.75mm, 2mm, 1mm, 425 μ , 212 μ , 150 μ and 75 μ) is carried out for about 10 – 15 minutes and then mass of soil retained on each sieve is weighed. knowing mass of soil used for sieving (retained on 75 μ) and mass of soil retained on each sieve after sieving percentage of mass retained and cumulative percentage retained was determined, percentage finer retained on any sieve is determined by subtracting cumulative percentage from 100.

Soil slurry passing through 75 μ is oven dried and is used for sedimentation analysis by using hydrometer. About 50gm of this soil is mixed with 125ml of 4% calgon solution and sufficient water to produce 1000ml. Mixture is allowed to stand for 24hrs. Suspension is again mixed with electrical high speed stirrer with dispersion cup. Suspension is then taken in measuring cylinder and cylinder is turned end to end to ensure uniform distribution of particles. Before taking any measurements, hydrometer is suspended in the suspension and the readings were recorded at regular intervals of time (0.5, 1, 2, 5, 10, 15, 30, 60, 120, and 240, 480 and 1440 minutes), hydrometer reading were then corrected for meniscus, temperature and dispersion agent correction. Knowing the geometrical parameters of hydrometer effective depth at which hydrometer readings were taken is determined by using

$$H_e = H + 0.5 * \left[h - \frac{V_h}{A} \right] \quad (3.16)$$

where H – depth of center of hydrometer bulb from the water level, A – c/s area of cylinder, V_h is volume of hydrometer bulb, h is the length of hydrometer bulb. Percent finer than particle size D was calculated by using an equation

$$N = \frac{G}{(G-1)} \frac{R}{W_s} \times 100, \quad (3.17)$$

where G – specific gravity of soil and W_s dry weight of oven dry soil in suspension, size of particle D in turn was computed by using

$$D(mm) = K \sqrt{(H_e(cm)/t(min))} \quad (3.18)$$

where K is constant and is given by

$$K = \sqrt{\frac{30\eta}{G-1}} \quad (3.19)$$

where η is viscosity of water in gm-s/cm². Grain size distribution curve is plotted using combined analysis between particle size and percent finer for sieve analysis as well as sedimentation analysis; in sedimentation analysis % finer based on total weight is taken for plotting graph which can be calculated by using

$$N_T = N \frac{W}{W_f} \quad (3.20)$$

Where W – total weight of soil taken for sieve analysis, W_f – weight of soil passing 75 μ sieve

3.4 SOFT COMPUTING MODELING:

3.4.1 Artificial Neural Network:

Neural network is a group of interconnected artificial neurons that can be used as a computational model for information processing. These are non-linear statistical data modeling tools used to develop a relationship between input and output. Mathematically, an ANN can be treated as universal approximates having ability to learn from examples without the need of explicit physics.

3.4.1.1 Feed-Forward Back propagation Network (FFBP)

A FFBP network has an input layer an output layer and one or more hidden layers between the input and output layer. Information in a neural network passes from the input to the output side (Figure. 3.1). Hidden layers enhance the network's ability to model complex functions. The data passing through the connections from one neuron to another are manipulated by weights that control the strength of a passing signal. The neurons in one layer are connected to those in the next, but not to those in the same layer. Thus, the output of a node in a layer is only dependent on the inputs it receives from previous layers and the corresponding weights.

The strength of the signal passing from one neuron to the other depends on the weight of the interconnections. Each node multiplies every input by its weight, sums the product, and then passes the sum through a transfer function to produce its result (Figure. 3.5). This transfer function is generally a steadily increasing S-shaped curve, called a sigmoid function. The attenuation at the upper and lower limbs of the 'S' constrains the raw sums smoothly within fixed limits. The transfer function also introduces a nonlinearity that further enhances the network's ability to model complex functions.

3.4.1.2 Training a neural network

The process of training ANN models involves optimization of various parameters and is similar to calibration of a hydrological model. Generally, ANN models do not have any prior knowledge about the problem. The data enters the network through the input layer. The nodes in the input layer are not computational nodes and simply broadcast the data over weighted connections to the hidden nodes. The ANNs are trained with a

set of known input and output pairs called the training set. In the training process, the weights are optimized to get a specific response from ANN. The network weights are initialized based on some previous experience or with a set of random values. These initial values of weights are then corrected during a training (learning) process

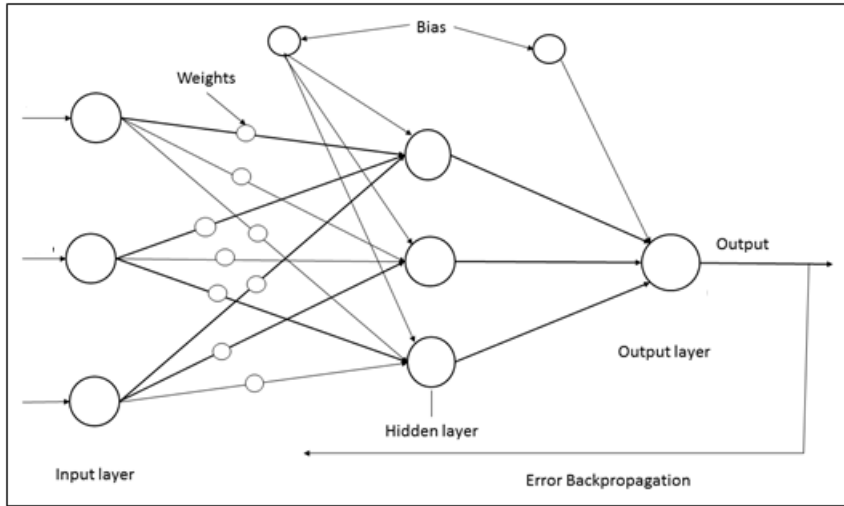


Fig 3.5 Architecture of FFBP neural network

The weights in the hidden and output layer neurons are calculated using Eqs. 3.21 and 3.22, respectively

$$w(N + 1) = w(N) - \eta \delta \phi \quad (3.21)$$

$$w(N + 1) = w(N) + \eta x \sum_{q=1}^r \delta_q \quad (3.22)$$

Where w is training weight, N is the number of iteration, x is input value, η is learning weight and ϕ is the output. δ is defined as $2\varepsilon_q \partial \phi / \partial I$, where I is the sum of the weighted inputs, q is neuron index of the output layer, and ε_q is error signal. The above training method is the standard back propagation training method. In the training process, estimated outputs are compared to the known outputs, then the errors occurred are back propagated to obtain the appropriate weight adjustments necessary in minimizing the errors. The neural network model stops iteration for training when the error becomes smaller than the target error. This error signal is propagated back and the weights are adjusted to reduce the difference between desired and computed outputs. The process of adjusting weights is continued until the required level of accuracy is obtained between target values and computed outputs. After learning, the

weights are frozen. Then a dataset that the ANN has not encountered before is presented to validate its performance. Depending on the outcome, the ANN has to be either retrained or can be implemented for its designated use.

3.4.2 Fuzzy Logic:

Fuzzy logic is a tool that is used to solve problems with imprecise parameters and insufficient information. Fuzzy sets are an aid in providing information in a more human comprehensible or natural form, and can handle uncertainties at various levels. In fuzzy systems, the knowledge can be captured in terms of rules and linguistic variables. The concepts and operational algorithms are given in many textbooks, for example Mukaidono (2001), Klir and Yuwan (1995), Trillas and Eciolaza (2015).

Fuzzy Logic Systems will differ from each other based on the rule types. Common one being “if situation then decision” rules, built by human operators’ experience and knowledge (Sugeno, 1985). This sort of rules conveys preference and helps to decide (Yager and Zadeh, 1992). Robustness of fuzzy control depends on expert’s knowledge coupled with the statistical properties of the empirical data (Kacprzyk and Pedrycz, 2015) .The development of a Fuzzy Logic System, according to the Mamdani model (Mamdani, 1974), requires following steps as shown in fig 3.6

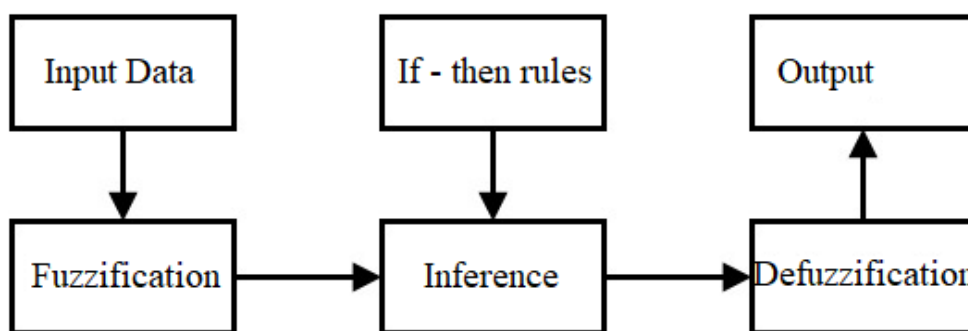


Fig 3.6 Simple architecture of Fuzzy logic model.

- i) Variables are “fuzzified” through the use of membership functions that define the membership degree to fuzzy sets. A fuzzy subset A of a universe of discourse U is characterized by a membership function $\mu_A(x)$, which associates each element $x \in U$, a membership $\mu_A(x)$ in the interval [0,1] that represents the grade of membership in A

(Sayed and Razavi, 2000). The key ideas are that fuzzy logic allows for something to be partly this and partly that, rather than having being either all this or all that; and that the degree of “belongingness” to a set or category can be described numerically by a membership number between 0 and 1. This transformation of real valued inputs into a degree of membership to a particular fuzzy set is called “fuzzification”.

ii) Rule evaluation. The fuzzified data are applied to the precedents of the fuzzy rules. If a given rule has different precedents, a unique number that represents the result of the precedents evaluation may be obtained by using the fuzzy operant AND and OR. This unique number is then exercised to the subsequent membership function.

iii) Aggregation. The fuzzy membership functions of all rule gains are consolidated into a single fuzzy set.

iv) Defuzzification. The cumulative output fuzzy set is transformed into a crisp value. For the defuzzification, many methods are there, but the most common is the centroid technique,

3.4.3 Adaptive Neuro-Fuzzy Inference System (ANFIS)

Jang (1993) proposed a method that used neural network learning algorithm for constructing a set of fuzzy if-then rules from stipulated input output pairs. Fundamentally, ANFIS is a functional equivalent of fuzzy inference systems endowed with neural learning capabilities. An ANFIS model combines the transparent and linguistic representation of a fuzzy system with learning ability of ANN. This allows them to be trained in performing input/output mapping as an ANN model. ANFIS comes with an additional benefit of being able to provide a set of rules on which the model is based.

Typically, ANFIS network architecture consists of five different layers (Figure.3.7). Each layer contains several nodes described by the node function. Let O_i^j denote the output of the i^{th} node in layer j .

Each node in Layer 1 is an adaptive node with node output defined as

$$O_i^1 = \mu A_i(x), \text{ for } i=1, 2, \dots \quad (3.23)$$

$$O_i^1 = \mu B_i(y), \text{ for } i=3, 4\dots \quad (3.24)$$

Where x (or y) is the input to the node; and A_i (or B_i) is a linguistic label associated with this node. The membership functions for A_i and B_i can be represented by various functions.

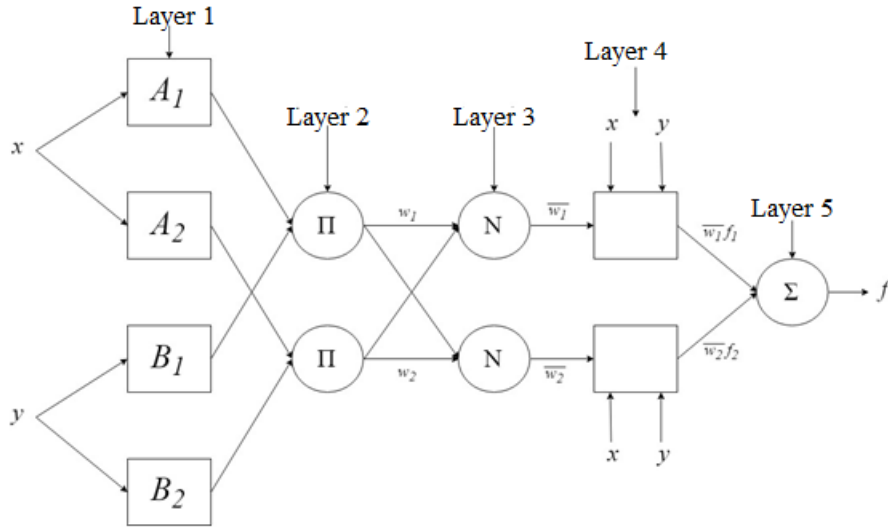


Figure. 3.7 Architecture of ANFIS model

In layer 2, each node Π multiplies incoming signal and output is the product of all the incoming signals.

$$O_i^2 = \omega_i = \mu A_i(x)\mu B_i(y), \text{ for } i=1,2\dots \quad (3.25)$$

Each node output represents the firing strength of a rule.

In layer 3, each node N calculates the ratio of the i^{th} rules firing strength to the sum of all rule's firing strengths.

$$O_i^3 = \bar{\omega}_i = \frac{\omega_i}{\omega_1 + \omega_2}, \text{ for } i=1, 2\dots \quad (3.26)$$

The normalized firing strengths are the output from this layer.

In layer 4, each node calculates the contribution of the i^{th} rule to the overall output

$$O_i^4 = \bar{\omega}_i f^i = \bar{\omega}_i (a_i x + b_i y + c_i), \text{ for } i=1,2\dots \quad (3.27)$$

Where $\bar{\omega}_i$ is the output of layer 3 and (a_i, b_i, c_i) is the parameter set. The parameter of this layer are known as consequent parameters.

In layer 5, the signal node calculates the final output as the summation of all input signals

$$O_i^5 = \text{overalloutput} = \sum \bar{\omega}_i f_i = \frac{\sum_i \omega_i f_i}{\sum_i \omega_i} \quad (3.28)$$

Thus, an adaptive network is functionally equivalent to a sugeno-type fuzzy inference system. In this study, Fuzzy c – means c lustering metod is used for ANFIS modeling algorithms. The purpose of clustering is to identify natural groupings of data from a large data set to produce a concise representation of a system's behavior.

Fuzzy c-means (FCM) is a data clustering technique in which a dataset is grouped into n clusters with every data point in the dataset belonging to every cluster to a certain degree. This method was developed by Dunn (1973) and improved by Bezdek (1981) and is frequently used in pattern recognition. For example, a certain data point that lies close to the center of a cluster will have a high degree of belonging or membership to that cluster and another datapoint that lies far away from the center of a cluster will have a low degree of belonging or membership to that cluster. The Fuzzy Logic Toolbox™ function fcm performs FCM clustering. It starts with an initial guess for the cluster centers, which are intended to mark the mean location of each cluster. The initial guess for these cluster centers is most likely incorrect. Next, fcm assigns every data point a membership grade for each cluster. By iteratively updating the cluster centers and the membership grades for each data point, fcm iteratively moves the cluster centers to the right location within a data set. This iteration is based on minimizing an objective function as presented in Zhang et al. (2008) that represent the distance from any given data point to a cluster center weighted by that data point's membership grade. To optimize the weighting exponent (m) in the FCM, genetic algorithms is used.

3.4.4 Support Vector Machine

The foundation of support vector machines (SVM) has been developed by Vapnik, (1995) and is gaining popularity due to many attractive features and promising

empirical performances. The formulation embodies structural risk minimization (SRM) principle, which has shown better performances than empirical risk minimization (ERM) which is employed by conventional neural networks. SRM minimizes an upper bound on the expected risk, as opposed to ERM that minimizes the error on the training data. It is this difference, which equips SVM with a greater ability to generalize, thus, achieving the goal of statistical learning. SVM comes with an advantage of using kernel trick to minimize both model complexities and prediction errors simultaneously. SVMs were initially developed to solve the classification problems, but recently they have been extended to the domain of regression problems. The procedure of support vector regression (SVR) is briefly discussed below

3.4.4.1 Support Vector Regression

The goal of a regression problem is by analyzing the input and their corresponding output values finding a function that describes the underlying relationship between them. This relationship may be assumed either linear or nonlinear. Once it is determined, using this relationship the output for any unseen data can be predicted.

For the given set of input samples $\{(x_i, y_i)\}_{i=1,2,\dots,m}$ in which $x \in R^n$ and $y \in R$, the linear support vector regression problem is the method in approximating the output $y \in R$ by a function $f(\cdot)$ of the form:

$$f(x) = w^T \cdot x + b \quad (3.29)$$

where $w \in R^n$ and $b \in R$ are obtained as the solution of the unconstrained minimization problem:

$$\min \frac{1}{2} \|w\|^2 + C X \frac{1}{m} \sum_{i=1}^m L(f(x_i)y_i) \quad (3.30)$$

where L is a loss function used for penalizing errors in prediction. The term $\frac{1}{m} \sum_{i=1}^m L(f(x_i)y_i)$, which is the average loss over the training samples, represents the empirical error or risk and $\frac{1}{2} \|w\|^2$ is the regularization term. Choosing higher values of C will increase the importance of the empirical risk relative to the regularization

term. Let us consider some of the popular loss functions namely quadratic, Huber and ϵ -insensitive error loss functions. The quadratic loss function is defined by:

$$L(f(x), y) = (f(x) - y)^2 \quad (3.31)$$

This is the conventional loss function used in least squares method. The Huber loss function is written as:

$$L(f(x), y) = \begin{cases} \frac{1}{2} (f(x) - y)^2 & \text{if } |f(x) - y| < \epsilon \\ \epsilon |f(x) - y| - \frac{\epsilon^2}{2}, & \text{otherwise} \end{cases} \quad (3.32)$$

Where ϵ is a parameter. Since the above two loss functions do not produce sparseness in the support vectors (Gunn, 1998; Vapnik, 1998) the ϵ -insensitive error loss function given by:

$$L(f(x), y) = \begin{cases} 0 & \text{if } |f(x) - y| < \epsilon \\ |f(x) - y| - \epsilon, & \text{otherwise,} \end{cases} \quad (3.33)$$

was introduced (Vapnik, 1998) as an approximation to Huber's loss function having sparseness property in the support vectors (Gunn, 1998). The support vector regression problem for linear function approximation with ϵ -insensitive error loss function will be defined as the following unconstrained minimization problem of the form (Vapnik, 1996; Gunn, 1998): *for* $(w, b) \in R^{n+1}$

$$\min \frac{1}{2} \|w\|^2 + C \sum_{i=1}^m |w^T \cdot x_i + b - y_i|_{\epsilon} \quad (3.34)$$

where, $|w^T \cdot x_i + b - y_i|_{\epsilon} = \max\{0, |w^T \cdot x_i + b - y_i| - \epsilon\}$ and $C > 0$ is a parameter.

The above problem can be reformulated as a constrained quadratic optimization problem (Lee et al., 2005) with parameters $C > 0$ and $\epsilon > 0$, defined by:

$$\text{for } (w, b, \xi, \xi^*) \in R^{N+1+2m} \min \frac{1}{2} w^T \cdot w + C \sum_{i=1}^m (\xi_i + \xi_i^*) \quad (3.35)$$

$$\text{subject to } \begin{cases} y_i - w^T \cdot x_i - b \leq \epsilon + \xi_i \\ w^T \cdot x_i - b - y_i \leq \epsilon + \xi_i^* \\ \text{and } \xi_i, \xi_i^* \geq 0 \quad \forall i = 1, 2, \dots, m \end{cases} \quad (3.36)$$

where, ξ_i, ξ_i^* are slack variables.

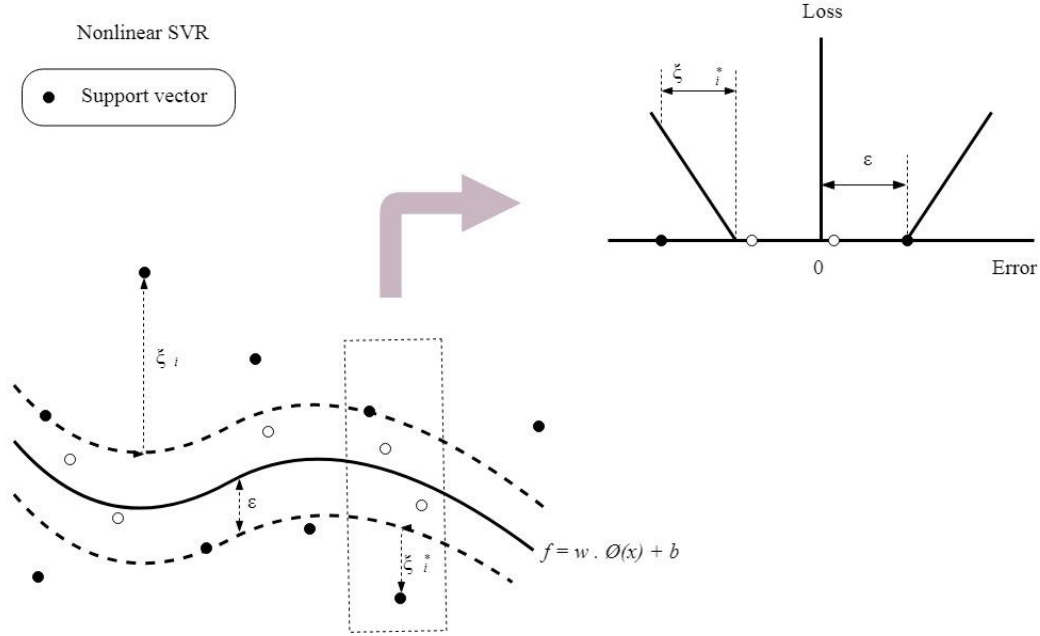


Fig 3.8 Nonlinear support vector regression with ϵ – insensitive loss function

For the nonlinear support vector regression model as depicted in fig 3.8, the input data is mapped into a higher dimensional feature space via a kernel function, $K(\cdot, \cdot)$ and the linear support vector regression is performed in the feature space. Typically let the input data be transformed into a higher dimensional feature space by the transformation $\phi = R^n \rightarrow R^N$ and let the support vector regression approximation function in the higher dimensional space be given by

$$f(x) = w^T \phi(x) + b \quad (3.37)$$

Then the SVR formulation can be written as a constrained optimization problem of the form:

$$\text{for } (w, b, \xi, \xi^*) \in R^{N+1+2m} \min \frac{1}{2} \|w\|^2 + C \sum_{i=1}^m (\xi_i + \xi_i^*) \quad (3.38)$$

$$\text{subject to } \begin{cases} y_i - w^T \cdot \phi(x_i) - b \leq \epsilon + \xi_i \\ w^T \cdot \phi(x_i) - b - y_i \leq \epsilon + \xi_i^* \\ \text{and } \xi_i, \xi_i^* \geq 0 \quad \forall i = 1, 2, \dots, m \end{cases} \quad (3.39)$$

Where, ξ_i, ξ_i^* are slack variables

3.4.5 Extreme Learning Machine:

Amongst various neural networks, feed forward neural network is favorite one for the researchers due to its inherent advantages such as capability of directly mapping complicated nonlinear data from input samples. Architecture of ELM model is given below in Fig 3.9.

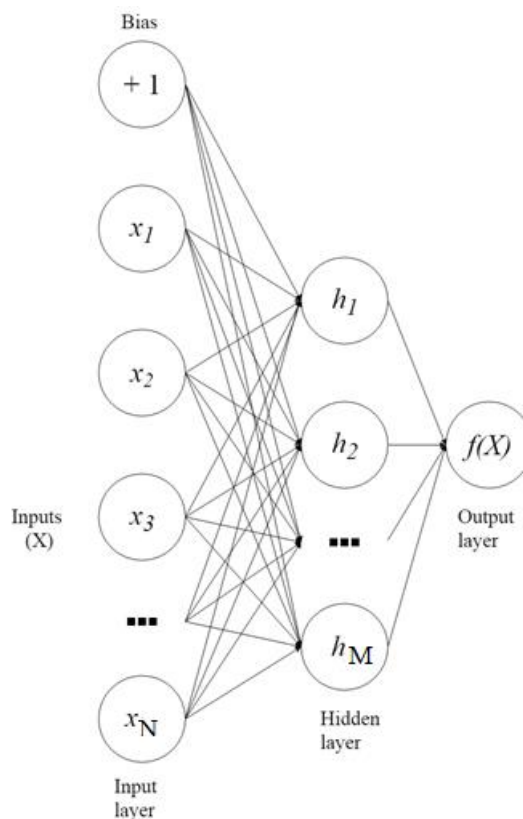


Fig 3.9 Architecture of ELM model

This network architecture has one input layer, one output layer and hidden layers (one or more). Extreme learning machine is learning algorithm for single layered feed forward network (SLFN) having multiple advantages such as high-speed learning, best generalization, and least error in training with smaller norm weights.

Extreme learning machine were originally proposed for SLFNs and then it was extended to the generalized SLFNs. Essentially ELM trains the SLFN in following stages first it maps the feature randomly and then tends to solve it for linear parameters. The weights are chosen randomly in ELM. Tamura and Tateishi (1997) and Huang (2004) found that SLFNs with randomly adopted input weights can

efficiently learn distinct training examples with minimum error. On choosing the input weights and hidden layer biases the SLFN can be considered as a linear system and the output weights analytically determined by simple generalized inverse operation of the hidden layer output matrices. This simplified approach makes ELM work faster than the feed forward algorithm.

The basic theory of ELM can be given as follows:

For N arbitrary distinct inputs (x_j, y_j) with $x_i \in \mathbb{R}^d$ with M hidden nodes and activation function f can be modeled as the following sum

$$\sum_{j=1}^M \beta_j f(w_j x_j + b_j), \mathbf{i} \in \{1, 2, \dots, N\} \quad (3.40)$$

Where w_j are the input weights to the j th neuron in the hidden layer, b_j the biases and β_j are the output weights. In the case where the SLFN would perfectly approximate the data, the relation is

$$\sum_{j=1}^M \beta_j f(w_j x_j + b_j) = y_i, \mathbf{i} \in \{1, 2, \dots, N\} \quad (3.41)$$

Which can compactly written as

$$H\beta = Y$$

Where H the hidden layer output matrix is defined as

$$\begin{pmatrix} f(w_1 x_1 + b_1) & \cdots & f(w_M x_1 + b_M) \\ \vdots & \ddots & \vdots \\ f(w_1 x_N + b_1) & \cdots & f(w_M x_N + b_M) \end{pmatrix} \quad (3.42)$$

$$\text{Where } \beta = (\beta_1 \dots \beta_M)^T \text{ and } Y = (y_1 \dots y_N)^T \quad (3.43)$$

Considering the randomly initialized first layer of the ELM and the training inputs, the hidden layer output matrix H can be computed. Given H and the target outputs, output weight β can be solved by finding the least square solution to the linear system defined by Eq. (3.42). This solution is given by $\beta = H^m Y$, where H^m is the Moore–Penrose generalized inverse of the matrix H . More details on the ELM algorithm can be found in the original paper (Huang et al., 2006).

3.5 SOIL DATA COLLECTION

Soil data collection in this study included the measurement carried out at three stations and three different depths under different land use and land cover. At each

station 100 sampling points and three depths (300 readings) so overall 900 sets of readings having estimated values of Saturated hydraulic conductivity, dry bulk density, particle density (G), sand, silt, clay, porosity and organic matter. For analysis purpose dataset was segregated station wise (College, Mulegaon and Punanaka) as well as depth wise (15cm, 30cm and 45cm). For each analysis, there were 300 data set. Eighteen (Six sets X three modeling techniques) models (Table 3.2) were developed using ANFIS, SVM and ELM.

Table 3.2 Various models proposed in the study

Dataset	MODEL		
	ANFIS	SVM	ELM
College	ANFIS – C	SVM – C	ELM – C
Mulegaon	ANFIS – M	SVM – M	ELM – M
Punanaka	ANFIS – P	SVM – P	ELM – P
15cm depth	ANFIS – 15	SVM – 15	ELM – 15
30cm depth	ANFIS – 30	SVM – 30	ELM – 30
45cm depth	ANFIS – 45	SVM – 45	ELM – 45

3.6 DATA PREPROCESSING:

Data set was tested for the normal distribution by using statistical techniques i.e. skewness as well as QQ plot and it was found that they are not normally distributed so in order to get normal distribution data were log transformed (Airmun and Amin., 2009; Hu et al., 2013). The QQ plot before transformation of data after transformation of data is shown in Fig 3.10. Each data set is then normalized between 0.05 - 0.95 by using min – max normalization. As the numerical values of parameters differs greatly with the output, normalized value x_{new} of any observed value x having its maximum value x_{max} and minimum value x_{min} is computed by using equation

$$x_{new} = 0.05 + 0.9 \left[\frac{x - x_{min}}{x_{max} - x_{min}} \right] \quad (3.44)$$

The output obtained by modeling technique is then denormalised by using

$$x = \frac{(x_{new} - 0.05)(x_{max} - x_{min})}{0.9} \quad (3.45)$$

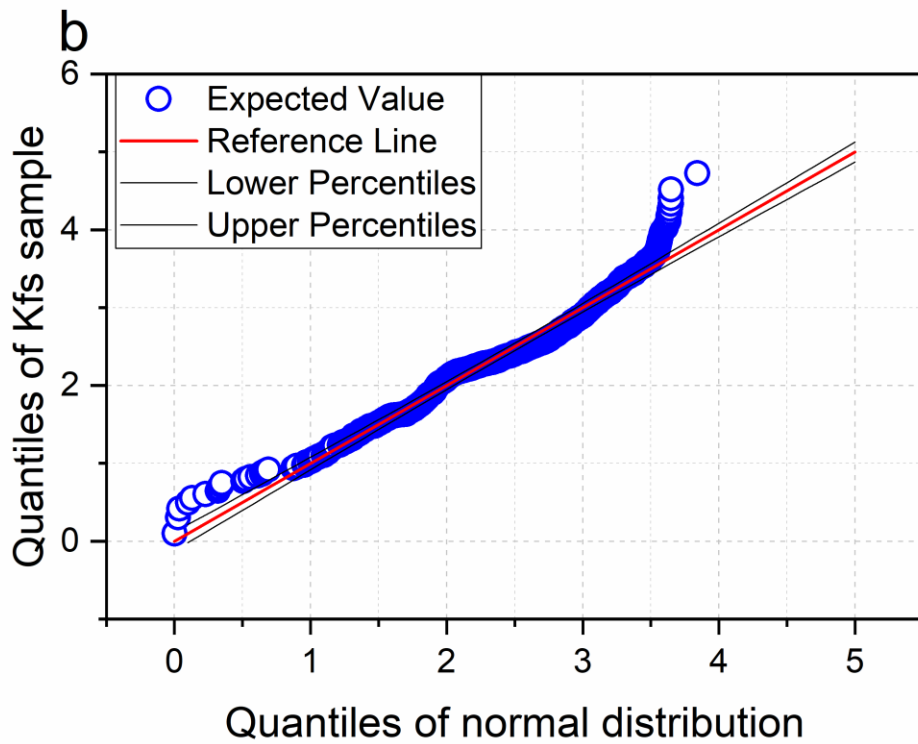
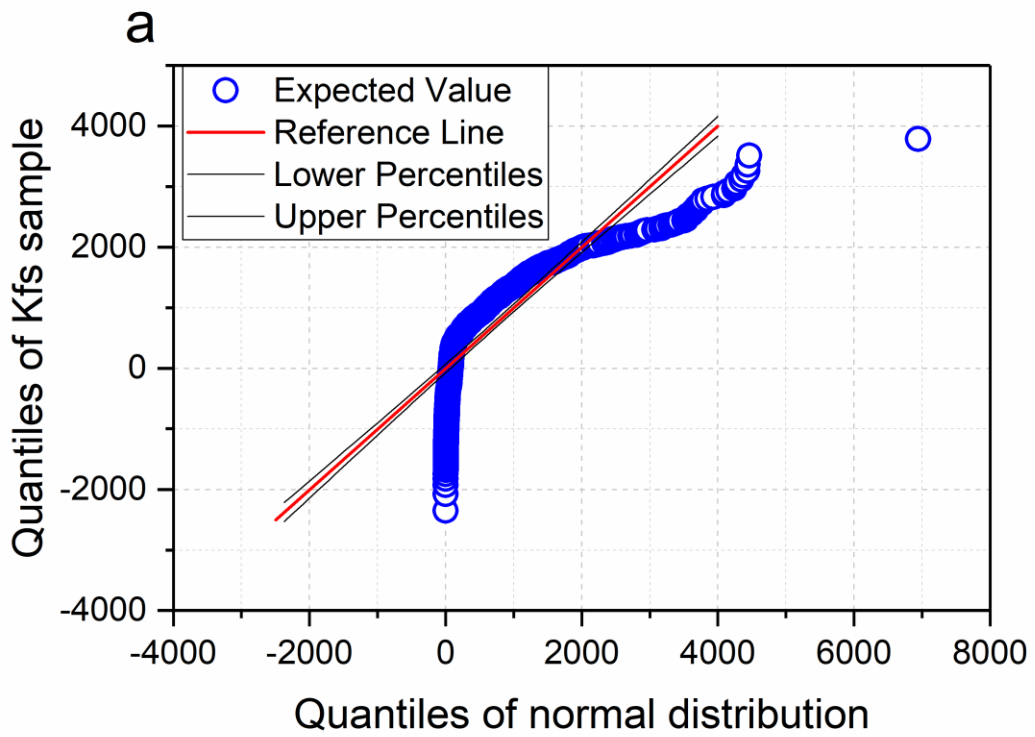


Fig 3.10 QQ Plot for saturated hydraulic conductivity. (a) before transformation and (b) After transformation

3.7 SELECTION OF INPUT PARAMETERS:

Based on the literature the possible factors affecting were assumed bulk density (BD), porosity(n) , sand% (S) , silt % (Si), clay % (C), Organic matter (OM). Amongst these parameters, most influential parameters were determined by using stepwise regression having significance at $P < 0.01$. The Input parameters selected for various sample dataset are as given in Table 3.3

Table 3.3 Input parameters selected based on stepwise regression for various dataset

S.N.	Dataset	Input parameters
1	College	Porosity (n), Sand % (S), clay % and bulk density (BD).
2	Mulegaon	Porosity (n), Sand % (S), clay % and bulk density (BD).
3	Punanaka	Porosity (n), Sand % (S), Silt % (Si) and bulk density (BD)
4	15cm depth	Porosity (n), Sand % (S), Silt % (Si) and bulk density (BD)
5	30cm depth	Porosity (n) and bulk density (BD)
6	45cm depth	Porosity (n), Sand % (S) and bulk density (BD)

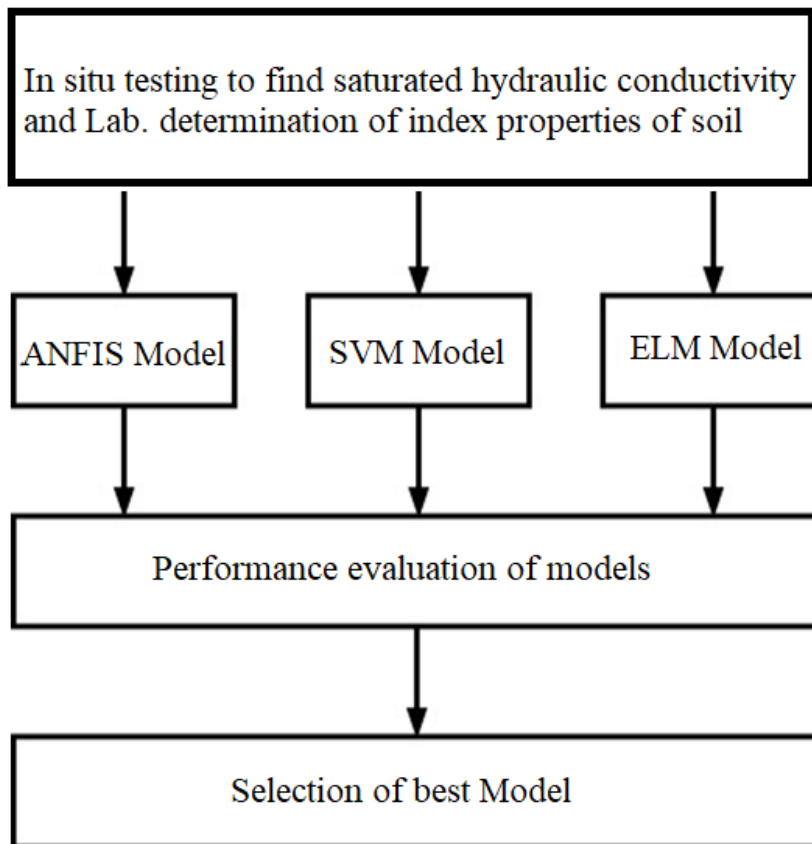


Figure 3.11 Flow chart of the methodology used in the study

In this study, an attempt is made to evaluate the performance of different soft computing models for estimating saturated hydraulic conductivity in Deccan trap (Solapur). The performance of ANFIS, SVM and ELM were compared by using statistical parameters and the best model is selected. Flow chart for the process involved in developing the model is presented in Figure 3.11. The results obtained from various models are discussed in subsequent chapters.

3.8 MODEL PERFORMANCE CRITERIA:

Performance measure metrics were calculated by using the parameters; O – observed value of parameter, P – predicted value of the parameter, O_{max} - maximum value of observed variable, used to assess the model O_{min} – minimum value of the observed variable, O_{avg} – average value of observed variable, and P_{avg} – average predicted value of variable N – number of observations.

3.8.1 Coefficient of correlation (R):

$$R = \frac{\sum_{i=1}^N (O_i - O_{avg})(P_i - P_{avg})}{\sqrt{\sum_{i=1}^N ((O_i - O_{avg}))^2} \sqrt{\sum_{i=1}^N (P_i - P_{avg})^2}} \quad (3.46)$$

Pearson (sample or product – moment) correlation coefficient (R) was introduced by Galton in 1877 and developed later by Pearson. It measures the strength and direction of the linear relation between variables. This is the best known and most commonly used type of correlation coefficient; its value can be anything in between – 1 to + 1. Correlation coefficient 0.9 to 1.0 is interpreted as very high correlation, 0.7 – 0.89 high correlations, 0.5 – 0.69 moderate correlations, 0.3 – 0.49 low correlation and < 0.3 as very low correlation.

A correlation of -1.0 indicates a perfect negative correlation (A change in the value of one variable predicts a change in the opposite direction in the second variable). A correlation of 1.0 indicates a perfect positive correlation (A change in the value of one variable will predict a change in the same direction in the second variable). A correlation of 0.0 indicates zero or no relationship between the two variables. Correlations may or may not indicate causal relations. Reversely, causal relations from some variable to another variable may or may not result in a correlation between the two variables. Correlations are very sensitive to outliers; a single unusual observation may have a huge impact on a correlation. Such outliers are easily detected by a quick inspection a scatterplot.

3.8.2 Root mean square error (RMSE)

$$RMSE = \sqrt{\frac{\sum_1^N (O-P)^2}{N}} \quad (3.47)$$

RMSE is the square root of the variance of the residuals. It indicates the absolute fit of the model to the data, i.e. how close the observed data points are to the models predicted value. Its unit is same as the unit of the variable thus can be better interpreted. Lower value of the RMSE is an indication of good model

3.8.3 Mean relative error (MRE)

$$MRE = \frac{1}{N} \sum_1^N \left(\frac{O-P}{O} \right) \quad (3.48)$$

It is the mean of error relative to the observed value of the parameter. This error is relative to the size of the item being measured. The relative error is very useful when we wish to compare things that are measured in different units. RE is expressed as a percentage and has no units. Its value close to zero indicates model is good

3.8.4 Normalized root mean square error (NRMSE)

$$NRMSE = \frac{RMSE}{O_{max} - O_{min}} \quad (3.49)$$

Normalizing the RMSE facilitates the comparison between datasets or models with different scales. Though there is no consistent means of normalization in the literature, common choices are the mean or the range (defined as the maximum value minus the minimum value) of the measured data, and often expressed as a percentage, where lower values indicate less residual variance

3.8.5 Nash–Sutcliffe model efficiency coefficient (NSE)

$$NSE = 1 - \left[\frac{\sum_1^N (O-P)^2}{\sum_1^N (O - O_{avg})^2} \right] \quad (3.50)$$

The Nash–Sutcliffe coefficient was used to access efficiency of the models.. NSE varies between $-\infty$ and 1. A value of 1 indicates a perfect agreement and a value of zero indicates that the model does not explain any part of the initial variance.

CHAPTER 4

RESULTS AND DISCUSSION

Results obtained from the field experimentation and various developed model has been analyzed and discussed here. In this part of the study, statistical analysis of various soil parameters, variability of soil parameters, textural distribution of soil, soil structure effect on saturated hydraulic conductivity, land use land cover effect on saturated hydraulic conductivity and performance analysis of ANFIS, SVM and ELM model is discussed.

4.1 STATISTICAL ANALYSIS:

Statistical analysis of the samples result tested in the laboratory and in the field is done for all samples (900), and subdivided samples for modeling purpose (College, Mulegaon, Punanaka, 15cm depth, 30cm depth and 45cm depth) to know the mean value, standard deviation, minimum and maximum value of each soil parameter being tested.

Maximum value of log saturated hydraulic conductivity (K_{fs}) was observed (Table 4. 1) at Punanaka (3.842 m yr^{-1}) and minimum value at College site (0.002 m yr^{-1}), standard deviation at college site was more (0.804) as compared to other two sampling stations i.e. 0.598 at Punanaka and 0.621 at Mulegaon.

Correlation coefficient of various soil parameters with the saturated hydraulic conductivity (logarithmic terms) is depicted in Table 4.2. Porosity shown strong influence with correlation coefficient of 0.9 as compared with other. It is obvious for more flow to take place through a porous media it should have more porosity. Next factor having its dominance in controlling K_{fs} is bulk density it has negative impact on K_{fs} with its maximum value of -0.90, density is mass per unit volume. More the density means more number of particles in a given volume thereby reducing the void space and hence conductivity. Other parameters have shown least correlation except sand content which is also positively correlated with the K_{fs} .

Table 4.1: Summary statistics of soil parameters samples at all three sites and all three depths (15cm, 30cm and 45cm)

		Mean	SD	Kurtosis	Skewness	Minimum	Maximum
CO		2.067	0.804	-0.505	-0.231	0.002	3.638
MU	Kfs(m yr ⁻¹)	2.576	0.621	-1.073	-0.167	0.506	3.647
PN		2.610	0.598	-0.575	-0.330	1.098	3.842
CO		1.622	0.073	-0.954	0.030	1.504	1.761
MU	Porosity (%)	1.668	0.053	-0.962	0.174	1.504	1.773
PN		1.699	0.055	-0.243	-0.292	1.517	1.786
CO		1.265	0.319	-0.453	0.458	0.699	1.944
MU	% sand	1.394	0.281	-0.600	0.636	0.778	1.944
PN		1.492	0.296	-1.043	0.000	0.845	1.940
CO		1.472	0.389	2.108	-1.296	0.000	1.924
MU	% clay	1.407	0.392	0.494	-0.904	0.000	1.914
PN		1.311	0.417	0.034	-0.690	0.000	1.914
CO		1.461	0.305	-0.495	-0.513	0.301	1.903
MU	% silt	1.440	0.313	1.448	-0.935	0.000	1.863
PN		1.415	0.306	1.473	-0.969	0.000	1.863
CO		3.152	0.044	-0.619	-0.785	3.053	3.203
MU	BD (kg.m ⁻³)	3.128	0.044	-1.443	-0.162	3.047	3.202
PN		3.099	0.040	-0.690	0.263	3.042	3.201
CO		0.923	0.287	20.751	-3.684	-1.495	1.174
MU	OM(g kg ⁻¹)	0.981	0.118	6.767	-1.589	0.273	1.144
PN		0.391	0.227	1.002	-1.085	-0.541	0.712
CO		0.396	0.015	-1.194	-0.362	0.370	0.427
MU	G	0.406	0.010	0.493	-0.155	0.369	0.437
PN		0.408	0.017	-1.007	0.561	0.372	0.452

All soil parameters are in logarithmic terms, CO – college site, MU – Mulegaon site & PN – Punanaka site

Table 4.2 Correlation coefficient of various soil parameters with saturated hydraulic conductivity sampled at college (CO), Mulegaon (MU) and Punanaka (PN)

	Kfs (m yr ⁻¹)	Porosity %	Sand %	Clay %	Silt %	BD (kg m ⁻³)	OM (g kg ⁻¹)	G
CO	1.00	0.90	0.76	-0.43	-0.14	-0.87	0.28	0.73
MU	1.00	0.88	0.58	-0.42	-0.28	-0.90	-0.05	0.23
PN	1.00	0.70	0.73	-0.59	-0.36	-0.71	0.10	0.58

All soil parameters are in logarithmic terms, CO – college site, MU – Mulegaon site & PN – Punanaka site

4.1.1 College site:

Maximum value of mean Kfs (2.883 m yr⁻¹) was observed at 15cm depth and minimum value of mean was 1.261 at 45cm depth (Table 4.3) Maximum standard deviation (0.601) was observed at 45 cm depth and minimum value of 0.344 was observed at 30cm depth in college.

Table 4.3. Summary statistics of soil parameters sampled at College site, (15cm, 30cm and 45cm depth)

		Mean	SD	Kurtosis	Skewness	Minimum	Maximum
CO15		2.883	0.379	0.709	-0.548	1.538	3.638
CO30	Kfs(m yr ⁻¹)	2.058	0.344	1.238	0.449	1.215	3.205
CO45		1.261	0.601	2.961	0.750	0.002	3.595
CO15		1.697	0.041	-1.383	-0.157	1.597	1.761
CO30	Porosity %	1.630	0.010	-0.318	-0.615	1.606	1.646
CO45		1.539	0.040	13.865	3.418	1.504	1.744
CO15		1.594	0.223	-1.159	0.246	1.041	1.940
CO30	% sand	1.528	0.282	-0.656	-0.514	0.699	1.919
CO45		0.972	0.204	8.070	2.312	0.699	1.944
CO15		1.244	0.448	0.817	-1.011	0.000	1.898
CO30	% clay	1.528	0.282	-0.656	-0.514	0.699	1.919
CO45		1.645	0.301	3.685	-1.654	0.301	1.924
CO15		CO15	0.000	1.378	0.301	0.052	-0.571
CO30	% silt	1.543	0.286	-0.180	-0.869	0.778	1.892
CO45		1.462	0.307	-1.134	-0.219	0.845	1.903
CO15		3.103	0.032	-0.961	0.393	3.053	3.186
CO30	BD (kg.m ⁻³)	1.543	0.286	-0.180	-0.869	0.778	1.892
CO45		3.192	0.021	27.810	-5.249	3.066	3.203
CO15		0.993	0.126	-0.895	-0.461	0.728	1.174
CO30	OM(g kg ⁻¹)	1.031	0.079	-1.037	-0.184	0.878	1.158
CO45		0.744	0.420	7.798	-2.273	-1.495	1.171
CO15		0.405	0.011	-1.520	0.031	0.390	0.427
CO30	G	0.405	0.003	-1.200	-0.007	0.400	0.410
CO45		0.378	0.011	4.411	2.314	0.370	0.417

All soil parameters are in logarithmic terms, CO – college site, MU – Mulegaon site & PN – Punanaka site

Table 4.4 Correlation coefficient of various soil parameters sampled at college (15cm, 30cm and 45cm depth).

	Kfs (m yr ⁻¹)	Porosity %	Sand %	Clay %	Silt %	BD (kg m ⁻³)	OM (g kg ⁻¹)	G
CO15	1.00	0.61	0.72	-0.48	-0.32	-0.63	-0.04	0.44
CO30	1.00	0.54	0.18	-0.06	0.16	-0.56	-0.11	-0.56
CO45	1.00	0.78	0.07	0.07	-0.09	-0.71	-0.02	0.66

All soil parameters are in logarithmic terms, CO – college site, MU – Mulegaon site & PN – Punanaka site

Positive skewness of 0.750 was observed at 45cm depth in college and negative skewness of 0.548. Minimum value of saturated hydraulic conductivity (0.002 myr^{-1}) was observed at 45cm depth. Porosity, sand content and bulk density have strong influence on the value of Kfs. Bulk density has negative correlation whereas porosity and sand has positive correlation as depicted in Table 4.4.

4.1.2 Mulegaon site

Table 4.5 Summary statistics of soil parameters, sampled at Mulegaon site (15cm, 30cm and 45cm depth)

		Mean	SD	Kurtosis	Skewness	Minimum	Maximum
MU15		2.937	0.475	0.782	-0.995	1.510	3.647
MU30	Kfs(m yr^{-1})	2.824	0.466	0.672	-0.818	1.262	3.631
MU45		1.966	0.390	7.735	1.781	0.506	3.641
MU15		1.707	0.047	-0.022	-0.819	1.548	1.760
MU30	Porosity %	1.678	0.040	0.533	-0.470	1.528	1.739
MU45		1.619	0.030	17.765	2.917	1.504	1.773
MU15		1.646	0.256	-0.883	-0.467	1.041	1.944
MU30	% sand	1.341	0.201	1.961	0.701	0.903	1.944
MU45		1.194	0.157	7.173	2.074	0.778	1.934
MU15		1.126	0.414	-0.278	-0.229	0.000	1.863
MU30	% clay	1.523	0.303	1.774	-1.186	0.301	1.908
MU45		1.571	0.281	2.557	-1.131	0.301	1.914
MU15		1.340	0.348	1.576	-0.923	0.000	1.863
MU30	% silt	1.472	0.276	1.969	-1.008	0.301	1.851
MU45		1.509	0.287	-0.601	-0.610	0.699	1.857
MU15		3.095	0.036	-0.290	0.828	3.054	3.189
MU30	BD (kg.m^{-3})	3.118	0.032	-0.703	0.493	3.070	3.196
MU45		3.172	0.023	21.727	-4.435	3.047	3.202
MU15		0.993	0.102	-1.154	-0.293	0.785	1.144
MU30	OM(g kg^{-1})	0.977	0.095	-0.973	-0.015	0.788	1.144
MU45		0.972	0.150	7.438	-2.186	0.273	1.141
MU15		0.409	0.012	-1.201	-0.354	0.378	0.426
MU30	G	0.401	0.009	-0.491	0.041	0.374	0.417
MU45		0.407	0.006	26.964	-0.718	0.369	0.437

All soil parameters are in logarithmic terms, CO – college site, MU – Mulegaon site & PN – Punanaka site

Mean Kfs was found more (2.937) at 15cm depth (Table 4.5) as compared to 30cm and 45cm depth. Influence of porosity (positive) and that of bulk density (negative) were found predominant (Table 4.6). Sand content had control over Kfs only at 15cm

depth and its effect at 30cm depth and 45 cm depth was insignificant as at larger depth texture of soil becomes finer.

Table 4.6 Correlation coefficient of various soil parameters sampled at Mulegaon site (15cm, 30cm and 45cm depth)

	Kfs (m yr ⁻¹)	Porosity %	Sand %	Clay %	Silt %	BD (kg m ⁻³)	OM (g kg ⁻¹)	G
MU15	1.00	0.86	0.87	-0.62	-0.48	-0.88	0.02	0.63
MU30	1.00	0.77	0.02	-0.01	-0.05	-0.80	0.09	0.18
MU45	1.00	0.69	-0.04	-0.07	-0.06	-0.74	-0.43	0.42

All soil parameters are in logarithmic terms, CO – college site, MU – Mulegaon site & PN – Punanaka site

4.1.3 Punanaka site

Table 4.7 Summary statistics of soil parameters sampled at Punanaka site (15cm, 30cm and 45cm depth)

	Mean	SD	Kurtosis	Skewness	Minimum	Maximum
PN15	3.161	0.296	1.067	-0.393	1.996	3.842
PN30	Kfs(m yr ⁻¹)	2.320	0.493	0.517	0.130	3.649
PN45		2.333	0.540	-0.841	-0.324	3.268
PN15		1.760	0.023	8.889	-2.795	1.786
PN30	Porosity %	1.687	0.030	-0.564	0.057	1.749
PN45		1.649	0.038	2.756	-1.566	1.720
PN15		1.785	0.162	-0.037	-1.049	1.940
PN30	% sand	1.350	0.234	0.125	0.359	1.898
PN45		1.338	0.230	0.197	0.395	1.898
PN15		0.981	0.406	-0.065	-0.152	1.857
PN30	% clay	1.471	0.312	0.190	-0.744	1.914
PN45		1.487	0.312	0.315	-0.808	1.914
PN15		1.224	0.317	2.023	-1.022	1.740
PN30	% silt	1.513	0.245	-0.288	-0.737	1.863
PN45		1.502	0.258	0.115	-0.834	1.863
PN15		3.055	0.016	9.650	2.941	3.135
PN30	BD (kg.m ⁻³)	3.108	0.022	0.288	0.417	3.187
PN45		3.136	0.027	-0.067	0.778	3.201
PN15		0.450	0.082	0.501	0.119	0.655
PN30	OM(g kg ⁻¹)	0.585	0.086	22.112	-3.638	0.712
PN45		0.140	0.190	1.343	-0.791	0.574
PN15		0.428	0.011	2.883	-1.368	0.452
PN30	G	0.399	0.009	-0.839	0.742	0.419
PN45		0.395	0.007	1.965	-0.376	0.410

All soil parameters are in logarithmic terms,

Mean value, maximum value and minimum value of saturated hydraulic conductivity at 30cm and 45 cm depth was found roughly same (Table 4.7) in the logarithmic scale. The Pearson correlation coefficient of index properties of soil with saturated hydraulic conductivity is shown in Table 4.8. At 15 cm depth, Soil texture has shown strong influence in controlling the value of Kfs. Sand content has dominated over all other parameter with correlation coefficient of 0.57, followed by silt content (-0.48) and then clay content (-0.44) whereas at 45cm depth, porosity, sand, clay and bulk density has shown strong influence.

Table 4.8 Correlation coefficient of various soil parameters sampled at Punanaka site (15cm, 30cm and 45cm depth)

	Kfs (m yr ⁻¹)	Porosity %	Sand %	Clay %	Silt %	BD (kg m ⁻³)	OM (g kg ⁻¹)	G
PN15	1.00	0.12	0.57	-0.44	-0.48	-0.10	0.01	0.14
PN30	1.00	0.31	0.07	-0.12	-0.03	-0.32	-0.07	0.15
PN45	1.00	0.71	0.92	-0.57	0.04	-0.71	-0.05	-0.13

All soil parameters are in logarithmic terms,

4.1.4 At 15 cm depth

Table 4.9 Correlation coefficient of various soil parameters sampled at 15 cm depth in college site, Mulegaon site and Punanaka site with saturated hydraulic conductivity.

	Kfs (m yr ⁻¹)	Porosity %	Sand %	Clay %	Silt %	BD (kg m ⁻³)	OM (g kg ⁻¹)	G
CO15	1.00	0.61	0.72	-0.48	-0.32	-0.63	-0.04	0.44
MU15	1.00	0.86	0.87	-0.62	-0.48	-0.88	0.02	0.63
PN15	1.00	0.12	0.57	-0.44	-0.48	-0.10	0.01	0.14

All soil parameters are in logarithmic terms

Saturated hydraulic conductivity at 15cm depth (Table 4.9) is found to be regulated by porosity, sand, clay, and silt content, however bulk density found influencing at college and Mulegaon but at Punanaka, it has no control over Kfs its correlation was very poor amounting 0.01. Clay content also has shown negative correlation with saturated hydraulic conductivity at all three stations. Range of Kfs at all three locations (maximum – minimum) was more or less same (Table 4.10). Standard deviation was found more at Mulegaon (0.475) as compared to other sites, and average value of Kfs (3.161m yr⁻¹) was found more at 15cm depth in Punanaka site.

Table 4.10 Summary statistics of soil parameters at 15cm depth sampled at College site, Mulegaon site and Punanaka site

		Mean	SD	Kurtosis	Skewness	Minimum	Maximum
CO15		2.883	0.379	0.709	-0.548	1.538	3.638
MU15	Kfs(m yr ⁻¹)	2.937	0.475	0.782	-0.995	1.510	3.647
PN15		3.161	0.296	1.067	-0.393	1.996	3.842
CO15		1.697	0.041	-1.383	-0.157	1.597	1.761
MU15	Porosity (%)	1.707	0.047	-0.022	-0.819	1.548	1.760
PN15		1.760	0.023	8.889	-2.795	1.655	1.786
CO15		1.594	0.223	-1.159	0.246	1.041	1.940
MU15	% sand	1.646	0.256	-0.883	-0.467	1.041	1.944
PN15		1.785	0.162	-0.037	-1.049	1.230	1.940
CO15		1.244	0.448	0.817	-1.011	0.000	1.898
MU15	% clay	1.126	0.414	-0.278	-0.229	0.000	1.863
PN15		0.981	0.406	-0.065	-0.152	0.000	1.857
CO15		1.378	0.301	0.052	-0.571	0.301	1.813
MU15	% silt	1.340	0.348	1.576	-0.923	0.000	1.863
PN15		1.224	0.317	2.023	-1.022	0.000	1.740
CO15		3.103	0.032	-0.961	0.393	3.053	3.186
MU15	BD (kg.m ⁻³)	3.095	0.036	-0.290	0.828	3.054	3.189
PN15		3.055	0.016	9.650	2.941	3.042	3.135
CO15		0.993	0.126	-0.895	-0.461	0.728	1.174
MU15	OM(g kg ⁻¹)	0.993	0.102	-1.154	-0.293	0.785	1.144
PN15		0.450	0.082	0.501	0.119	0.258	0.655
CO15		0.405	0.011	-1.520	0.031	0.390	0.427
MU15	G	0.409	0.012	-1.201	-0.354	0.378	0.426
PN15		0.428	0.011	2.883	-1.368	0.390	0.452

All soil parameters are in logarithmic terms, CO – college site, MU – Mulegaon site & PN – Punanaka site

4.1.5: At 30cm depth

Statistical summary of soil parameters sampled at 30cm depth in college, Mulegaon and Punanaka site is shown in Table 4.11. Maximum value of Kfs was found at Punanaka site (3.649) slightly bigger in logarithmic scale than Mulegaon site (3.631). Kurtosis at college site (30cm) was found more than other two locations. Average saturated hydraulic conductivity was more at Mulegaon site (2.824). Sand texture has insignificant control over saturated hydraulic conductivity as depicted in Table 4.12. Only porosity and bulk density has shown strong positive and negative correlation.

Table 4.11 Summary statistics of soil parameters sampled at 30 cm depth sampled at College site, Mulegaon site and Punanaka site

		Mean	SD	Kurtosis	Skewness	Minimum	Maximum
CO30		2.058	0.344	1.238	0.449	1.215	3.205
MU30	Kfs(m yr ⁻¹)	2.824	0.466	0.672	-0.818	1.262	3.631
PN30		2.320	0.493	0.517	0.130	1.112	3.649
CO30		1.630	0.010	-0.318	-0.615	1.606	1.646
MU30	Porosity %	1.678	0.040	0.533	-0.470	1.528	1.739
PN30		1.687	0.030	-0.564	0.057	1.595	1.749
CO30		1.229	0.137	4.213	0.665	0.903	1.869
MU30	% sand	1.341	0.201	1.961	0.701	0.903	1.944
PN30		1.350	0.234	0.125	0.359	0.845	1.898
CO30		1.528	0.282	-0.656	-0.514	0.699	1.919
MU30	% clay	1.523	0.303	1.774	-1.186	0.301	1.908
PN30		1.471	0.312	0.190	-0.744	0.477	1.914
CO30		1.543	0.286	-0.180	-0.869	0.778	1.892
MU30	% silt	1.472	0.276	1.969	-1.008	0.301	1.851
PN30		1.513	0.245	-0.288	-0.737	0.778	1.863
CO30		3.163	0.010	-0.701	0.343	3.146	3.184
MU30	BD (kg.m ⁻³)	3.118	0.032	-0.703	0.493	3.070	3.196
PN30		3.108	0.022	0.288	0.417	3.062	3.187
CO30		1.031	0.079	-1.037	-0.184	0.878	1.158
MU30	OM(g kg ⁻¹)	0.977	0.095	-0.973	-0.015	0.788	1.144
PN30		0.585	0.086	22.112	-3.638	-0.001	0.712
CO30		0.405	0.003	-1.200	-0.007	0.400	0.410
MU30	G	0.401	0.009	-0.491	0.041	0.374	0.417
PN30		0.399	0.009	-0.839	0.742	0.389	0.419

All soil parameters are in logarithmic terms, C30 – College site at 30cm depth, M30 – Mulegaon site at 30cm depth and P30 – Punanaka site at 30cm depth.

Table 4.12 Correlation coefficient of various soil parameters sampled at 30cm depth in college site, Mulegaon site and Punanaka site with saturated hydraulic conductivity.

	Kfs (m yr ⁻¹)	Porosity %	Sand %	Clay %	Silt %	BD (kg m ⁻³)	OM (g kg ⁻¹)	G
CO30	1.00	0.54	0.18	-0.06	0.16	-0.56	-0.11	-0.56
MU30	1.00	0.77	0.02	-0.01	-0.05	-0.80	0.09	0.18
PN30	1.00	0.31	0.07	-0.12	-0.03	-0.32	-0.07	0.15

All soil parameters are in logarithmic terms, C30 – College site at 30cm depth, M30 – Mulegaon site at 30cm depth and P30 – Punanaka site at 30cm depth

4.1.6: At 45 cm depth

Minimum value of saturated hydraulic conductivity (0.002) was found at college site and large value (0.601) of standard deviation. Least value at college site was due to predominance of fine texture soil at 45 cm depth at college site - soil texture found decreasing with depth. (Table 4.13).

Table 4.13 Summary statistics of soil parameters 45 cm sampled at College site, Mulegaon site and Punanaka site

		Mean	SD	Kurtosis	Skewness	Minimum	Maximum
CO45		1.261	0.601	2.961	0.750	0.002	3.595
MU45	Kfs(m yr ⁻¹)	1.966	0.390	7.735	1.781	0.506	3.641
PN45		2.333	0.540	-0.841	-0.324	1.098	3.268
CO45		1.539	0.040	13.865	3.418	1.504	1.744
MU45	Porosity %	1.619	0.030	17.765	2.917	1.504	1.773
PN45		1.649	0.038	2.756	-1.566	1.517	1.720
CO45		0.972	0.204	8.070	2.312	0.699	1.944
MU45	% sand	1.194	0.157	7.173	2.074	0.778	1.934
PN45		1.338	0.230	0.197	0.395	0.845	1.898
CO45		1.645	0.301	3.685	-1.654	0.301	1.924
MU45	% clay	1.571	0.281	2.557	-1.131	0.301	1.914
PN45		1.487	0.312	0.315	-0.808	0.477	1.914
CO45		1.462	0.307	-1.134	-0.219	0.845	1.903
MU45	% silt	1.509	0.287	-0.601	-0.610	0.699	1.857
PN45		1.502	0.258	0.115	-0.834	0.699	1.863
CO45		3.192	0.021	27.810	-5.249	3.066	3.203
MU45	BD (kg.m ⁻³)	3.172	0.023	21.727	-4.435	3.047	3.202
PN45		3.136	0.027	-0.067	0.778	3.087	3.201
CO45		0.744	0.420	7.798	-2.273	-1.495	1.171
MU45	OM(g kg ⁻¹)	0.972	0.150	7.438	-2.186	0.273	1.141
PN45		0.140	0.190	1.343	-0.791	-0.541	0.574
CO45		0.378	0.011	4.411	2.314	0.370	0.417
MU45	G	0.407	0.006	26.964	-0.718	0.369	0.437
PN45		0.395	0.007	1.965	-0.376	0.372	0.410

All soil parameters are in logarithmic terms, CO45 – College site at 45cm depth, MU45 – Mulegaon site at 45cm depth and PN45 – Punanaka site at 15cm depth.

The Pearson's correlation coefficient for soil parameters samples at 45cm depth in various sites is as shown in Table 4.13. Bulk density has strong negative correlation (~ -0.7) and porosity has shown strong positive correlation (~ 0.7). Soil texture failed to hold its control on Kfs except at Punanaka station. This indicates some extrinsic factors might be influencing Kfs value.

Table 4.14 Correlation coefficient of various soil parameters sampled at 45cm depth in college site, Mulegaon site and Punanaka site with saturated hydraulic conductivity.

	Kfs (m yr ⁻¹)	Porosity %	Sand %	Clay %	Silt %	BD (kg m ⁻³)	OM (g kg ⁻¹)	G
CO45	1.00	0.78	0.07	0.07	-0.09	-0.71	-0.02	0.66
MU45	1.00	0.69	-0.04	-0.07	-0.06	-0.74	-0.43	0.42
PN45	1.00	0.71	0.92	-0.57	0.04	-0.71	-0.05	-0.13

All soil parameters are in logarithmic terms, CO45 – College site at 45cm depth, MU45 – Mulegaon site at 45cm depth PN45 – Punanaka site at 45cm depth,

4.2 VARIABILITY OF SOIL PARAMETERS

Coefficient of variation of Kfs in logarithmic scale (Fig 4.1) is 40% at college, which is higher than its variation at remaining two sampling location. Organic matter content (OM) has shown large coefficient of variation amounting nearly 60% at Punanaka site and has least variation at Mulegaon site; which is due to difference in land use at these sites Mulegaon being agricultural land sampled during fallow period and Punanaka is open bare land. Variability of porosity, bulk density and specific gravity in logarithmic scale was found insignificant at all three depths (Fig 4.2, Fig 4.3 and Fig 4.4).

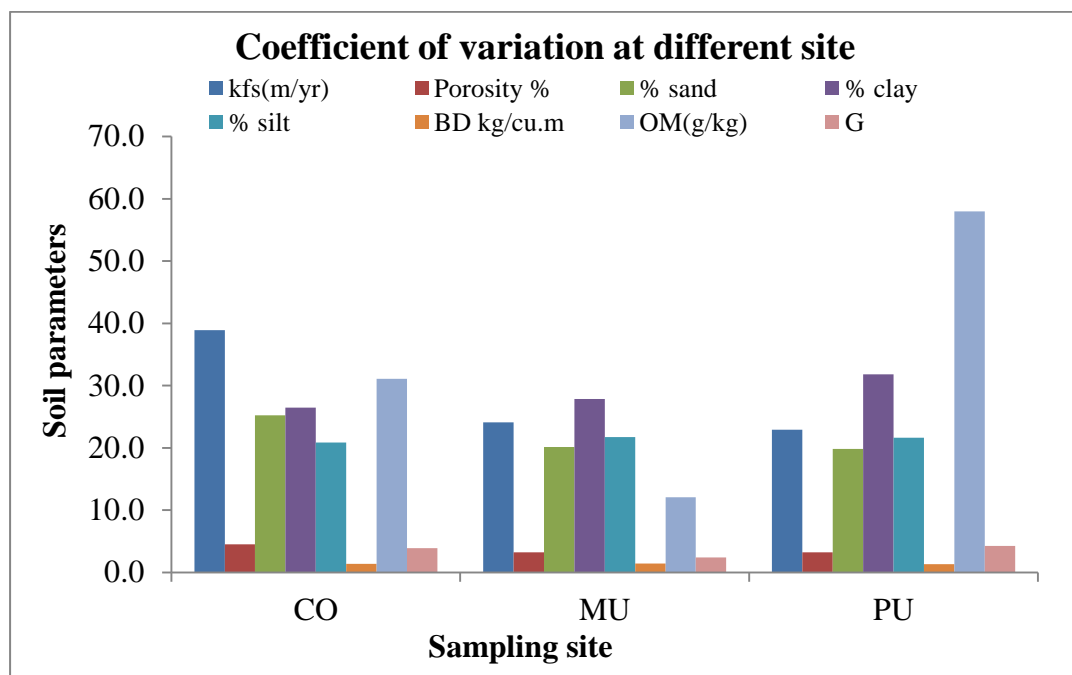


Fig 4.1 Coefficient of variation in percentage of various soil parameters sampled at three sites.

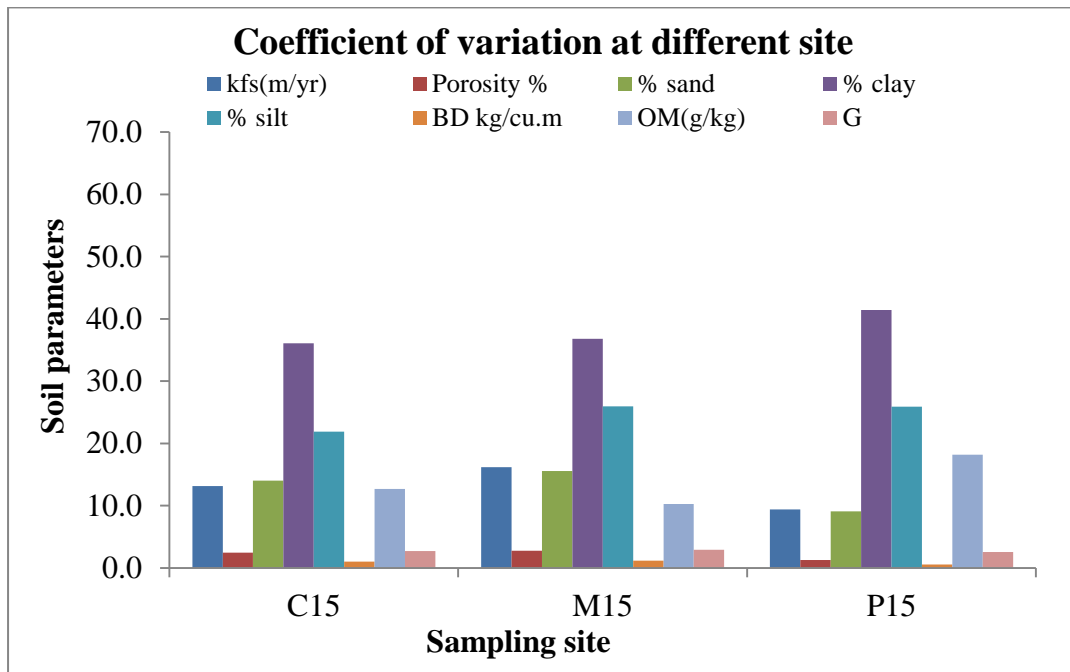


Fig 4.2 Variation of coefficient of variation of soil parameters sampled and tested at (15cm depth) all three sampling locations.

Variability of clay is dominant (~ 40%) at 15cm depth, in all locations. (Fig 4.2). Variability of most of the parameters was between 10% - 20% at 30cm depth (Fig 4.3) and variability of the organic matter (OM) was found very large at College and Punanaka (~ 60% – 70%) which implies amount of organic matter was not uniformly spread in the college site and Punanaka site which is attributed to land use and land cover effect.

Variability of Kfs was found more at college site at a depth of 45cm (Fig 4.4) as compared to that at Mulegaon and Punanaka at same depth indicating resistance offered by soil to flow through it is uniform at Mulegaon and Punanaka whereas at college site it is not uniform may be due to heterogeneity of pores and their interconnectivity.

Maximum value of Kfs was found at Punanaka site as compared to that at other two sites which can be attributed to macro holes due to earthworm, biological activities, it being a bare land receives less disturbance due to men and animals thus its structure pores, and pore connectivity will remain intact.

Minimum value of Kfs was observed at college site, as this site a pasture land and is dominated by clay texture. The reason for this can be more intervention by cattles and

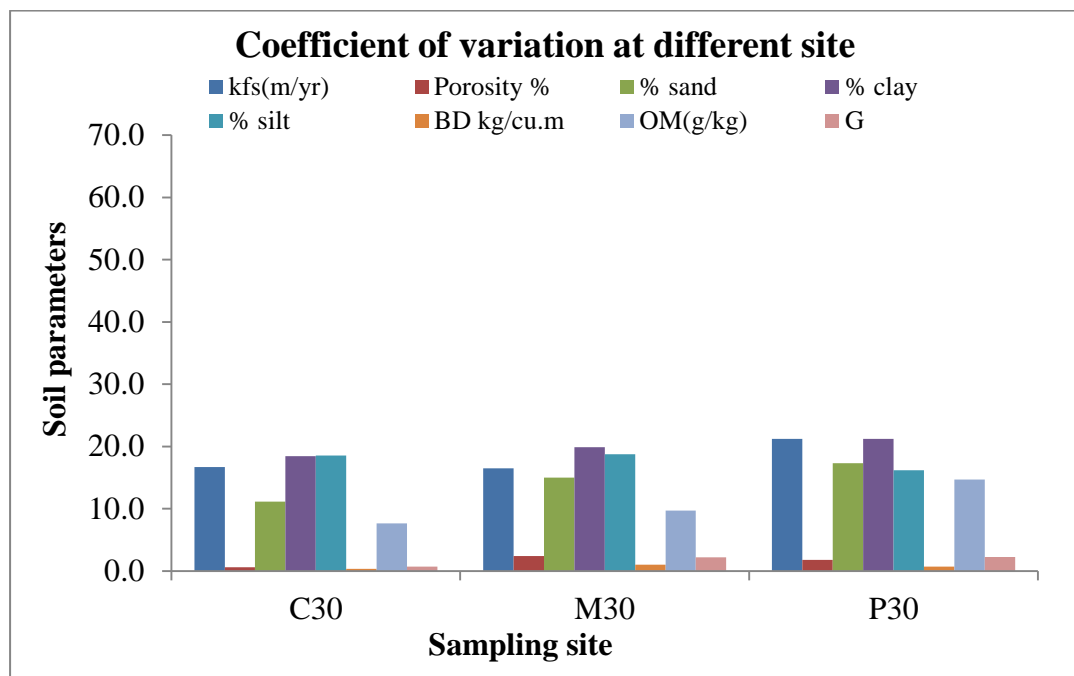


Fig 4.3 Variation of coefficient of variation of soil parameters sampled and tested at (30cm depth) all three sampling locations.

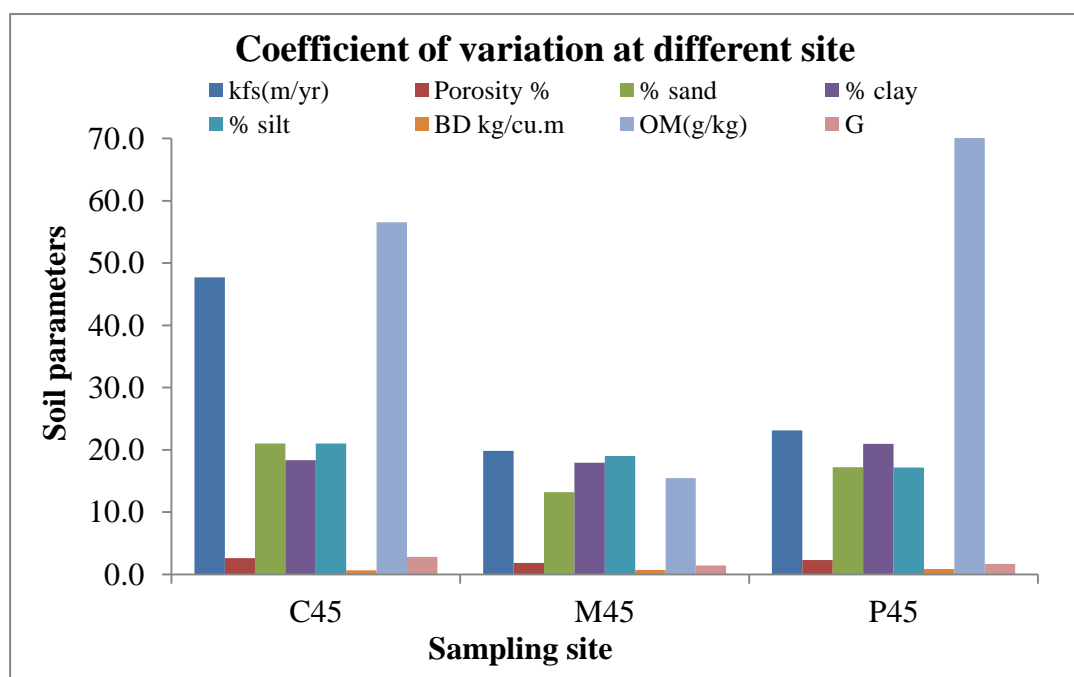


Fig 4.4 Variation of coefficient of variation of soil parameters sampled and tested at (45cm depth) all three sampling locations.

human beings, having more repetitive movement for grazing purpose thus by pores and pore connectivity will get blocked by compaction.

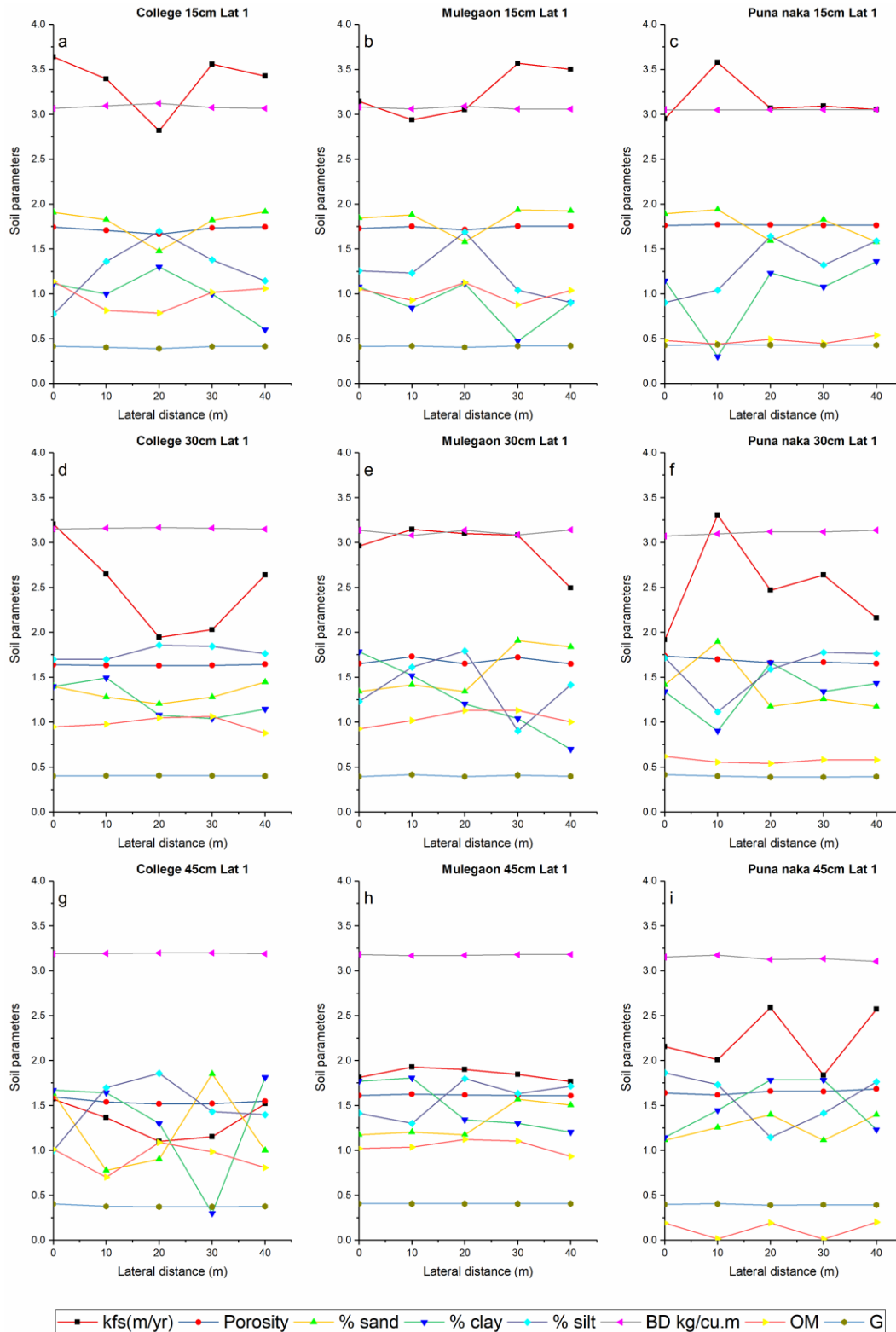


Fig 4.5 Variations of soil parameters along lateral direction at lateral 1 in college, Mulegaon and Punanaka site, at 15cm depth, 30cm depth and 45cm depth.

Variation in Porosity, bulk density and specific gravity of the soil at all three depths and along all lateral in all three sampling station was found to be insignificant. In general hydraulic conductivity was found declining with depth. Kfs was found declining towards centre at all depth and then again rising towards edge in college site at lateral 1 (Fig 4.5 a, d and g). Possible reason for which is topography of the ground at this location i.e. depression towards centre from either side. Mulegaon site has not shown any trend in the variation of Kfs along the lateral direction. Its trend is similar to that of variation of sand quantity at all three depths implying heterogeneity of soil and sand content controlling the Kfs. (fig 4.5 b, e, h). Punanaka also has not shown any trend. It is random variation reflecting heterogeneity of soil texture and structure caused by non-uniform compaction resulting from anthropogenic activity of floating population during their temporary stay in the bare land. Texture of soil has influence on Kfs at this site i.e. Sand content (Fig 4.5c, f and i) has shown positive trend with Kfs and clay content has negative impact on kfs.

The variation of Kfs in college at lateral 2 as depicted in Fig 4.6a, Fig 4.6d and Fig 4.6g ; was found similar to that at lateral 1, at all three depths, it was more at the edges and decreases towards centre. Sand content in the soil has similar kind of trend at 15cm and 30cm depth, but at 45cm it was different not following the trend of kfs. The reason being at 45cm depth amount of sand content was less as soil texture found decreasing with depth. There is no well-defined trend of soil texture at all three depths thus by indicating randomness in the variation. Changes in Kfs in Mulegaon and Punanaka (Fig 4.6) with respect to depth was found haphazard except at 45cm depth in Mulegaon. Here it was found uniform implying resistance to flow of water at 45 cm depth is same may be due to similar pore structure and there connectivity. Sand followed similar trend to that of Kfs thus is one of an important parameter controlling the Kfs at Mulegaon and Punanaka.

Bulk density, porosity and specific gravity have very negligible variability in the logarithmic scale at all stations and all depths (Fig 4.7). Variability of Kfs was found more at 45cm depth in college (Fig 4.7g), at 30cm depth in Mulegaon (Fig 4.7e) and 45cm depth in Punanaka (Fig 4.7i), which can be attributed to nonuniform compaction,

human intervention, cattles trampling, biological factors (wormholes, root holes etc.). Variation of all soil parameters found to be zigzag barring few soil parameters such as porosity bulk, density and specific gravity.

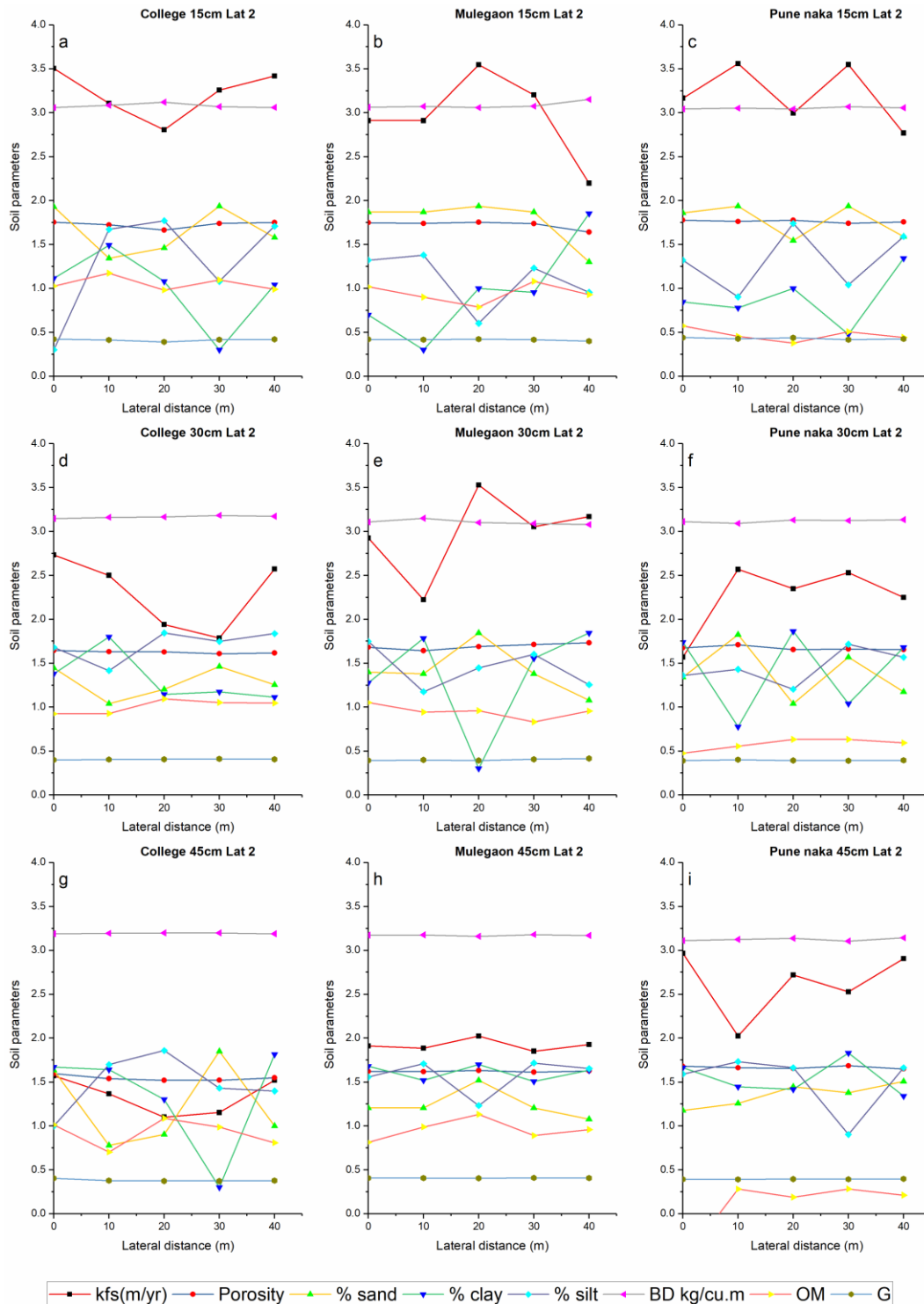


Fig 4.6 Variations of soil parameters along lateral direction at lateral 2 in college, Mulegaon and Punanaka site, at 15cm depth, 30cm depth and 45cm depth.

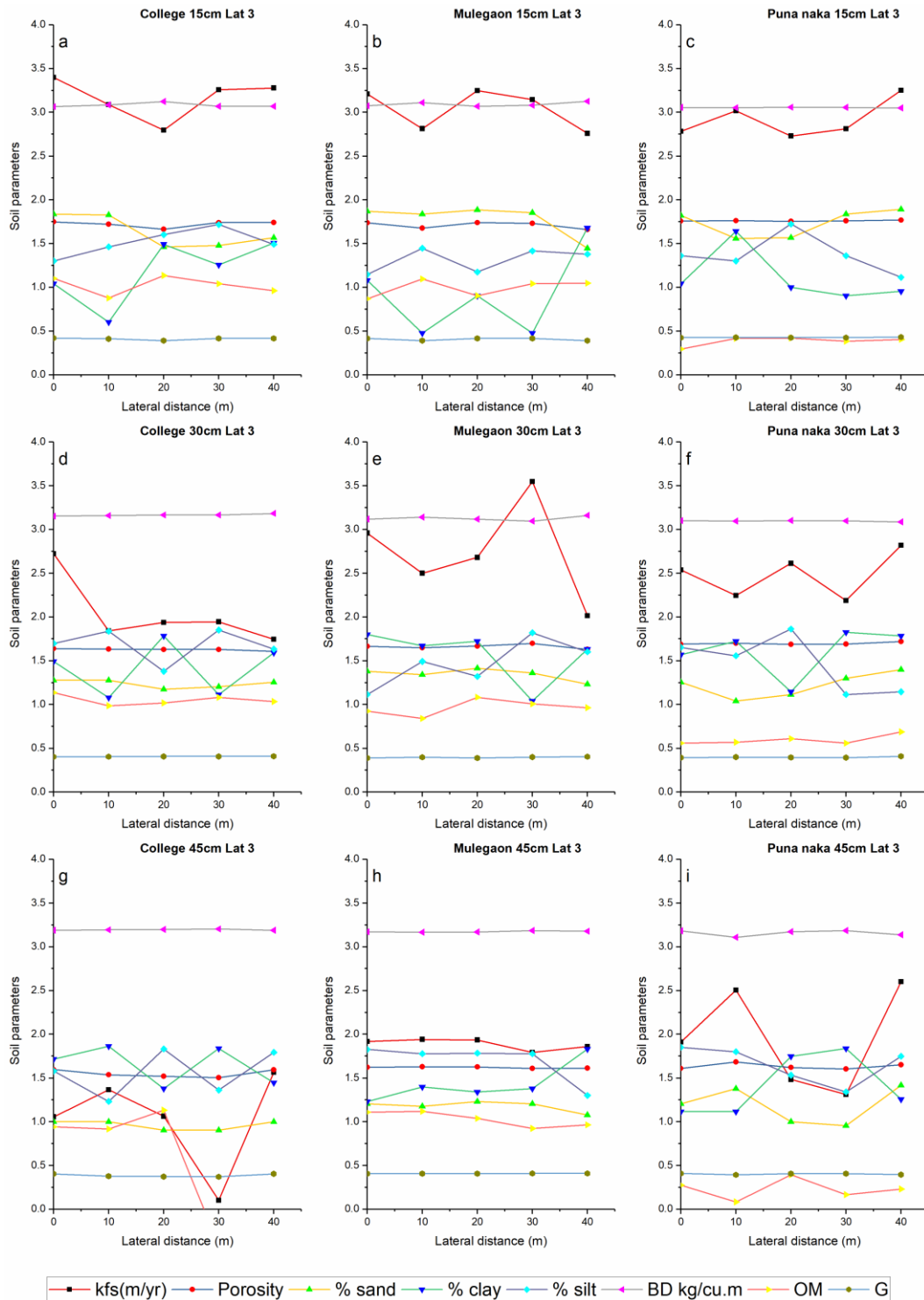


Fig 4.7 Variations of soil parameters along lateral direction at lateral 3 in college, Mulegaon and Puna naka site, at 15cm depth, 30cm depth and 45cm depth.

Abrupt variation in Kfs was found at 30cm and 45cm depth except in Mulegaon at 30cm depth as depicted in Fig 4.8. Possible reason can be attributed to subsurface biological activities along with spatial variation of compaction effect, due to

movement of living and non-living objects such as cattles grazing, human trespassing, and vehicle movements.

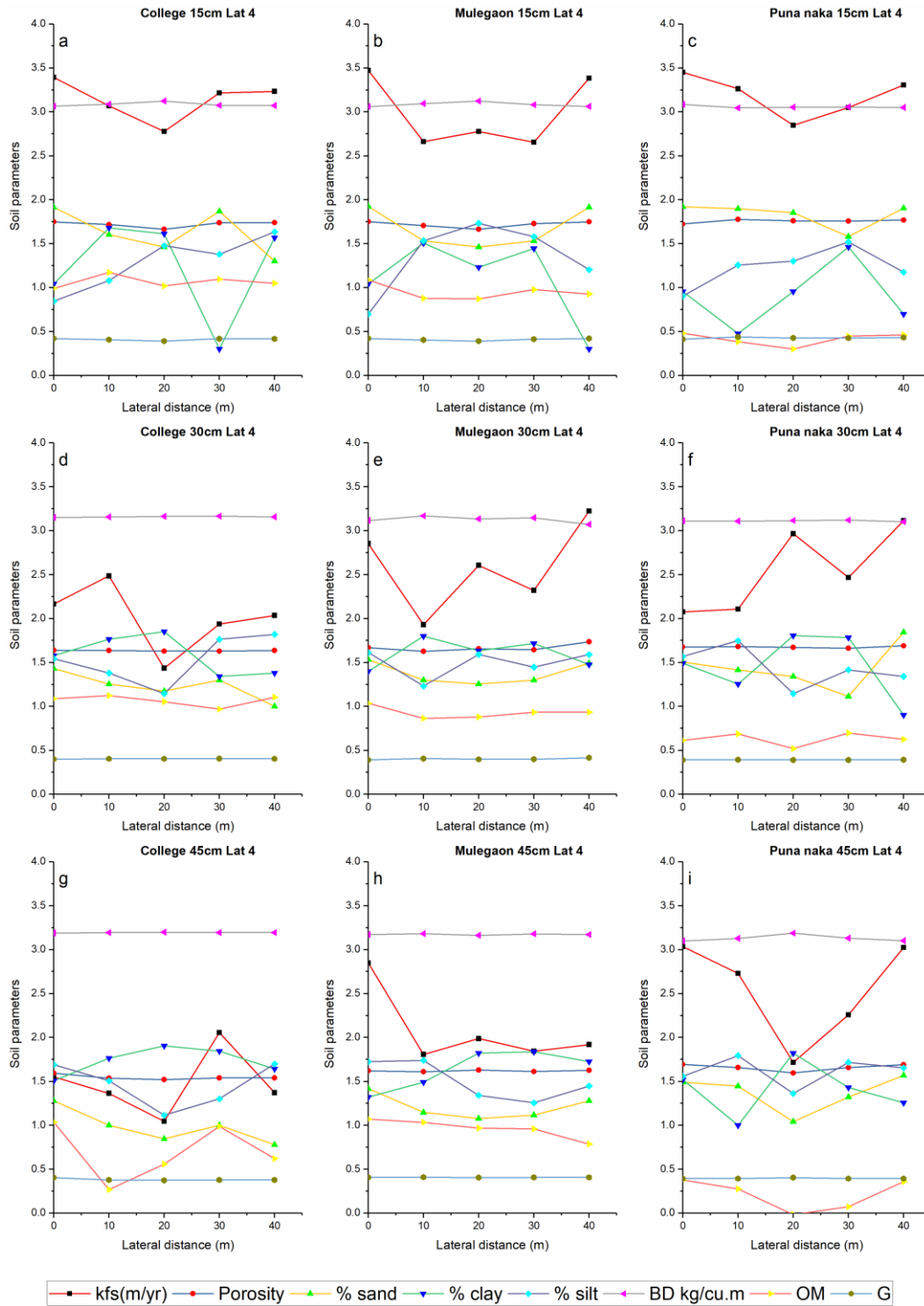


Fig 4.8 Variations of soil parameters along lateral direction at lateral 4 in college, Mulegaon and Punanaka site, at 15cm depth, 30cm depth and 45cm depth.

All these movements are not along well defined path so lead to nonuniform compaction. Soil texture though having non uniform distribution at all these

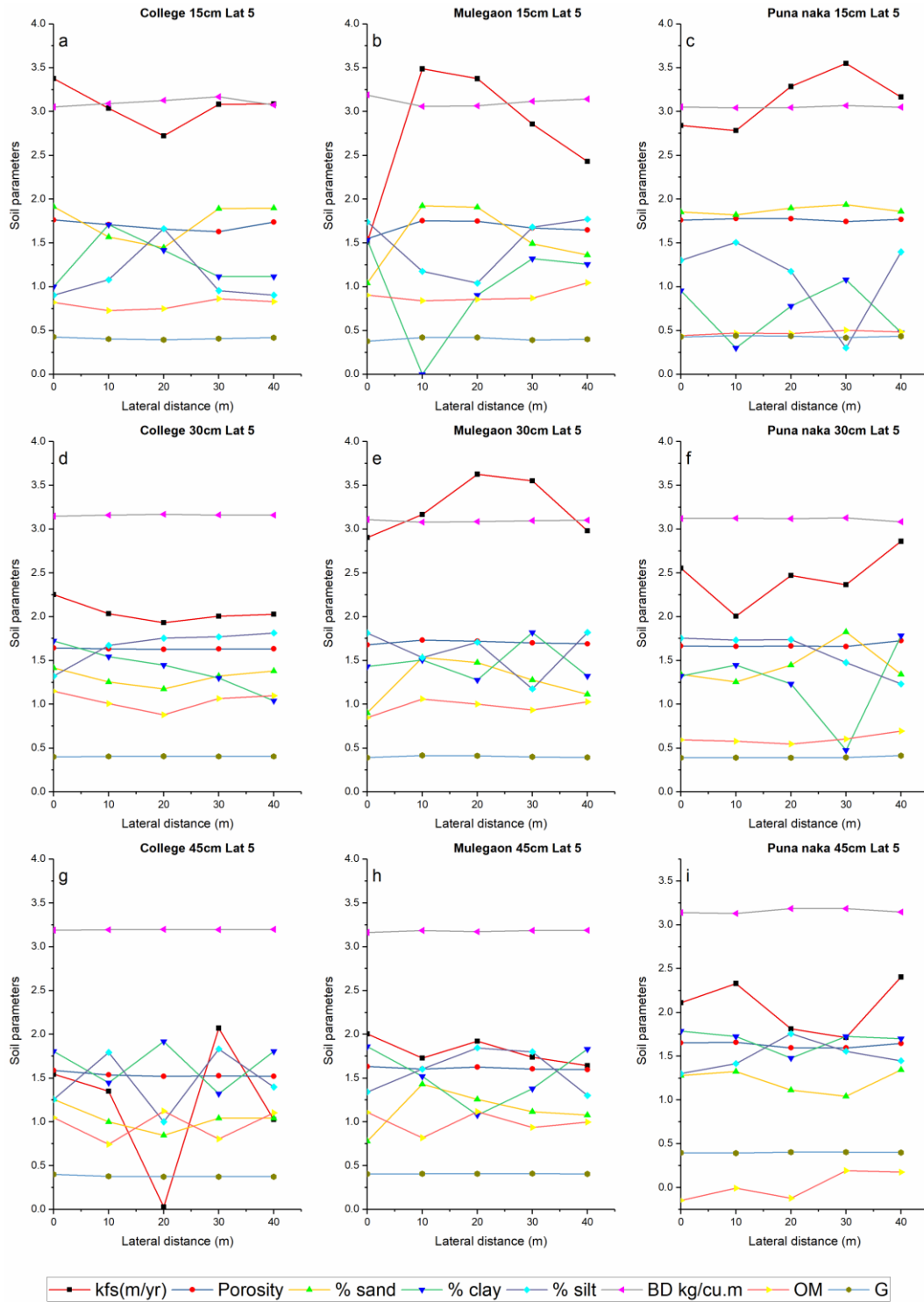


Fig 4.9 Variations of soil parameters along lateral direction at lateral 5 in college, Mulegaon and Punanaka site, at 15cm depth, 30cm depth and 45cm depth.

locations and depth, sand content has shown positive correlation with Kfs other two components has negligible influence on Kfs. Sand content failed to explain variation in Kfs at 45cm depth in college and Mulegaon because it was not following the trend of change of Kfs. However, at 45cm depth it has followed the trend to some extent (Fig 4.9). There is sharp decrease in Kfs at 45cm depth in college (Fig 4.8g) near 20m which might be due to localised effect of compaction, dominance of fine size texture at college site, some chemical changes in the subsurface soil. Sudden increase of Kfs at 15cm depth in Mulegaon was observed at 10m distance as depicted in Fig 4.9 b. It may be attributed to existence of macro pore due to root hole and/or wormhole (Mulegaon being agricultural land, root density and biological activities are predominant at this site).

Silt content has shown contrasting trend with respect to that of Kfs, for certain distance it was following the same trend and at other it was having opposite trend (Fig 4.10). In Mulegaon site, variation of Kfs at 15cm depth and 30cm has different trend. This change may be attributed to variation in structure of soil and thus the pore network that developed due to the structure. Sudden change in Kfs (Fig 4.10 b) was found predominant at 15cm in Mulegaon than in other two locations. The surface layer of soil (15cm) is very dynamic as it is the connection between the atmosphere and subsoil. The change that take place due to various factors at the interaction surface will be received by surface layer of soil thus leads to alteration in the structure and texture of soil spatially.

The saturated hydraulic conductivity in college site at a depth of 45 cm was less as compared to that at 15cm depth and 30cm depth. Also it was found decreasing along lateral direction at 7th lateral there was sudden drop (Fig 4.11g) at 30m distance. The possible reason may be local heterogeneity caused by cumulative effect of texture, structure, compaction, discontinuity of poreholes etc. Sand content (positively) and clay content (negatively) at 15cm depth (Fig 4.11b) followed trend of Kfs. However, silt content has shown contradictory variation with respect to Kfs.

Organic matter in college station at 15cm depth (Fig 4.12a) was found increasing along lateral direction which is beneficial as it helps in stability of soil aggregate and thus by prevent the destruction of structure of soil. Opposite variation was observed at

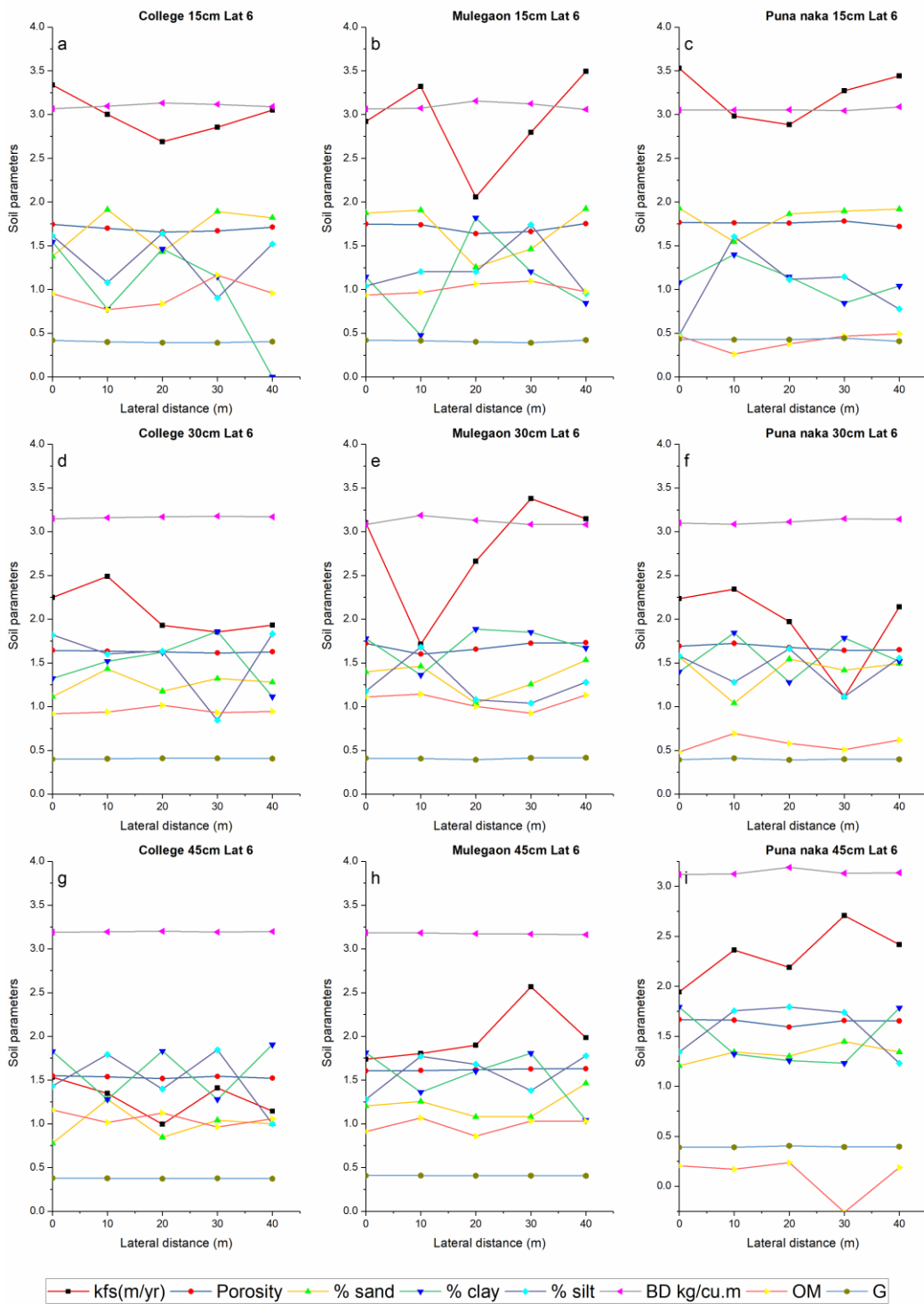


Fig 4.10 Variations of soil parameters along lateral direction at lateral 6 in college, Mulegaon and Puna naka site, at 15cm depth, 30cm depth and 45cm depth.

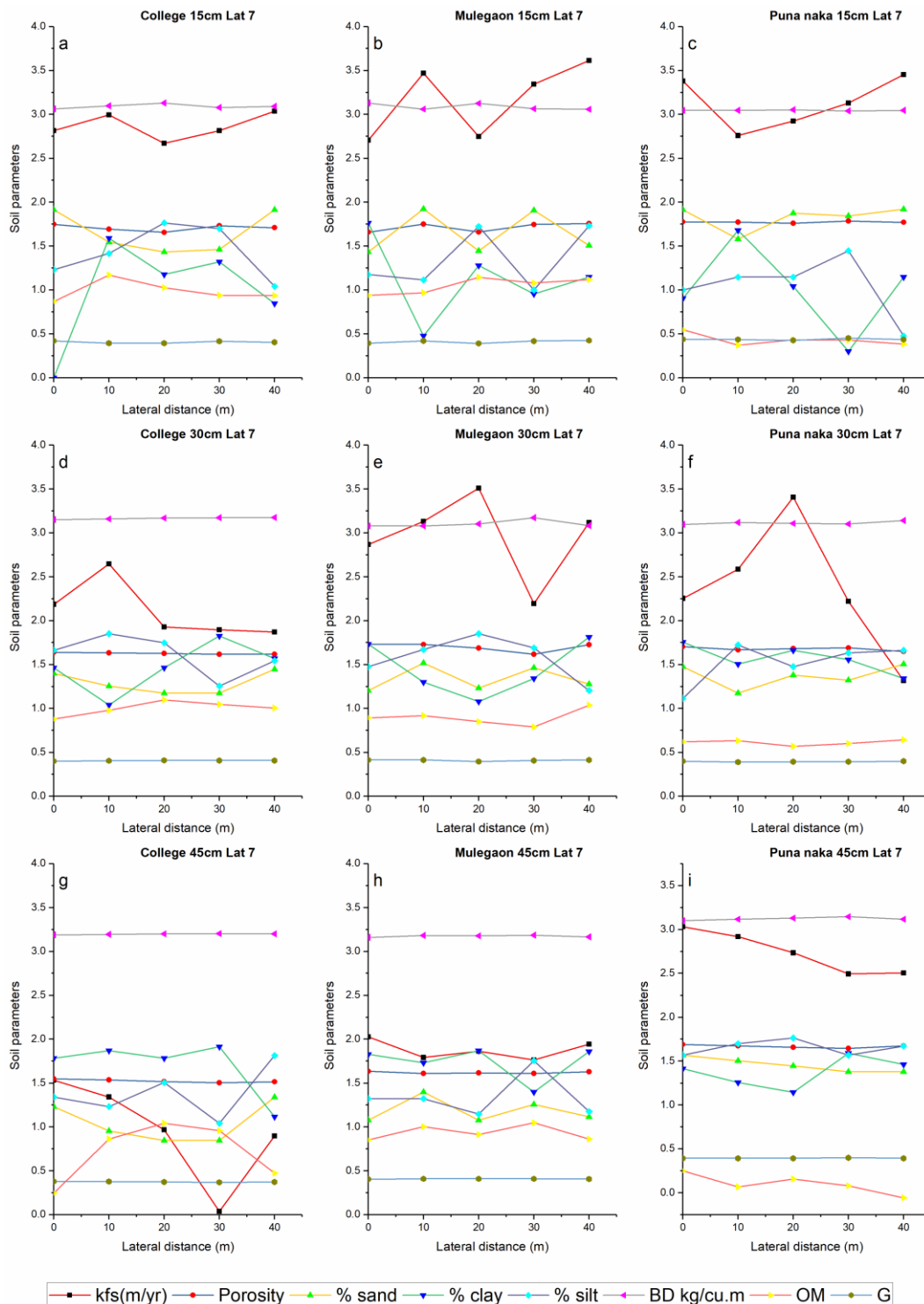


Fig 4.11 Variations of soil parameters along lateral direction at lateral 7 in college, Mulegaon and Punanaka site, at 15cm depth, 30cm depth and 45cm depth.

45cm depth in college site (sudden decrease in Ks at 30m distance) and that at Punanaka (Sudden increase in Kfs at 30m distance) i.e. at same depth Kfs at one place

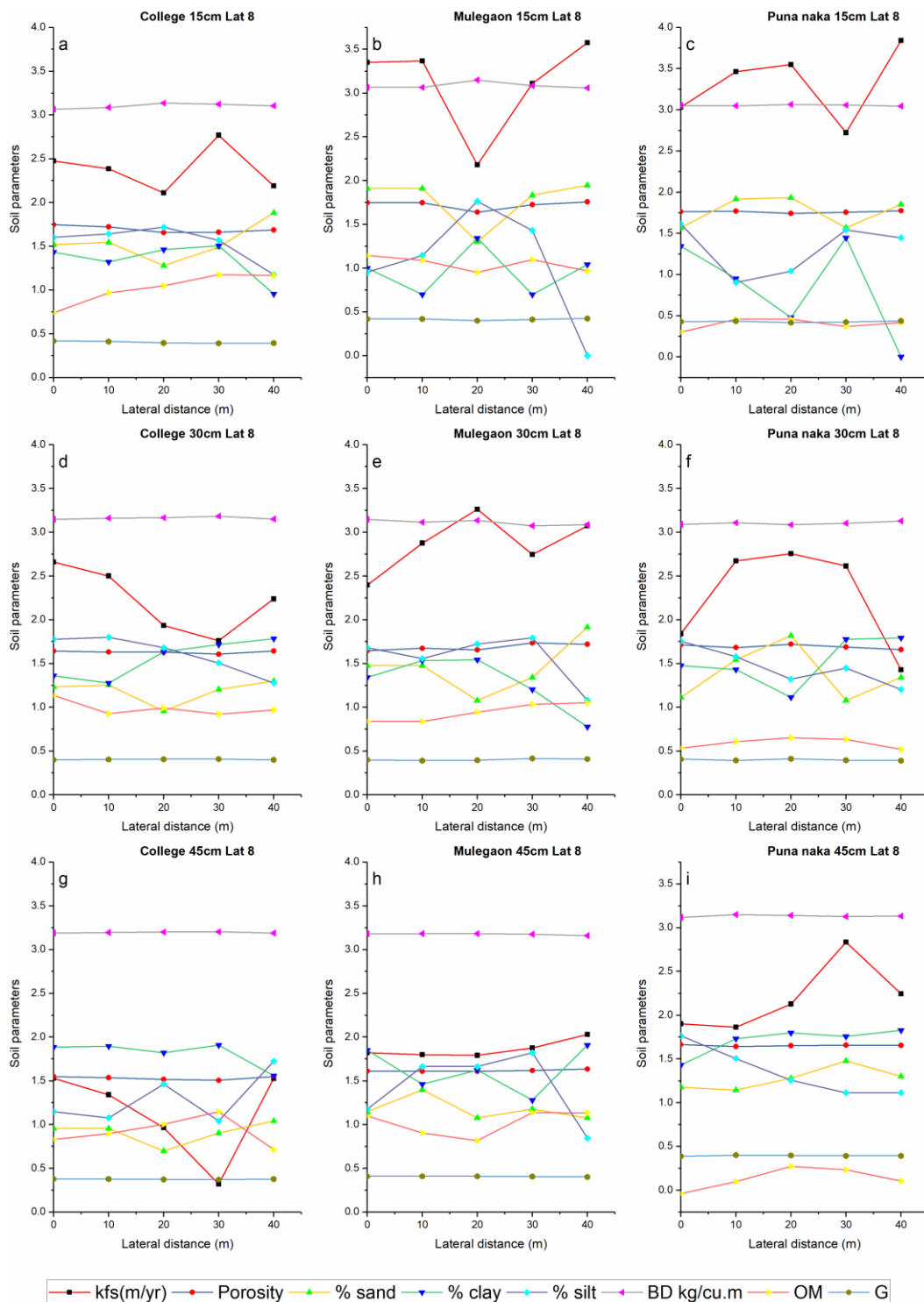


Fig 4.12 Variations of soil parameters along lateral direction at lateral 8 in college, Mulegaon and Punanaka site, at 15cm depth, 30cm depth and 45cm depth.

is decreased suddenly (Fig 4.12g) and at other place in increased suddenly (Fig 4.12i). This strongly supports the concept of heterogeneity of Kfs locally as well as spatially.

Although 30m distance is merely a coincidence as it has no role to play in heterogeneity. Variation of Kfs in Mulegaon site at 15cm depth (Fig 4.12b) seems to be controlled partially by clay content in the negative sense.

Zigzag kind of variation (increase – decrease – increase) in Kfs was observed at all three location along lateral 9, at a depth of 45cm in college (Fig 4.13g), at 15cm depth in Mulegaon (Fig 4.13b) and 30cm depth in Punanaka (Fig 4.13f). It is also similar at Mulegaon site at 15cm depth (Fig 4.13e) but the change is marginal.

Silt content at a depth of 15cm has negative impact on the Kfs for entire 40m lateral distance (Fig 4.14c), there was sudden decline of the value of silt content at a distance of 30m and then again plunge up at 40m the change in magnitude of Kfs was opposite to this but is relatively less. There was sudden decrease of Kfs at 30cm depth in Mulegaon (Fig 4.14e) at a lateral distance of 20m along 10th lateral the drop was local and again it jump back and then drop down again. The reason might be macro pore development and their interconnectivity, blockage etc. The improvement in the value of Kfs was observed at 15cm depth in Punanaka site along 10th lateral from 0m to 10m, from 10m to 20m there was gradual increase in Kfs, between 20m and 30m there it dropped suddenly and then found to climb up gently (Fig 4.14i).

Silt content shown negative trend with respect to Kfs at 15cm depth (Fig 4.15a) in College site along 11th lateral however quantum of change in Kfs was considerable as compared to that in case of Silt. It implies some kind of nonlinear correlation of silt content is there with Kfs. Similar scenario was observed at Mulegaon and Punanaka site at 15cm depth. However at 30cm depth it is having mixed kind of trend with Kfs. There was sudden plunge in the Kfs at 30 cm depth in Punanaka (Fig 4.15f) along lateral 11th from 0 – 10m and then it picked up slowly in between 10m to 30m and then again it dropped down at 45cm depth. At 15 cm depth also Kfs shown similar trend, it dropped down gradually from 0m to 30m and then climb up between 30m to 40m. Soil texture (sand content and silt content) was found to have control (Fig 4.16 a) over the Kfs as they are following similar trend by sand content or opposite (clay content). Most of the time silt content has shown negative trend and sand content has shown positive trend except at few locations where some other factor may be

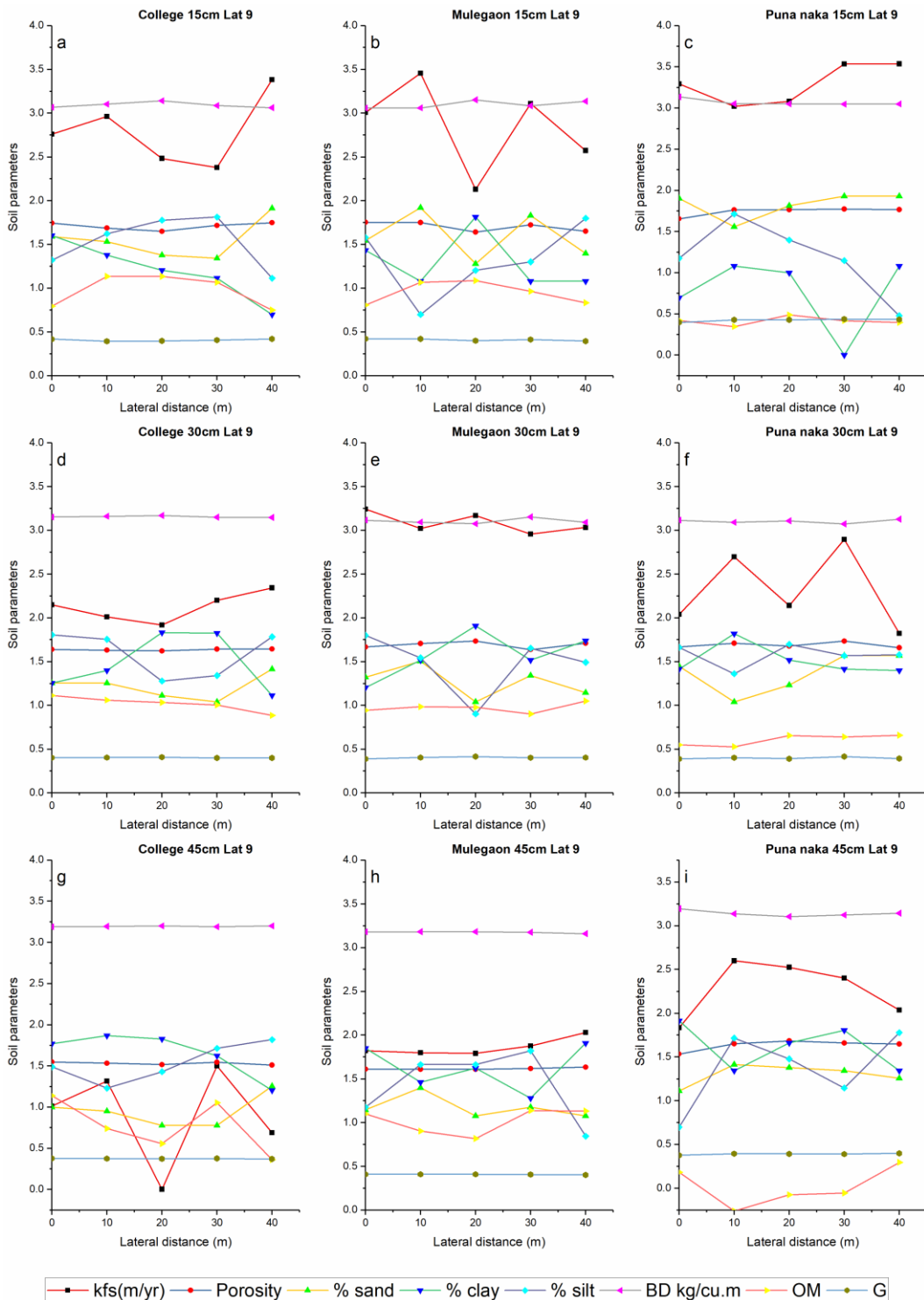


Fig 4.13 Variations of soil parameters along lateral direction at lateral 9 in college, Mulegaon and Punanaka site, at 15cm depth, 30cm depth and 45cm depth.

Dominating over the value of Kfs. Silt content was found to have positive trend with Kfs at 30cm depth in College along lateral 12. However, at same depth it was found to

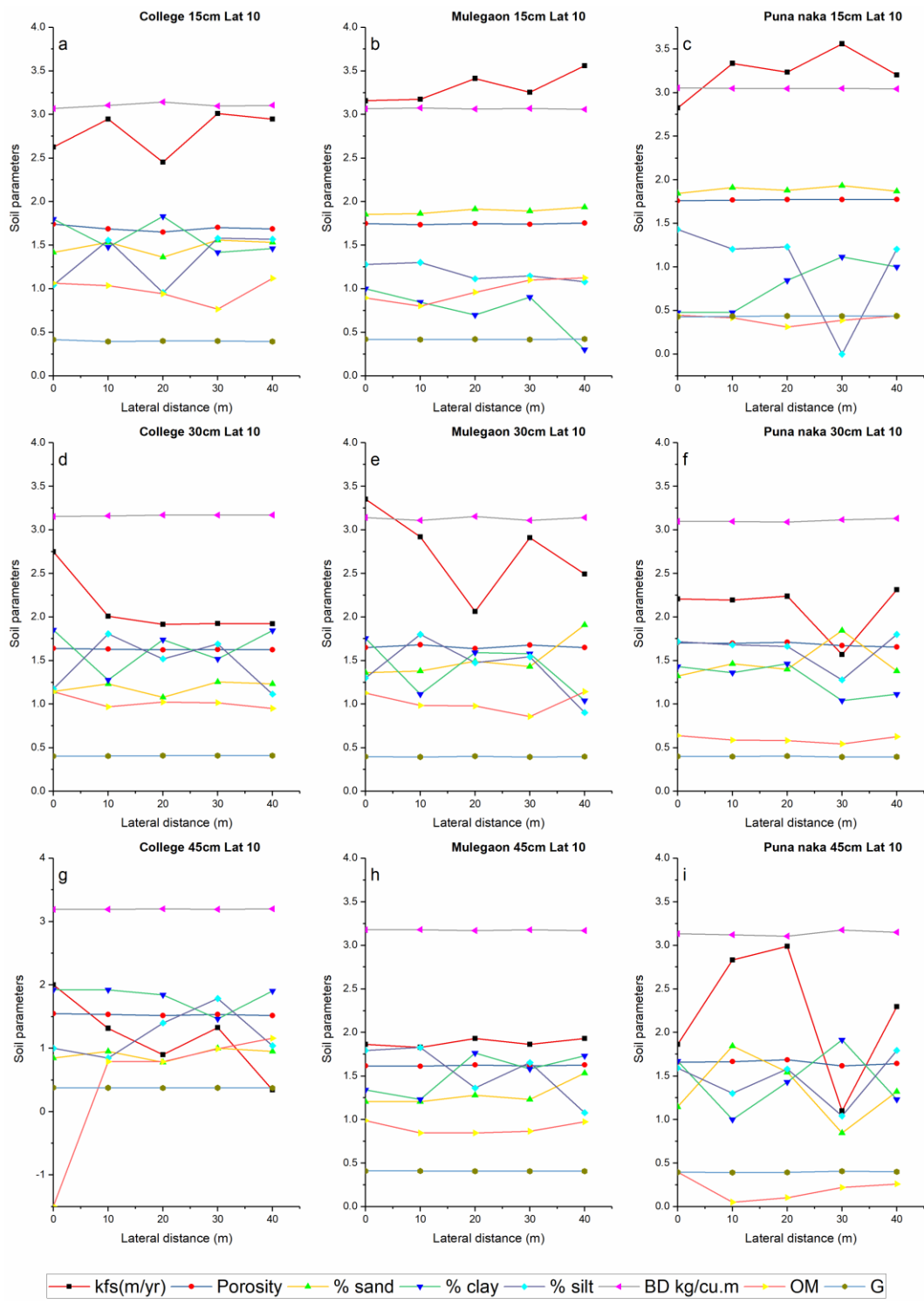


Fig 4.14 Variations of soil parameters along lateral direction at lateral 10 in college, Mulegaon and Punanaka site, at 15cm depth, 30cm depth and 45cm depth.

Have positive correlation with Kfs in Punanaka at 30cm depth. Substantial improvement of Kfs was observed at 45cm depth in Punanaka along lateral 12

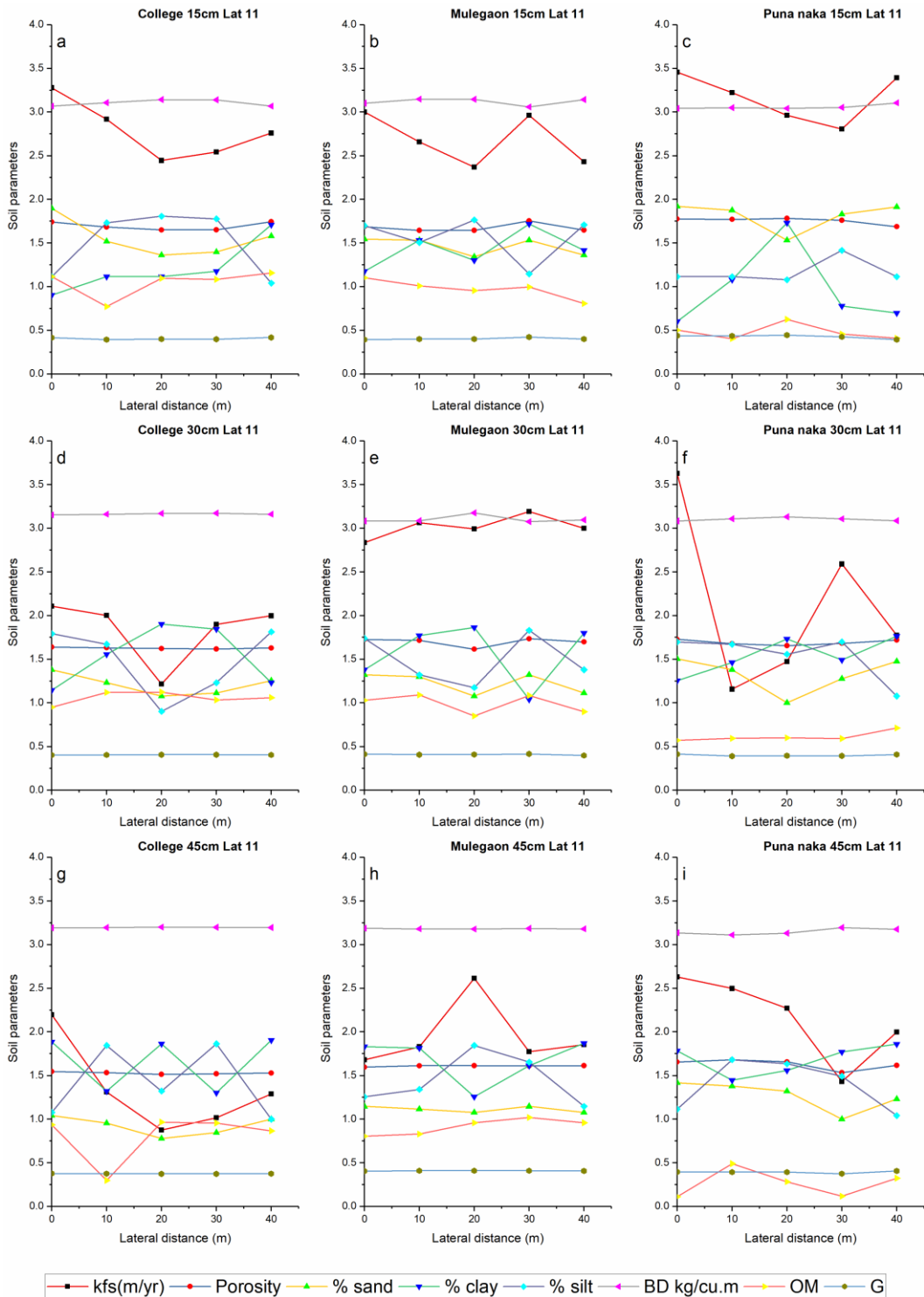


Fig 4.15 Variations of soil parameters along lateral direction at lateral 11 in college, Mulegaon and Punanaka site, at 15cm depth, 30cm depth and 45cm depth.

(Fig 4.16i). Clay content shown negative trend with respect to Kfs whereas silt and sand content shown positive correlation with Kfs. All three components of soil texture

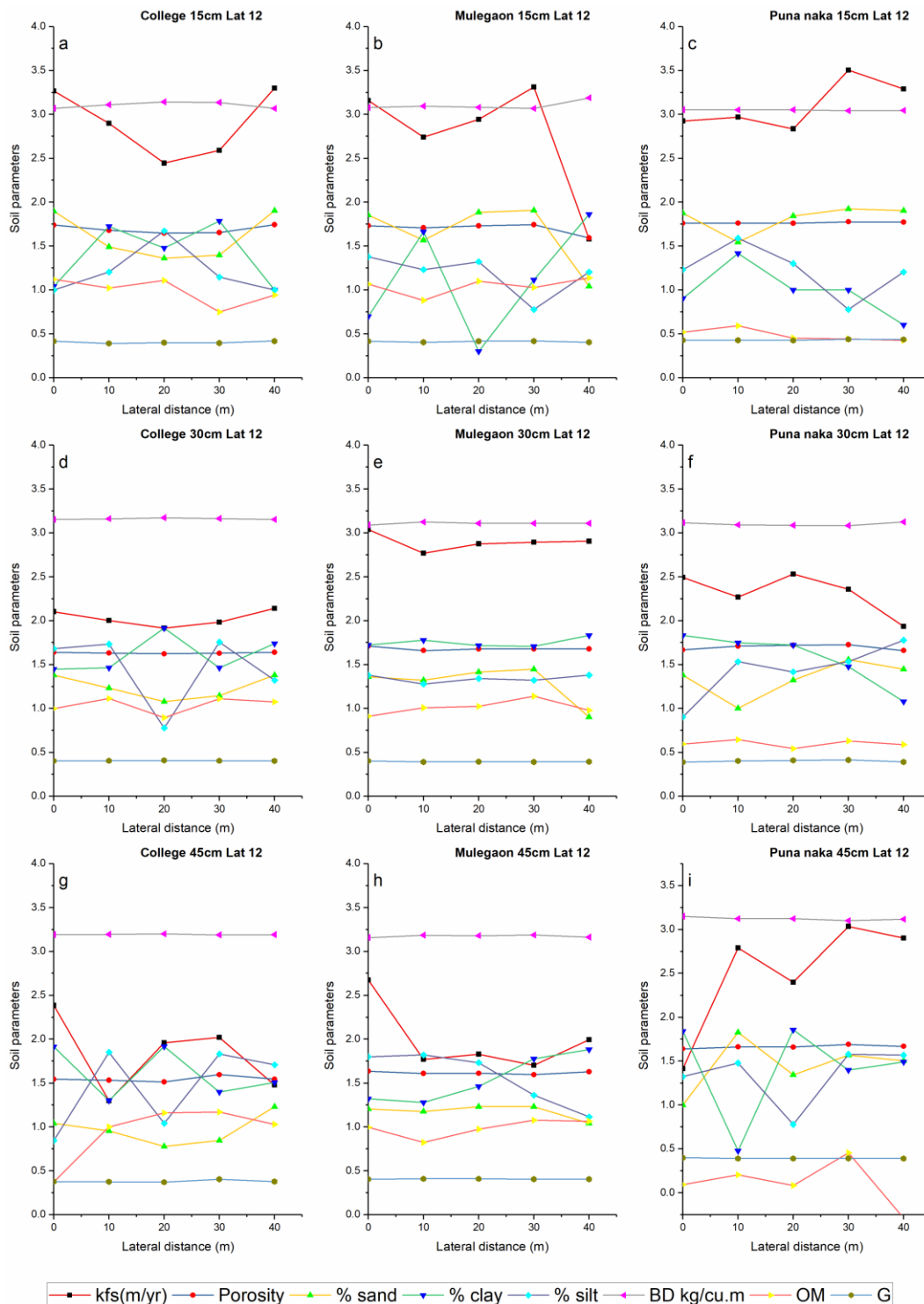


Fig 4.16 Variations of soil parameters along lateral direction at lateral 12 in college, Mulegaon and Puna naka site, at 15cm depth, 30cm depth and 45cm depth.

controlling the value of Kfs. Trend in the variation of the Kfs at 15cm depth, 30cm depth and 45 cm depth was not similar at all three sites of observations (Fig 4.17).

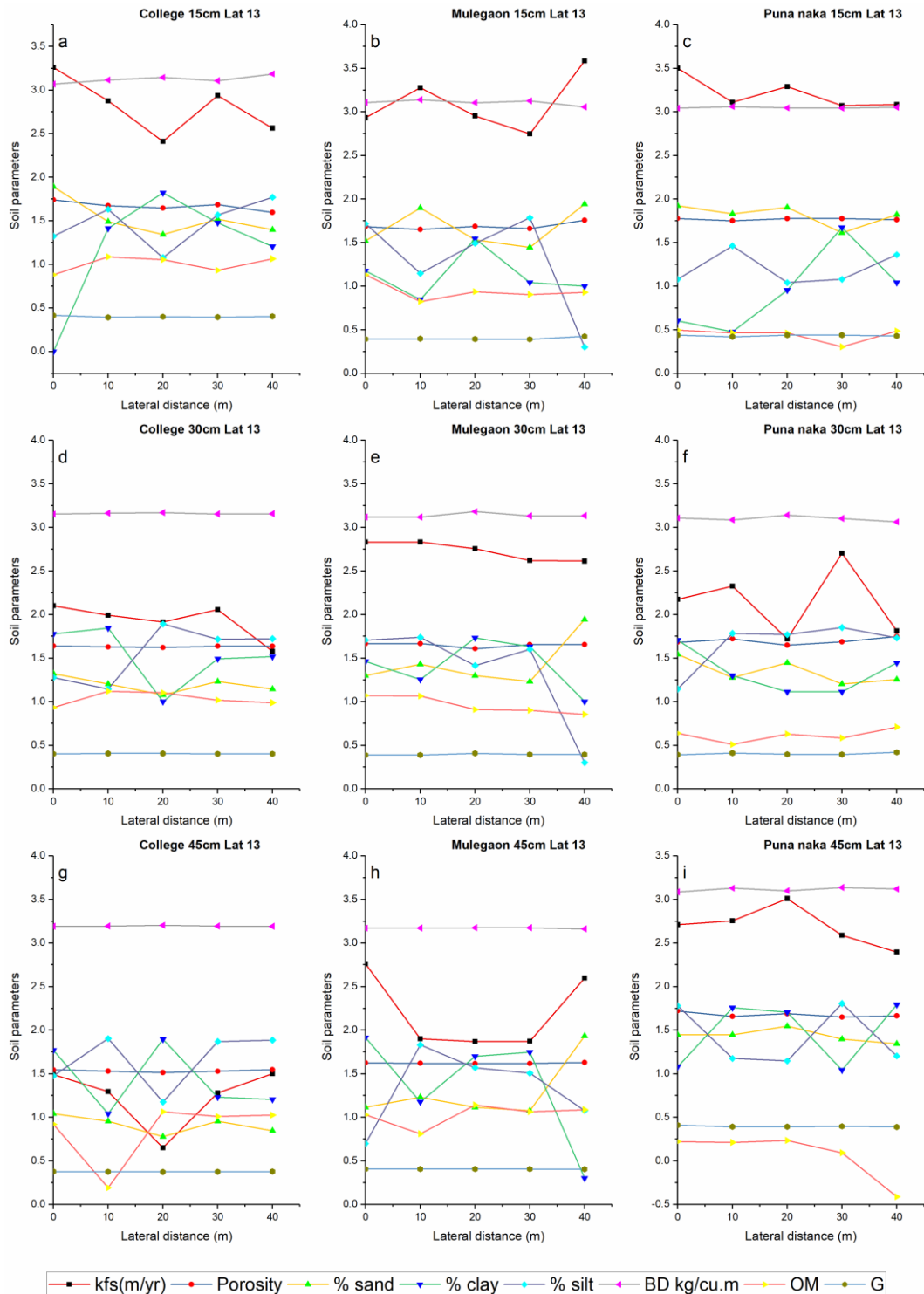


Fig 4.17 Variations of soil parameters along lateral direction at lateral 13 in college, Mulegaon and Punanaka site, at 15cm depth, 30cm depth and 45cm depth. Variation in Kfs at 45cm along 13th lateral was found steady along lateral. Sand content was following similar trend at all depth with respect to Kfs, thus a parameter having strong influence on it. Clay content at 15cm depth in College site (Fig 4.17 a)

was found increasing towards the middle of lateral from either side this may be attributed to topographical change (depression towards the center of lateral). Organic matter has not shown in specific trend along the lateral mixed trend was shown by it (increasing, steady and decreasing mixed in any order) thus implying the heterogeneity of it along all the laterals and at all depths of observations.

The sand content at 30 cm depth along 14th lateral in college site was found steady (Fig 4.18 d) in comparison with its variation at other sites and depths. The Kfs at 30cm depth went down gently in college site along lateral 14 (Fig 4.18d) and then up surged initially gently between 20m and 30m and then gradually went up between 30m and 40m. In Punanaka at a depth of 30 cm along lateral 14th Kfs rocketed up from 0 to 10m and then plunged down from 10m to 40m (Fig 4.18b).

Mulegaon site has shown (Fig 4.19b) decreasing trend (initially gradual and then sudden) towards the middle of lateral from either side at a depth of 15cm. Similar results are seen at 45cm in college site (Fig 4.19g) and at 30cm depth in college where variation is more gradual (Fig 4.19d). Variation of silt content and clay content were shown contrasting trends if one increase then other decreased at 30cm depth in Mulegaon (Fig 4.19e) Trend of variation of clay content was opposite to that of Kfs upto 30m along in Punanaka at 15cm depth (Fig 4.19c).

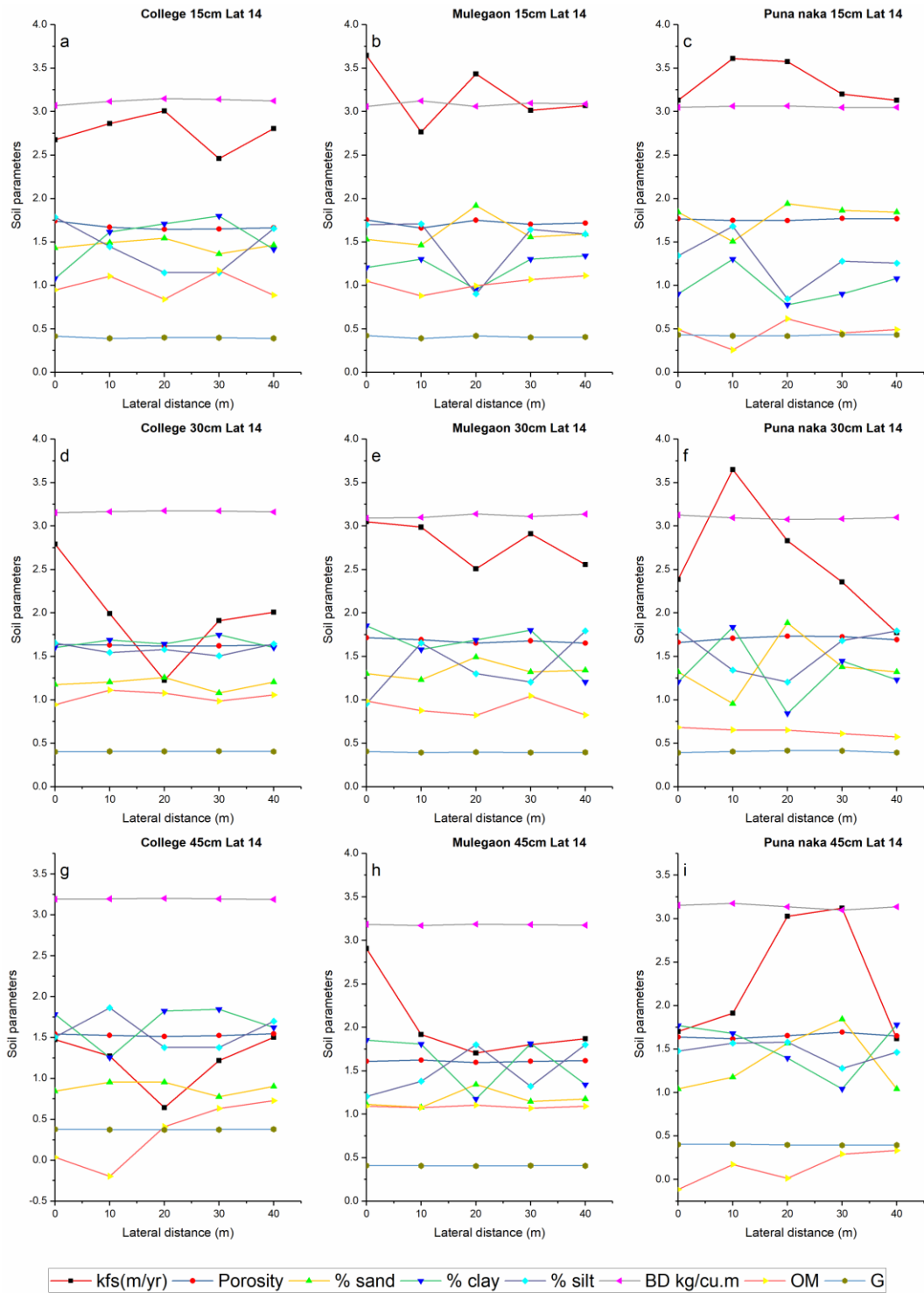


Fig 4.18 Variations of soil parameters along lateral direction at lateral 14 in college, Mulegaon and Punanaka site, at 15cm depth, 30cm depth and 45cm depth.

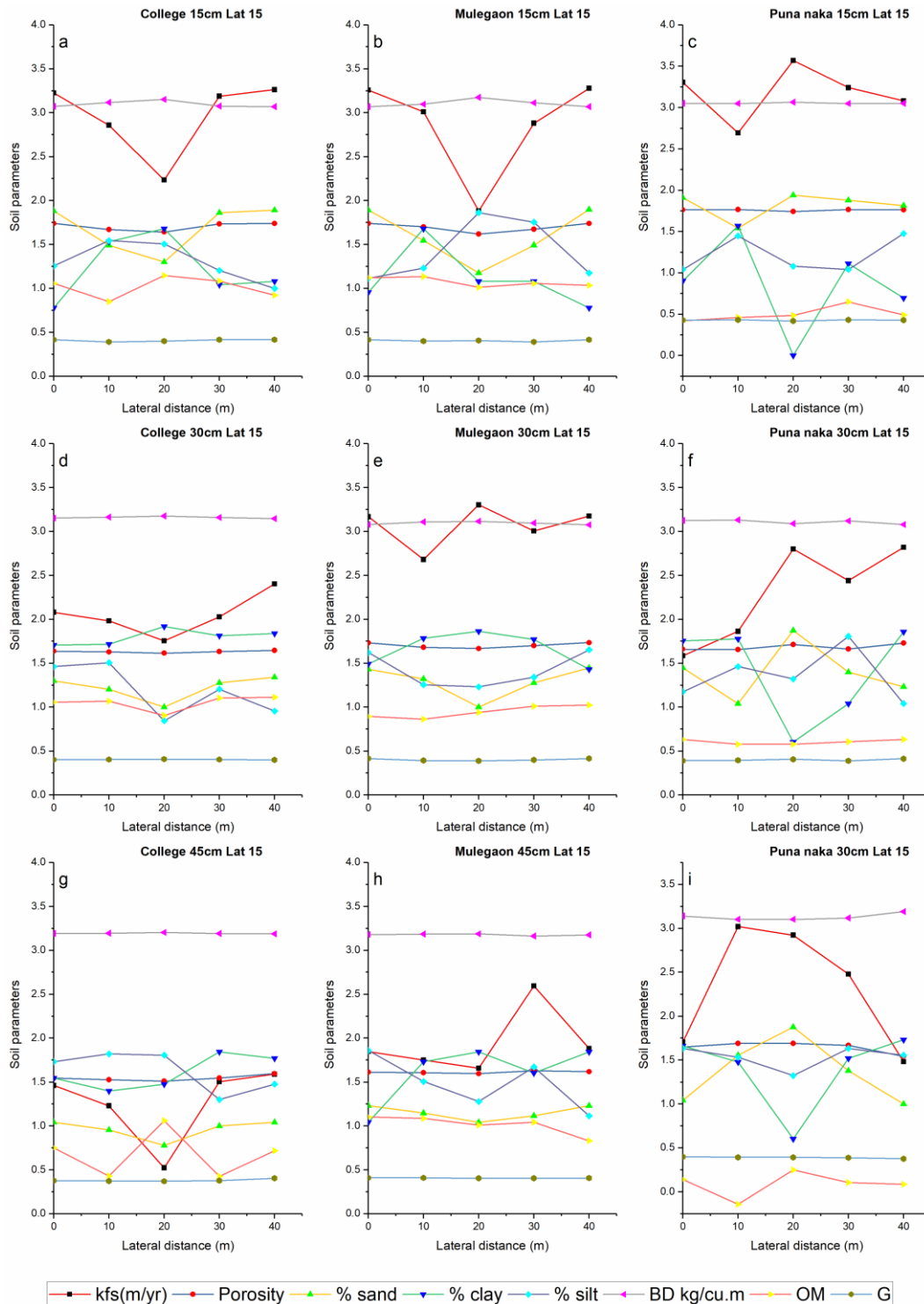


Fig 4.19 Variations of soil parameters along lateral direction at lateral 15 in college, Mulegaon and Puna naka site, at 15cm depth, 30cm depth and 45cm depth.

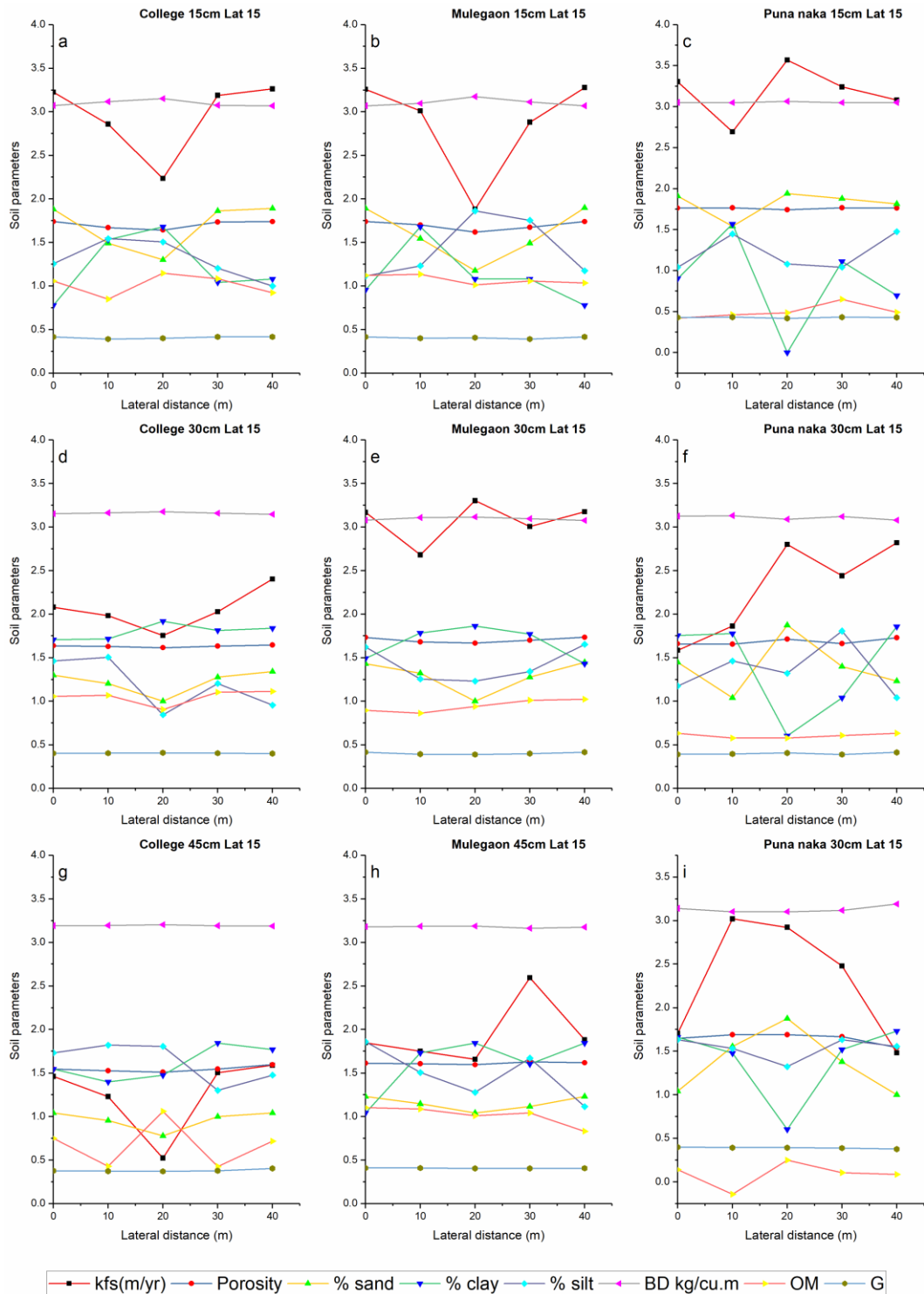


Fig 4.20 Variations of soil parameters along lateral direction at lateral 16 in college, Mulegaon and Puna naka site, at 15cm depth, 30cm depth and 45cm depth.

The Kfs at Punanaka has shown increase in its magnitude along lateral towards the centre of lateral from either side at 15cm, 30cm and 45cm depth (Fig 4.20c, 4.20f and 4.20i). In Mulegaon site at 30cm depth, Kfs was found increased abruptly between 0m to 10m along lateral 16th then remain steady between 10m to 20m and then again it drops down and finally become stable (Fig 4.20e). In college site (Fig 4.20d) at 30cm depth variation of Kfs was similar to that it has shown in Punanaka at 30cm depth but change in magnitude was quite low as compared to that in Punanaka. Clay content in Punanaka at 15cm depth was found to have inverse relation with Kfs showing sharp decrease in its value between 10m to 20m and 30m to 20m towards center of lateral (Fig 4.20c). Silt content has reciprocal trend in Mulegaon site at 15cm depth with respect to Kfs (Fig 4.20b). The variation of Kfs along the 17th lateral at college site resembled like opposite V at 15cm depth between 0 to 10m (Fig 4.21a) along lateral , and it was found like letter V at 30cm depth between 0 to 10m (Fig 4.21d), 10 to 30m at 45cm (Fig 4.21g). It was like a roof truss in Mulegaon at 15cm depth (Fig 4.21b), like letter M at 30cm depth (Fig 4.21e). In Punanaka at 15cm depth along 17th lateral variation of Kfs was like letter W (Fig 4.21c). Lot of variations in Kfs was observed having dissimilarities in their pattern revealing the spatial heterogeneity of it.

The sharp increase in Kfs was observed at 45cm depth along 18th lateral between 20m and 40m, in College site (Fig 4.22g). In Mulegaon too there was sharp increase in Kfs was noticed between 30m and 40m along 18th lateral (Fig 4.22e), steady increase in Kfs was noticed in Punanaka also at 30cm depth (Fig 4.22f). Kfs was found continuously falling from 10m to 40m in Mulegaon site at a depth of 30cm (Fig 4.22e). The kfs was rocketed up in college site (Fig 4.23g) at 45cm depth (30m to 40m), in Mulegaon it was found at a depth of 15cm (Fig 4.23b) between 10 to 20m , 30cm (Fig 4.23e), 45cm (Fig 4.23h) between 30m to 40m. In Punanaka it was found sharply increasing at a depth of 45cm between 10m to 30m (Fig 4.23i) and at 30cm depth it was increased gradually between 10m to 40m (Fig 4.23f). Sharp decrease in Kfs was observed at all three stations; between 0 to 10m in Mulegaon at 30cm depth (Fig 4.23b), between 0 to 20m in College (Fig 4.23g) and between 0 – 20m in Punanaka (Fig 4.23c).

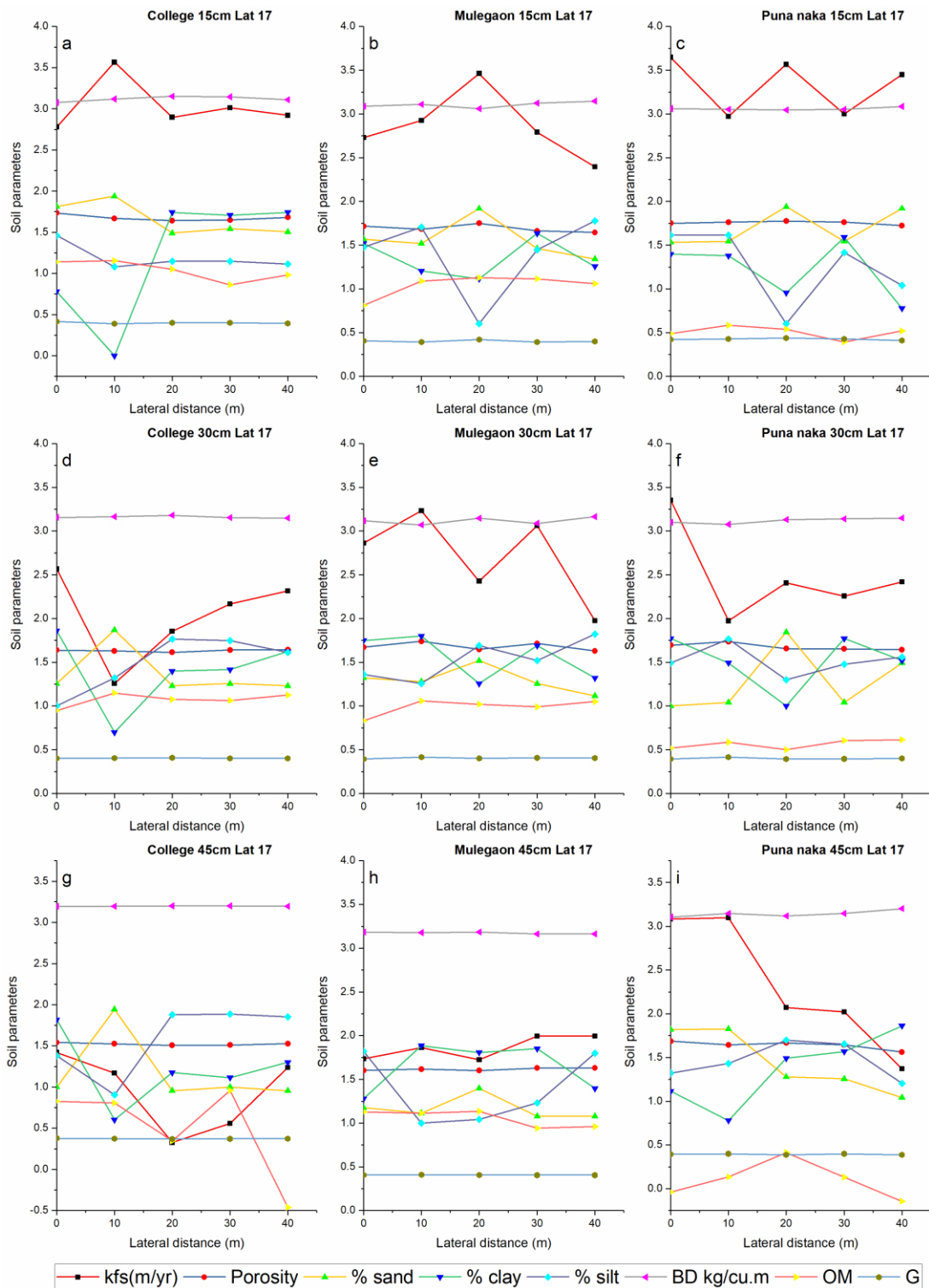


Fig 4.21 Variations of soil parameters along lateral direction at lateral 17 in college, Mulegaon and Punanaka site, at 15cm depth, 30cm depth and 45cm depth.

Zig zag kind of variation was observed at all stations and all depths along 20th lateral (Fig 4.24) at some depth there was sudden drop in the value of Kfs such as College

15cm depth between 10m 1nd 20m (Fig 4.24a), Mulegaon 30cm depth between 10m to 30m (Fig 4.24e) Surge in the Kfs value was observed in College at 45cm depth

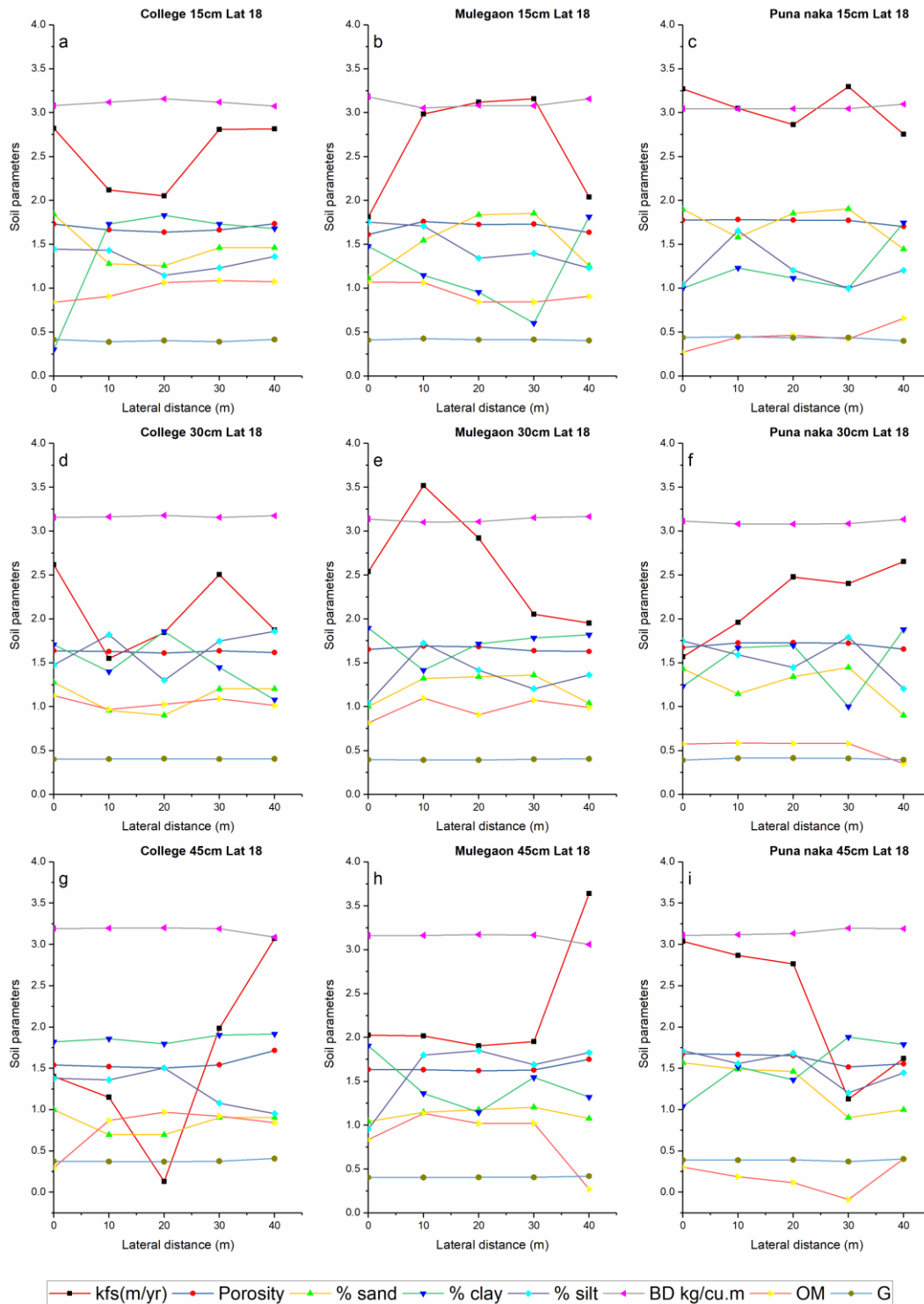


Fig 4.22 Variations of soil parameters along lateral direction at lateral 18 in college, Mulegaon and Punanaka site, at 15cm depth, 30cm depth and 45cm depth.

between 30m and 40m (Fig 4.24g), in Mulegaon at 45cm depth (Fig 4.24h) and gradual variation in Kfs was observed at remaining station and depth.

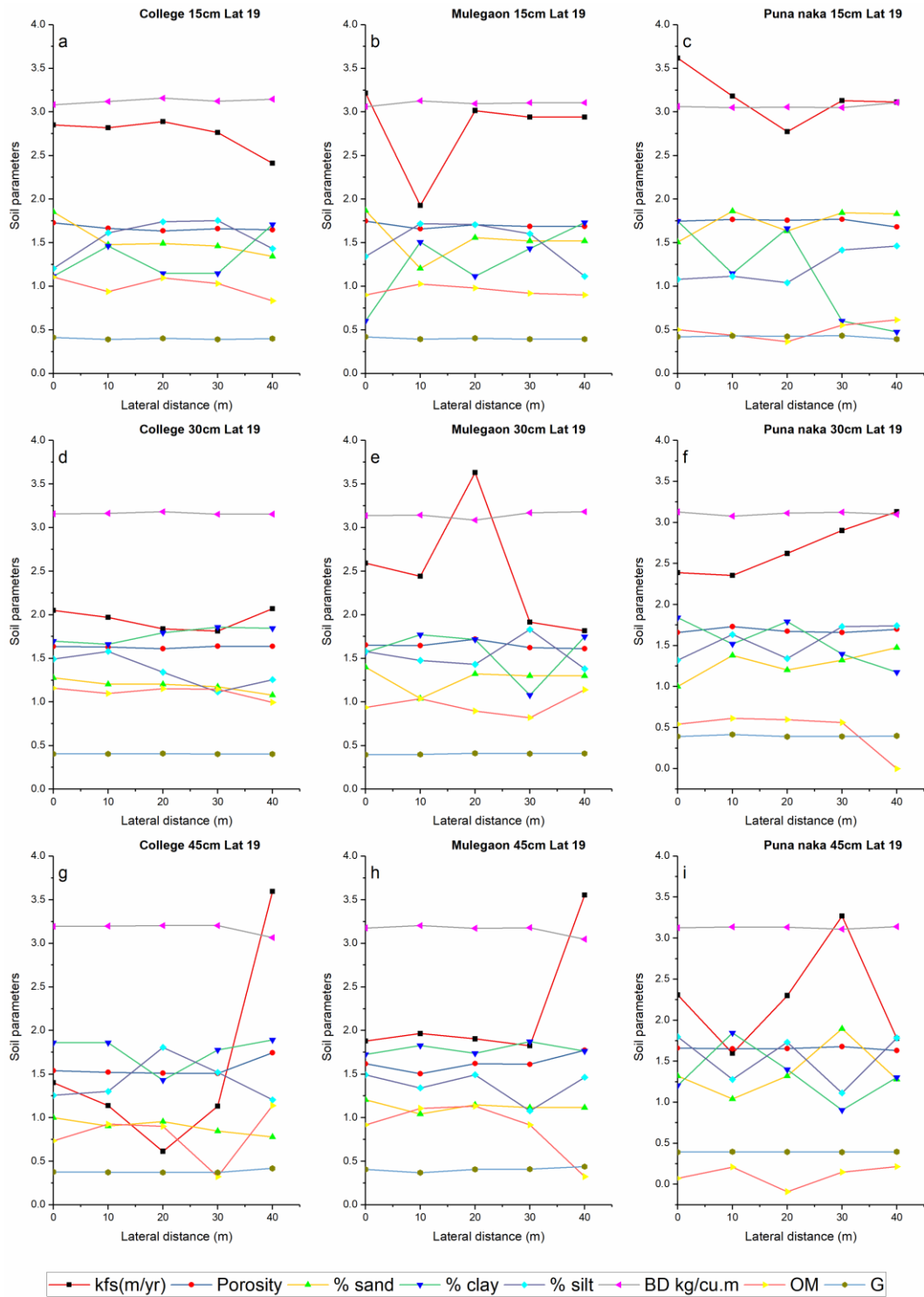


Fig 4.23 Variations of soil parameters along lateral direction at lateral 19 in college, Mulegaon and Punanaka site, at 15cm depth, 30cm depth and 45cm depth.

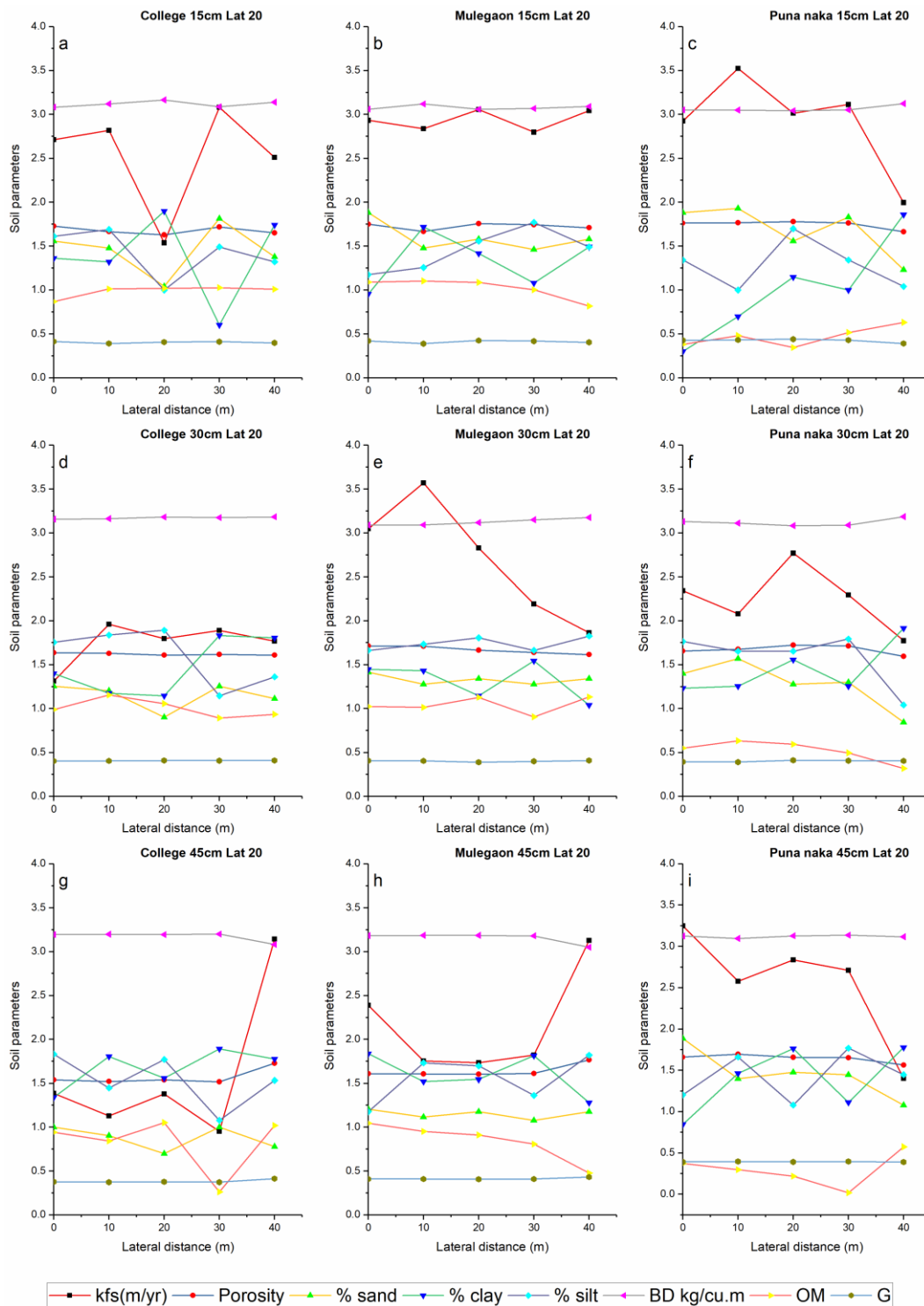


Fig 4.24 Variations of soil parameters along lateral direction at lateral 20 in college, Mulegaon and Punanaka site, at 15cm depth, 30cm depth and 45cm depth.

For clarity purpose, only the variation of Kfs with longitudinal distance at 15cm, 30cm and 45cm along particular longitude is shown (Fig 4.25, Fig 4.26 and Fig 4.27). Saturated hydraulic conductivity (Kfs) was found declining initially (fig 4.25) and then it increase and then uniform for some distance and then it was fluctuating. Similar kind of trend was observed at 30cm depth and 45cm depth (Fig 4.25a). Beyond 100m at 45cm depth Kfs at college site was found declining gradually till end. In Mulegaon, in the variation of Kfs , sharp decline was found at 15cm depth, 30cm depth and 45cm depth along longitudinal not necessarily at same position (Fig 4.25b). At few positions, trend at all depth found similar (increasing / decreasing), at few locations there is no similarity between variations at these depths was observed (Fig 4.25b). In Punanaka, non-uniform variation (up down up) kind of behaviour was observed (Fig 4.25c). Surface soil may be affected by various other parameters apart from the soil texture such as sealing grass roots microbiological activities etc.

In general, Kfs was found to be declining with depth barring few positions where Kfs at larger depth was found more than that at smaller depth (Fig 4.26). The fluctuation in the Kfs at 45cm in College (Fig 4.26a) and Mulegaon (Fig 4.26b) was found insignificant. Sudden drop in Kfs was observed at 70m along longitude, which is attributed to local depression along longitude. Sudden jerk in Kfs at 15cm depth in college was observed between 150m and 180m (Fig 4.26a). More or less uniform variation of Kfs was observed along the longitudinal 2 at college site, an indication of homogeneous structure of soil barring few positions. The disparity is due to various factors contributing change in pore size, shape and connectivity such as compaction, human intervention, and biological activities.

In Mulegaon site the variation in surface layer (15cm depth) was less than that at a depth of 30cm (Fig 4.26b) indication of dominance of subsurface activities in controlling Kfs by means of enhancing the pore geometry by roots, microorganism movement, wormholes and to some extent by rodents it being agricultural land. Fluctuation in variation of Kfs was more at 30cm depth and 45cm depth (Fig 4.26c). More jerks of fluctuations were observed at 30cm. Fluctuation in variation of Kfs was observed at all three depths in college (Fig 4.27a), Mulegaon (Fig 4.27b) and

Punanaka (Fig 4.27c). Relatively more ups and downs were observed at 45cm depth in College site as compared to other two sites.

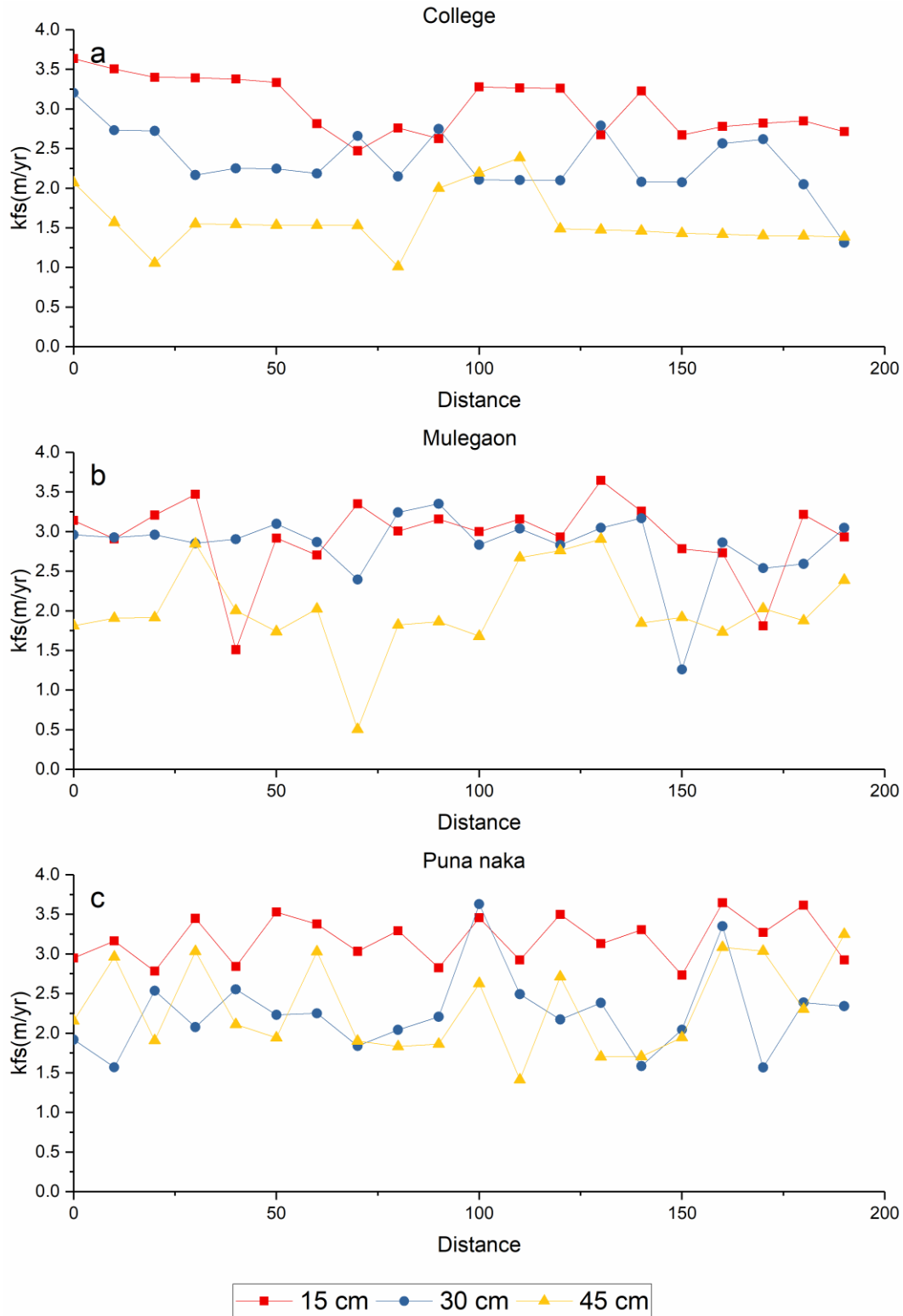


Fig 4.25 Variation of saturated hydraulic conductivity along the longitudinal 1 at 15cm, 30cm and 45cm depth in College, Mulegaon and Punanaka

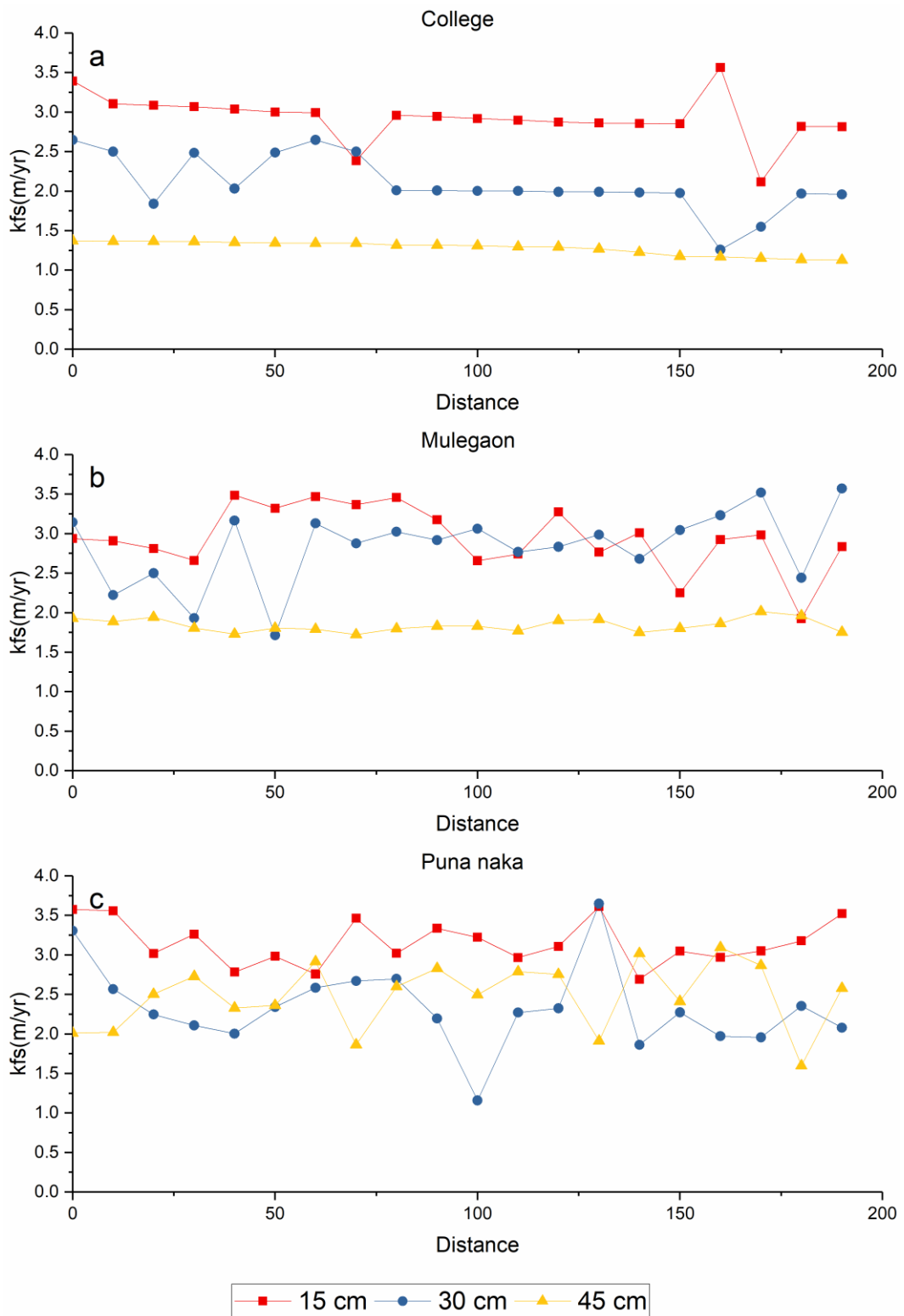


Fig 4.26 Variation of saturated hydraulic conductivity along the longitudinal 2 at 15cm, 30cm and 45cm depth in College, Mulegaon and Puna naka

In Mulegaon site, Kfs at 30cm depth at most of the positions (~ 50%) was found more than that at 15cm possibility of sealing and crusting in the surface layer cannot be overruled. Variation in the texture and structure may be also possible.

In college site at 15cm depth, (Fig 4.28a), trend in the variation was similar at 15cm depth and 30cm depth. However, at 45cm depth it was contrasting and large variation in Kfs was observed along longitude. Lot of crest and trough were observed implying heterogeneity of porous structure. In Mulegaon site, Kfs at 15cm (Fig 4.28b) was found less than that at 45cm (few position), Kfs at 30cm is more than that at 15cm. Possibly it is due to local heterogeneity in terms texture and structure of soil. In Punanaka Kfs was observed decreasing with depth along the longitude (Fig 4.28c).

In college site along longitude 5, Kfs was found decreasing with depth except at few location where Kfs at 45cm suddenly increased (Fig 4.29a) from lower value to higher value at 170m and for remaining distance it was found more than Kfs at 15cm and that at 30cm. In Mulegaon site, Kfs at three depths (Fig 4.29b) was found crossing each other violating the relation between them in terms of Kfs. In Punanaka the Kfs at 45 cm depth was found more than that at 30cm at most of the locations (Fig 4.29c).

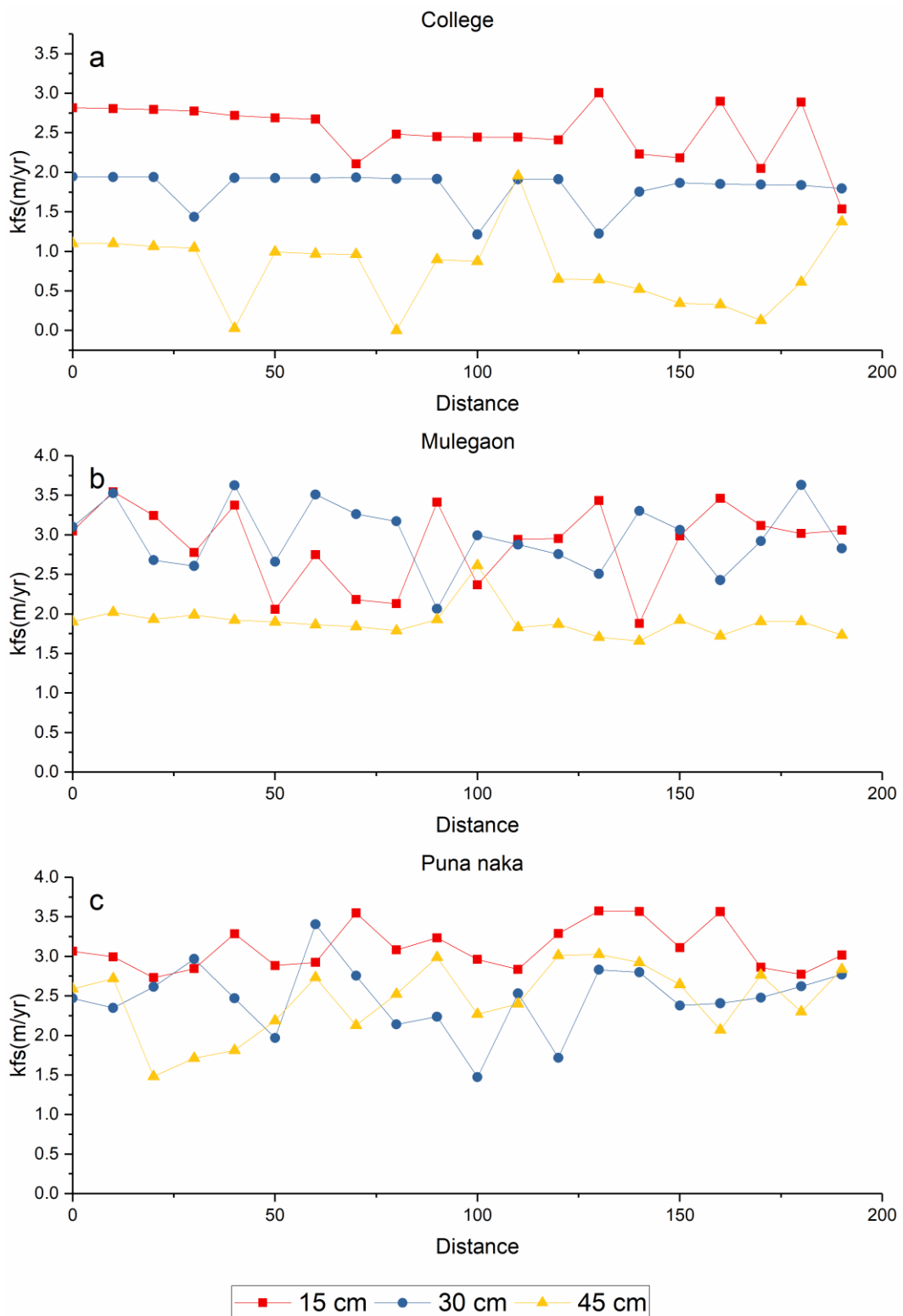


Fig 4.27 Variation of saturated hydraulic conductivity along the longitudinal 3 at 15cm, 30cm and 45cm depth in College, Mulegaon and Punanaka

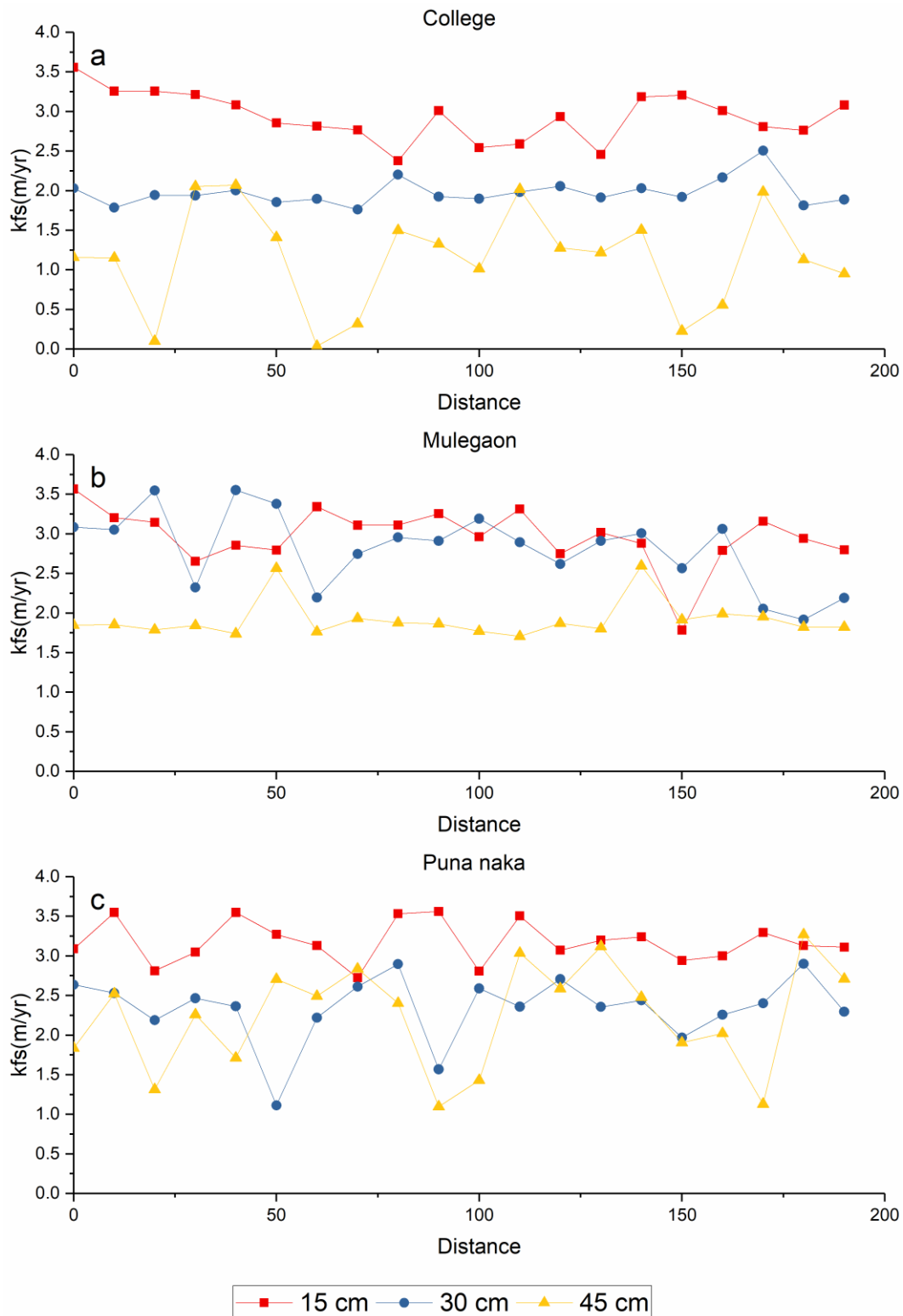


Fig 4.28 Variation of saturated hydraulic conductivity along the longitudinal 4 at 15cm, 30cm and 45cm depth in College, Mulegaon and Puna naka

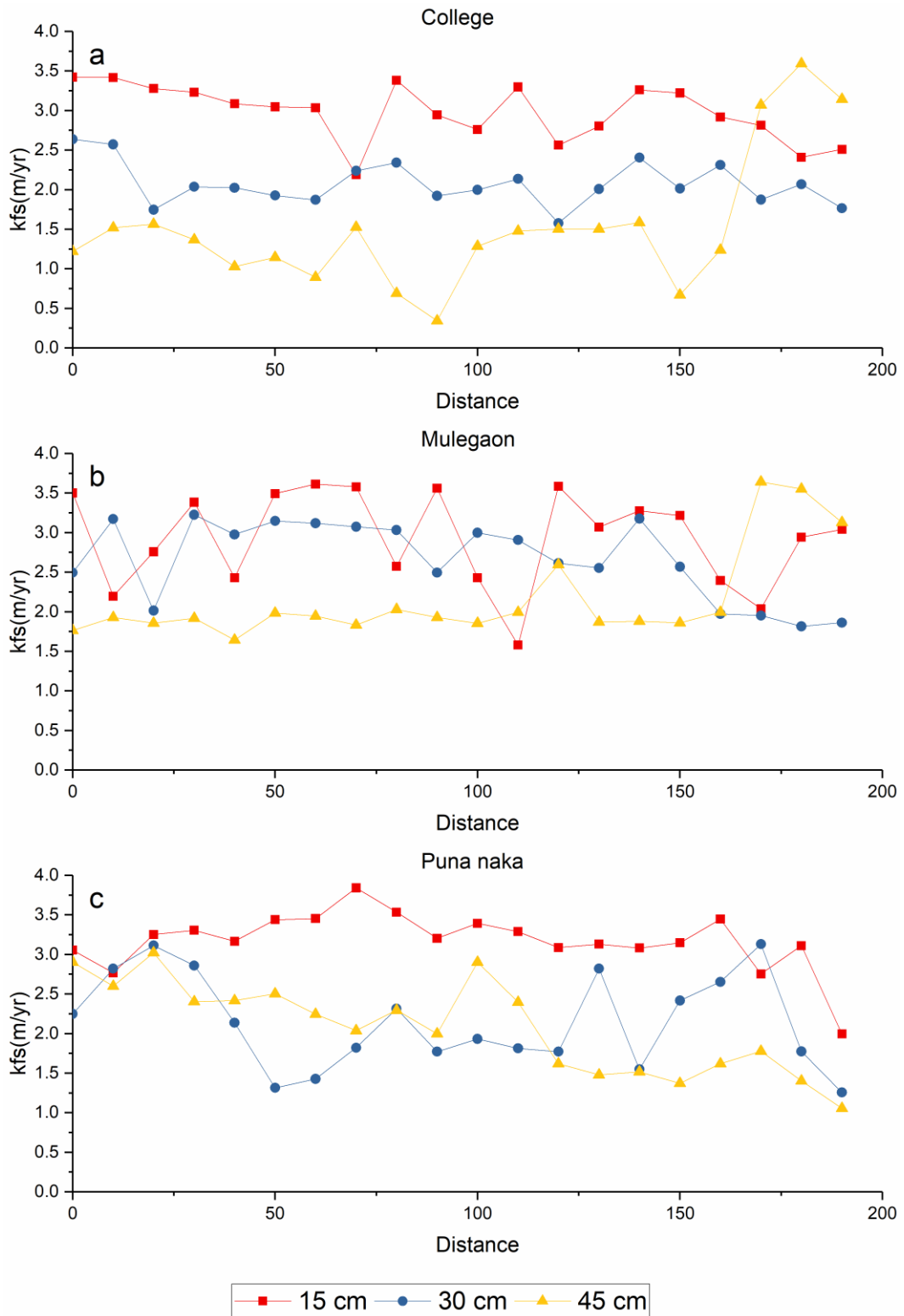


Fig 4.29 Variation of saturated hydraulic conductivity along the longitudinal 5 at 15cm, 30cm and 45cm depth in College, Mulegaon and Puna naka

4.3 TEXTURAL ANALYSIS OF SOIL

Blend of all textural class (Fig 4.30) was observed distributed at all sampling location; sandy texture was observed less as compared to clayey, silty, and loamy texture

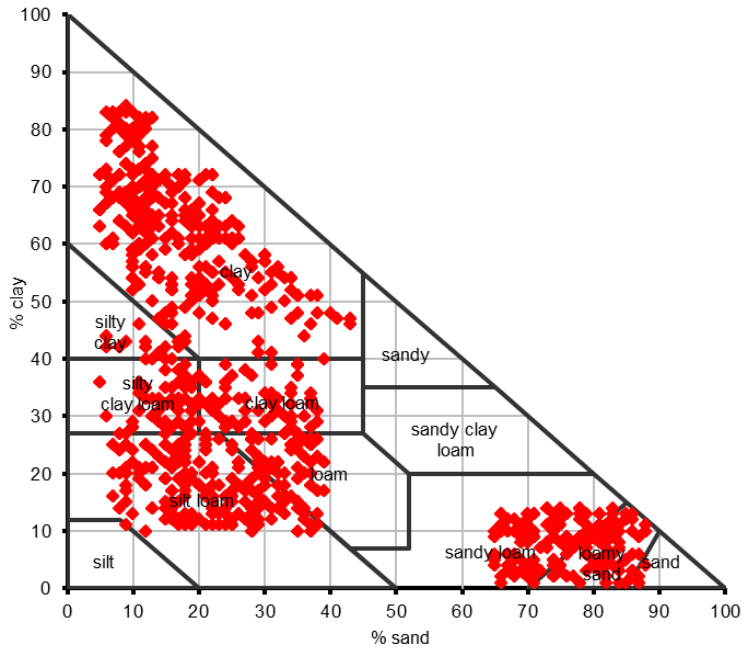


Fig 4.30 Textural distribution of soil across all three sites (College, Mulegaon and Punanaka)

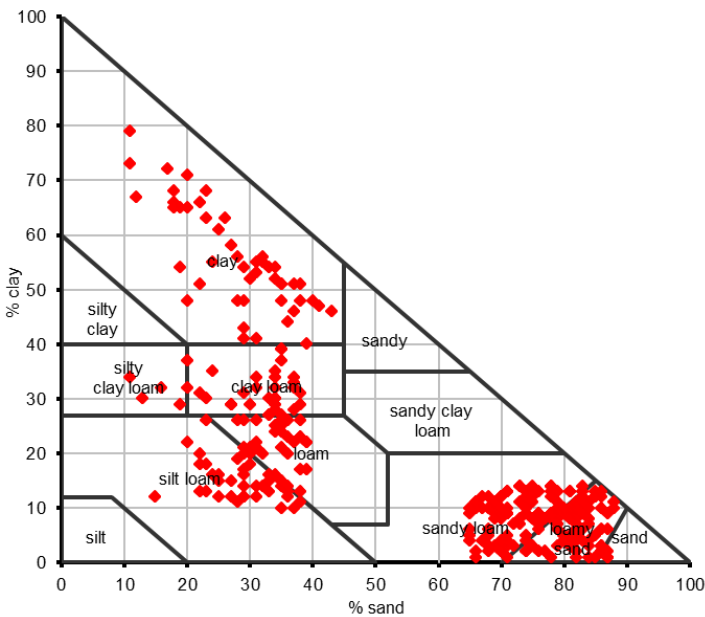


Fig 4.31 Textural distribution of soil across all three sites (College, Mulegaon and Punanaka) at 15cm depth.

Sand percentage available at 15cm depth is relatively more (Fig 4.31) as compared to other two textures so will have its dominance on saturated hydraulic conductivity at 15cm depth.

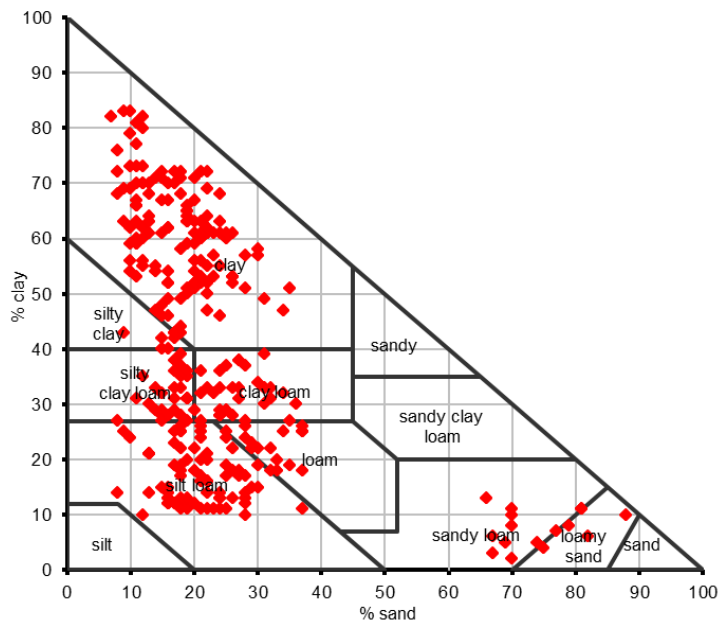


Fig 4.32 Textural distribution of soil across all three sites (College, Mulegaon and Punanaka) at 30cm depth.

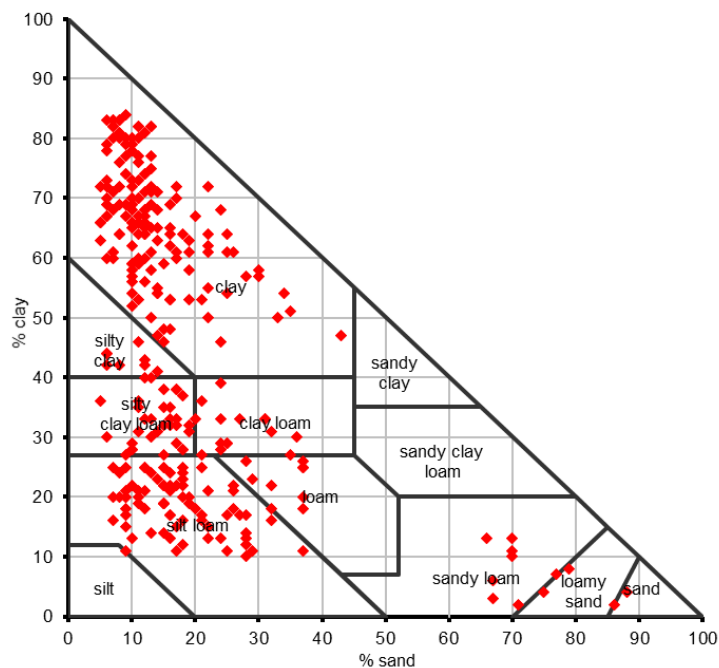


Fig 4.33 Textural distribution of soil across all three sites (College, Mulegaon and Punanaka) at 45cm depth.

Texture of soil (Fig 4.32 and 4.33) is more inclined towards silty, loamy and clayey texture. With depth soil texture changed from coarser to finer thus will have declining effect on the hydraulic conductivity, at few locations Kfs at 45cm found more Kfs at 15cm (Fig 4.29a and Fig 4.29b). The reason might be existence of root holes, wormholes in the soil at 45cm depth. There is no well-defined trend of variation of texture at all three depths implying randomness in its variation leading to heterogeneity of pore space and their interconnectivity.

4.4 LAND USE & LAND COVER

All the three land uses had similar statistical parameters for clay, silt and sand content (Table 4.1); the texture of these three sites were as shown in fig (4.6 – 4.8) as such there is no much difference in the overall texture of soil at these three locations; however there is noticeable difference in structure of soil, organic content of soil (Table 4.1). The effect of land cover and land use is predominant in the surface layer of soil (15cm depth) as compared to that at larger depth , although indirect effect of it is there to some extent on lower depth also. Land use and associated management (Mapa et al., 1986) are the most important and direct ways to affect soil structure and properties(Haynes et al., 1991; John et al., 2005; Ashagrie et al., 2007; Lehrsch et al., 2012). Mean value of Kfs at college site was 2.067 m yr^{-1} , that at Mulegaon was 2.576 m yr^{-1} and at Punanaka was 2.610 m yr^{-1} . This variation is attributed to change in land use of these three sites.

Mean value of Kfs at all three depths was least at College site (pastureland) as compared to other two sites, as it attracts cattle for grazing and the induced compaction, alteration in its structure. Similar results were obtained elsewhere by the by the researchers Tekin and Sabit (2006) found variability of Kfs in cultivated land was more than that in the virgin field by almost 2.5., Chen et al (2011) found that there is one order difference in the values of Ks at 25cm depth is lesser than that at surface soil for soil without vegetation.

4.5 MODELING:

Soft computing techniques namely ANFIS, SVM and ELM were used to develop pedotransfer function for the data measured at various depths below ground level and three different locations. Total data set from 3 sites and three depths (900) is split into smaller dataset for the modeling purpose into six subsets, which are as described below. Each sub data set has 300 data for all the parameters.

1. College station at all three depths (15cm, 30cm and 45cm)
2. Mulegaon station at all three depths (15cm, 30cm and 45cm)
3. Punanaka station at all three depths (15cm, 30cm and 45cm)
4. 15cm depth at all three location (College, Mulegaon and Punanaka)
5. 30cm depth at all three location (College, Mulegaon and Punanaka)
6. 45cm depth at all three locations. (College, Mulegaon and Punanaka)

Statistical analyses were carried out for all the samples. Results of statistical analysis were discussed in 4.1, for modeling purpose data need to be normally distributed which was checked by using QQ plot and it was found the Kfs is log normalized, thus all datas were log transformed (similar treatment was given by –Airmun and Amin., 2009; Hu et al., 2013). Data driven techniques usually perform well when the range of values of all parameters are same; to meet this requirement further datas were normalized by using an equation as discussed in section 3.5.

Normalized data at each sampling (location/depth) is split into two dataset one is used for training the network and validity of the model after training is tested by using other subset. Each dataset (300samples) were divided into six combinations for training and validation of each of these models. Optimum modeling parameters of each model were determined for all these six combination and the best model amongst them was determined based on the performance criteria. The details of these things are discussed below.

4.5.1 Training / testing data set: For each of three models following trials were carried out by segregating data into training and testing (validation) to determine the ideal model. For segregating data, data were arranged in order (descending / ascending) and then every nth element (3rd, 6th, 9th etc.) from this is segregated to get dataset for validation.

Table 4.15 Sample distribution for training and validating model

Trial	Training data set		Testing dataset	
	% of total data	No. of data	% of total data	No. of data
I	90	270	10	30
II	85	255	15	45
III	80	240	20	60
IV	75	225	25	75
V	70	210	30	90
VI	67	200	33	100

4.5.2 Development of Models.

a) ELM model

Three-layer architecture was adopted for ELM model development. The first layer (Input layer) used various soil parameters as inputs. The output layer had one neuron representing the estimated saturated hydraulic conductivity (Kfs). For the hidden layer maximum of 100 neuron were tested for each model. Initially one neuron was selected and subsequently the number of neurons was gradually increased up to 100 by an interval of 1. Radial basis activation function was employed for all ELM models tested.

Table 4.16 ELM model parameters.

Model	Hidden layer	Number of neurons in the hidden layer	Data used for training
ELM-CO	01	15	90 %
ELM-MU	01	28	70 %
ELM-PN	01	10	67 %
ELM-15	01	12	75 %
ELM-30	01	11	75 %
ELM-45	01	15	80 %

b) SVM model:

In this study, the SVM regression was performed in two stages i) training and ii) testing. Data were normalized between 0.05 and 0.95 before modeling. The normalized dataset was used to develop the SVM regression model. The output results obtained were denormalised. During training stage SVM parameters C (cost function), kernel width (γ) and insensitive value (ϵ) are optimized by using thorough grid search. These hyper parameters are interdependent and thus the possible combination of these three parameters will be chosen based on grid search method.

In grid search method is time consuming two step grid search method suggested by Hsu et al. (2003) was used wherein initially coarse grid search is applied keeping wide range for the parameters with big increment (say 2^{-15} to 2^{15} with increment of 2 in the exponent) to obtain the best region of these parameters. Then in that region finer grid search for each parameter. The hyperparameter were optimized by estimating the mean square error for every possible combination of these three parameters, the combination of hyper parameter which results in minimum value of mean square error during training will be taken as optimum hyperparameters. To avoid danger of over fitting four fold cross validation approach is used during training phase. LIBSVM software developed by Chang and Lin (2001) is used for analysis and calculation.

Table 4.17 SVM model parameters

Model	Hyper parameter			Number of Support vectors	Data used for training the model
	C	Gamma	epsilon		
SVM-CO	34.67	0.0323	0.00097656	38	90 %
SVM-MU	18.34	0.0418	0.0000488	35	70 %
SVM-PN	0.5548	16.2234	0.0078	33	67 %
SVM-15	0.1250	8.5742	0.0018	28	75 %
SVM-30	10.76	3.427	0.035	34	75 %
SVM-45	12.37	4.867	0.00043	42	80 %

c) ANFIS model:

In this model Fuzzy, c means (FCM) clustering algorithm is used to divide the dataset into clusters Fuzzy *C-means* (FCM) is a soft data clustering technique wherein each data point belongs to a cluster to some degree that is specified by a membership grade. (0 to 1). The algorithm used for clustering is described below

1). $U = [u_{ij}]$ matrix, $U^{(0)}$

At k – step: calculate the centers vectors $C^{(k)} = [c_j]$ with $U^{(k)}$

2) $C_i = \frac{\sum_{j=1}^n u_{ij}^m x_j}{\sum_{j=1}^n u_{ij}^m}$

3) Update $U^{(k)}, U^{(k-1)}$

4) $d_{ij} = \sqrt{\sum_{i=1}^n (x_i - c_i)^2}$

$$u_{ij} = \frac{1}{\sum_{k=1}^c \left(\frac{d_{ij}}{d_{ki}}\right)^{2/(m-1)}}$$

5) If $\|U(k+1) - U(k)\| < \varepsilon$ then stop; otherwise return to step 2

where m – any real number greater than 1 (~2) u_{ij} degree of membership of x_i in cluster j x_i is the i th of d – dimensional measured data

c_j is the d dimension center of cluster

ε is a termination criterion between 0 and 1,

k are the iteration steps.

Table 4.18 ANFIS model parameters.

Model	ANFIS model parameters		Data used for training
	No. of rules.	No. of clusters	
ANFIS – CO	14	12	90 %
ANFIS – MU	15	18	70 %
ANFIS – PN	13	18	67 %
ANFIS – 15	10	4	75 %
ANFIS – 30	17	6	75 %
ANFIS – 45	15	16	80 %

This procedure converges to a local minimum or a saddle point of J_m .

In fuzzy c-means algorithm the number of clusters has to be set arbitrarily, i.e. the number of clusters to be created by the clustering algorithm must be set manually on each algorithm execution; this is done repeatedly until we get optimal number of clusters based on the objective function. Numbers of clusters were tried manually between 2 and 20 with an increment of one. For each of the dataset.

4.5.3 Performance evaluation of models:

Performances of the models were tested by using coefficient of correlation (R), mean relative error (MRE), normalized root mean square error [(NRMSE), close to zero is better] and Nash – Sutcliffe efficiency (NSE).

The performance metrics of training dataset and testing dataset are shown in Table 4.17 to 4.22 for all six dataset segregated for modeling purpose. Scatter plot between observed and predicted value of the saturated hydraulic conductivity by using ELM, SVM and ANFIS are presented in Fig 4.33 to Fig 4.37.

a) College model:

Table 4.19 Performance comparison of models for College (90% training and 10% testing)

Model	Training			Testing		
	ELM	SVM	ANFIS	ELM	SVM	ANFIS
R	0.97	0.77	0.78	0.96	0.52	0.58
MRE	0.02	0.07	0.06	0.18	0.60	0.58
RMSE (myr ⁻¹)	73.01	257.12	217.52	219.03	771.37	652.55
NRMSE	0.02	0.07	0.06	0.06	0.21	0.18
NSE	0.95	0.16	0.60	0.90	0.18	0.15

R-value for training and testing for ELM model (0.97 and 0.96) performance was found good in comparison to other two models. MRE of ELM in training is 0.02 which (~0) and is less than that for other two models.(Table 4.19). In terms of NSE also ELM performance is very good during training and testing. NRMSE of SVM and ANFIS are relatively good for training however, for testing it is more in comparison to ELM. The scatterplot of observed v/s predicted Kfs is shown in fig 4.34 along with 1:1 line. The predicted values of Kfs by ELM methods are close to the 1:1 line in

comparison with that of other two methods both during and training and testing phase. Prediction by SVM method during training and testing by SVM were below 1:1 line indicating it fails to predict the Kfs, model is under fitting the values both during training and during testing phase.

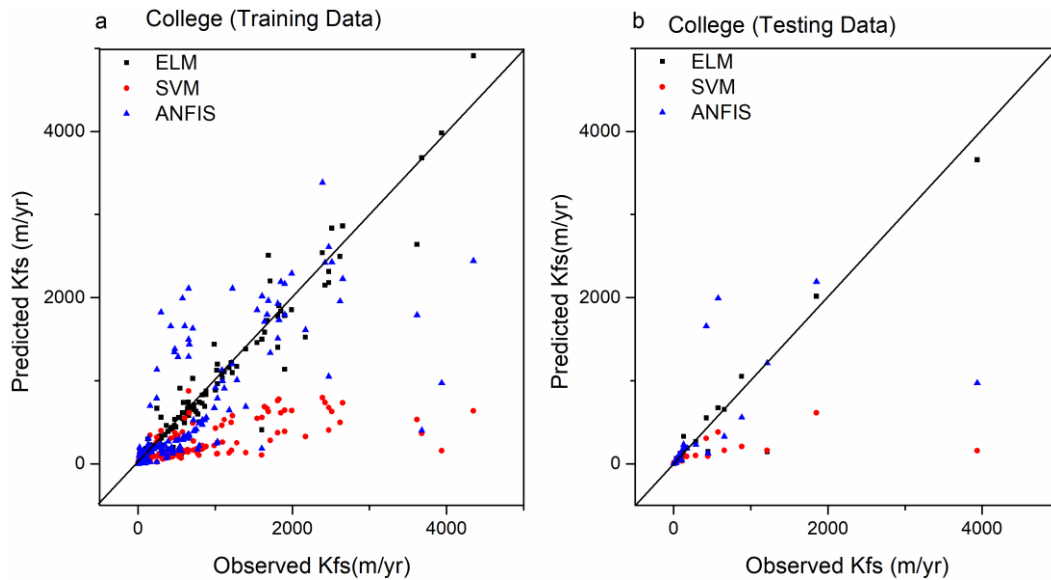


Fig 4.34 Scatter plot of predicted Kfs V/S observed Kfs for college station during training (a) and testing (b)

ANFIS prediction are scattered around 1:1 line minority values are over predicted (for smaller values of Kfs) and majority values are under predicted (for higher values of Kfs). Box plot of observed Kfs and estimated Kfs by ELM, SVM and ANFIS method is shown in Fig 4.35. median of observed Kfs and Kfs estimated by all methods is roughly same. Data distribution in lower quartile (0 – 25%) is dense in observed and predicted Kfs. Box plot of SVM both during training and testing is very compact implying values are very close (dense), it is very effective in predicting lower values but fails to predict higher values of Kfs. implying it fails to predict higher values of Kfs.

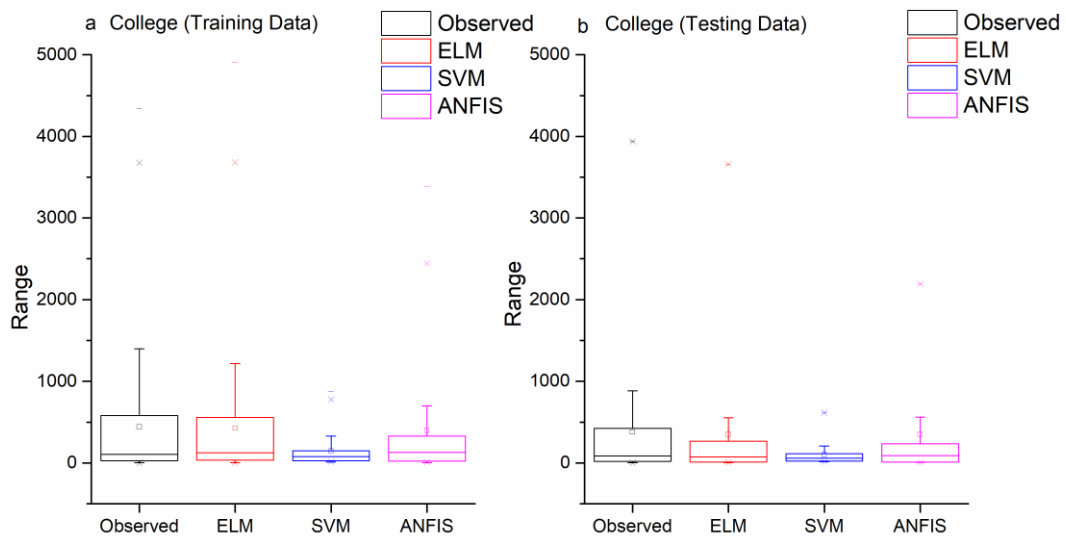


Fig 4.35 Box plot of Kfs, for observed and predicted values by ELM,SVM and ANFIS a) during training and b) during testing at College site.

b) Mulegaon Model:

In terms of statistical parameters, performance of ELM was found very good

Table 4.20 Performance comparison of models for Mulegaon (70% training data and 30% testing)

Model	Training			Testing		
	ELM	SVM	ANFIS	ELM	SVM	ANFIS
R	0.94	0.80	0.87	0.88	0.74	0.80
MRE	0.05	2.29	1.08	0.88	1.60	0.63
RMSE (myr ⁻¹)	332.23	978.60	495.34	411.91	631.70	378.04
NRMSE	0.07	0.22	0.11	0.09	0.14	0.09
NSE	0.87	0.48	0.72	0.58	0.34	0.64

Compared to SVM and ANFIS model as depicted in Table 4.20, both during training phase (R = 0.94) and testing phase (R = 0.88). SVM and ANFIS value for R are far below these values during training and testing. NRMSE for ELM is close to zero and NSE is close to one both are indicators of good model Performance.

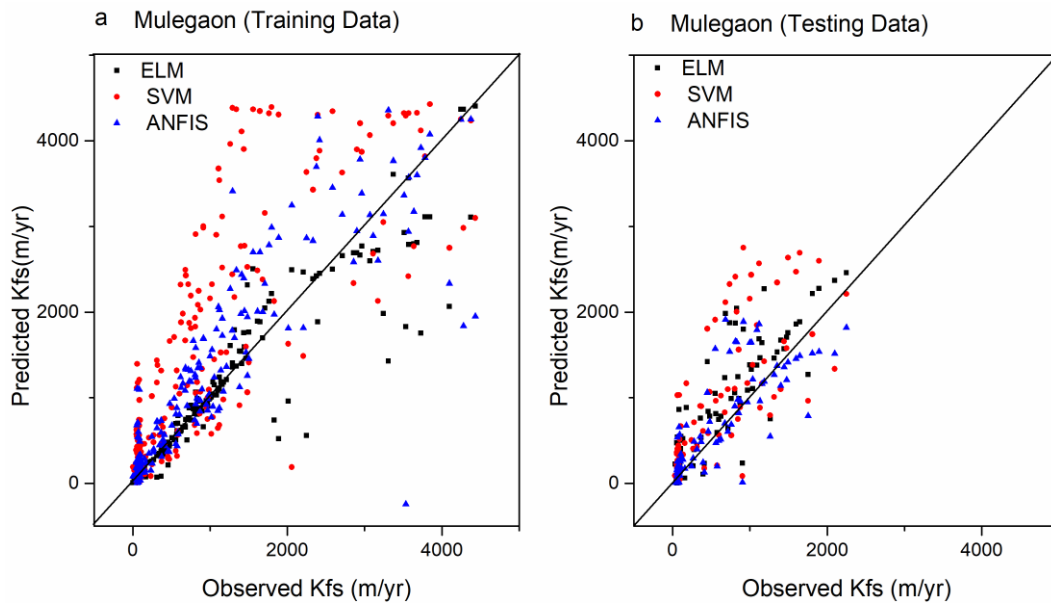


Fig 4.36 Scatter plot of predicted Kfs V/S observed Kfs for Mulegaon station during training (a) and testing (b)

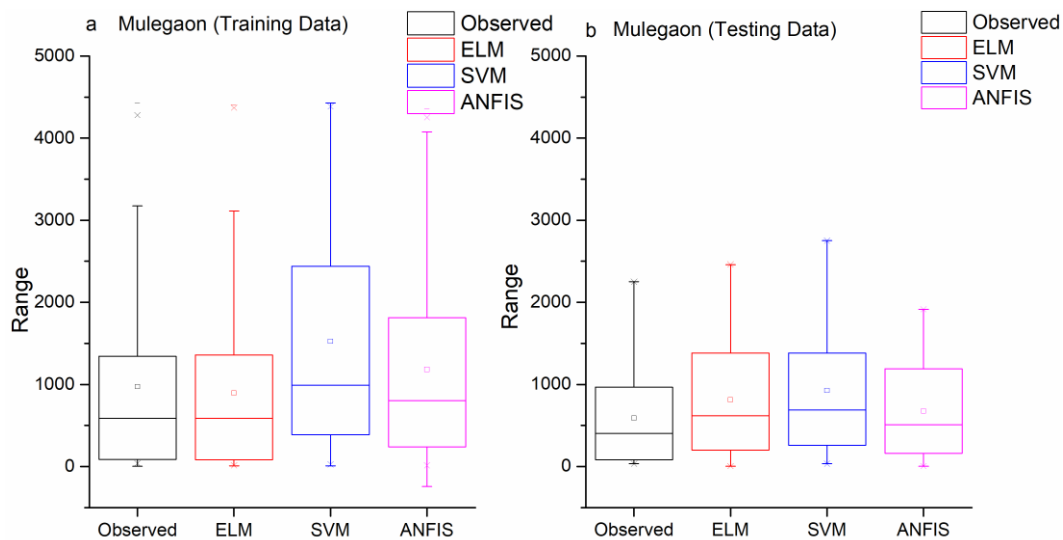


Fig 4.37 Box plot of Kfs, for observed and predicted values by ELM, SVM and ANFIS a) during training and b) during testing at Mulegaon site.

SVM was found relatively poor than ANFIS both during training and during testing. The scatterplot of observed v/s predicted Kfs is shown in fig 4.36a and 4.36b along with 1:1 line. Most of the predicted values of Kfs by ELM methods are close to the 1:1 line in comparison with that of other two methods both during and training and testing phase. During training the ELM under predicted the values while during testing it was over predicting. Prediction by SVM method during training and testing

was not satisfactory (over predicted). ANFIS prediction are scattered around 1:1 for smaller values of Kfs prediction by ANFIS was close to observed values but for higher values it was not able to predict accurately. Box plot for Observed Kfs and estimated Kfs by various methods is shown in Fig 4.37 Box plot of ELM is mirror image of that of observed indicating its excellent predictive capability during training. Box plot of SVM during training is highly distorted with respect to box plot for observed Kfs, implying poor predictive capability. During testing lower whisker for all is same. This indicates all model are efficient in predicting smaller values of Kfs.

c) Punanaka Model:

Correlation coefficient of ELM during training and testing was found more than 0.9.

Table 4.21 Performance comparisons of models for Punanaka (67% Training data and 33% Testing data)

Model	Training			Testing		
	ELM	SVM	ANFIS	ELM	SVM	ANFIS
R	0.99	0.85	0.85	0.94	0.63	0.78
MRE	0.07	1.91	0.90	0.71	1.41	1.44
RMSE (myr ⁻¹)	161.99	627.76	460.74	464.83	904.75	733.03
NRMSE	0.02	0.09	0.07	0.07	0.13	0.11
NSE	0.97	0.59	0.78	0.83	0.37	0.59

NSE value close to 1 during training with NRMSE close to zero sign of good model however its performance during testing was not at par with that during training phase (NSE = 0.62). SVM and ANFIS correlation coefficient during training and testing phase was same but in terms of MRE, NRMSE and NSE, SVM was found poor than ANFIS (Table 4.21), during training and testing. Barring few outliers, all predicted values (Fig 4.38a and Fig 4.38b) are closely spread along the line 1:1 by ELM method both during training and during testing phase. SVM was found overestimating the Kfs during training and testing whereas ANFIS prediction were found closely spread around the 1:1 line on either side of line 1:1, but for higher values it was found underestimating both during training and testing phase.

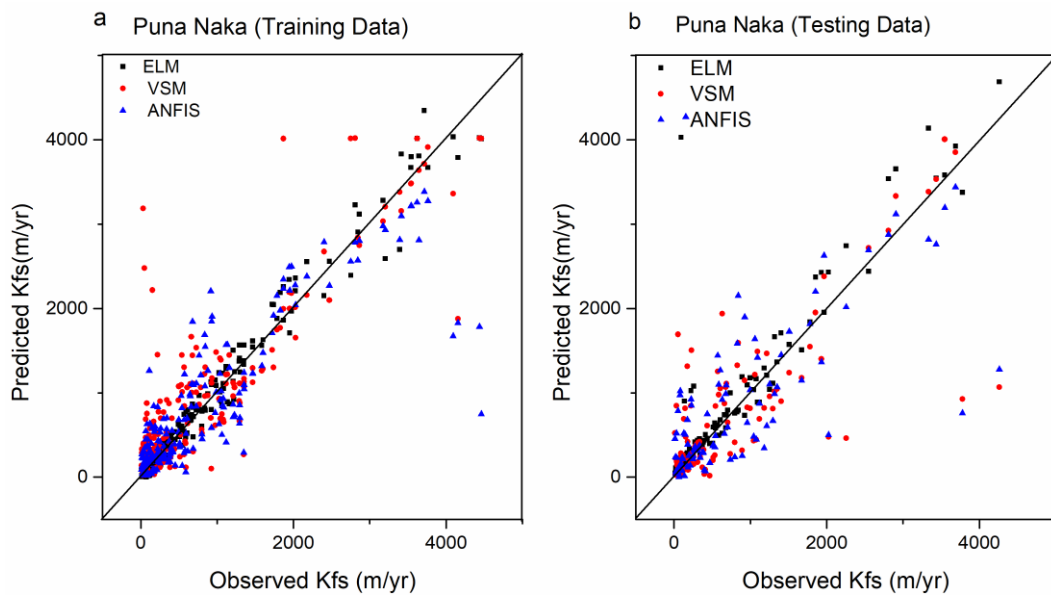


Fig 4.38 Scatter plot of predicted Kfs V/S observed Kfs for Puna Naka station during training (a) and testing (b)

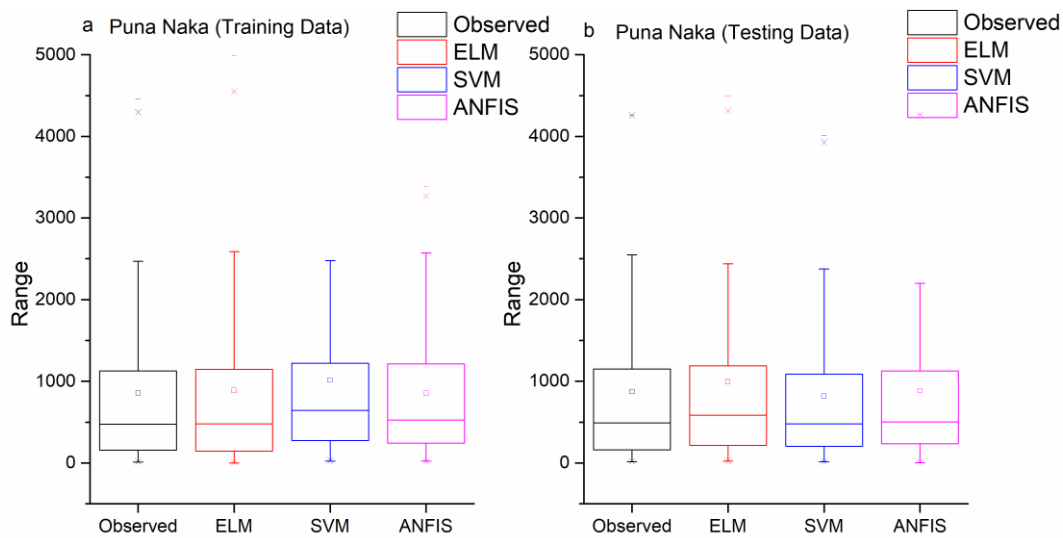


Fig 4.39 Box plot of Kfs, for observed and predicted values by ELM, SVM and ANFIS a) during training and b) during testing at Mulegaon site.

Box plot for observed Kfs and estimated Kfs by ELM, SVM and ANFIS is depicted in Fig 4.39. Data distribution in observed value of Kfs and predicted value of Kfs is identical during during training and testing. Median of observed Kfs and that predicted by ELM during training and testing is approximately same. However, slight variation is observed in median value predicted.

d) **15cm depth model:**

Table 4.22 Performance comparison of models for 15cm depth (75% training and 25% testing)

Model	Training			Testing		
	ELM	SVM	ANFIS	ELM	SVM	ANFIS
R	0.98	0.85	0.91	0.92	0.78	0.72
MRE	0.02	0.21	0.24	0.21	0.31	0.25
RMSE (myr ⁻¹)	198.71	559.91	429.49	527.09	762.39	838.11
NRMSE	0.03	0.08	0.06	0.08	0.11	0.12
NSE	0.96	0.72	0.83	0.81	0.59	0.51

The R-value during training / testing for ELM, SVM and ANFIS model performance was found good as depicted in Table 4.22. During training in terms of all performance parameters with NSE of 0.83 against that of 0.72 of SVM; however, performance of SVM was slightly better than ANFIS during testing. Performance of ELM was outstanding than other two methods during training and testing phase with NSE of 0.96 during training and 0.81 during testing.

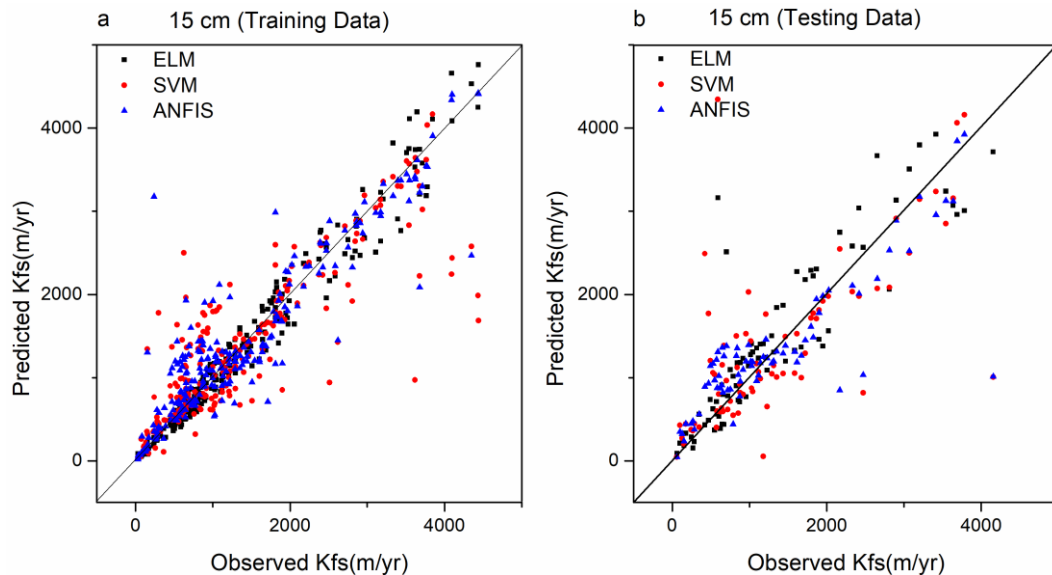


Fig 4.40 Scatter plot of predicted Kfs V/S observed Kfs for 15cm depth during training (a) and testing (b)

ELM prediction values are close to the observed values as depicted in Fig 4.40a and Fig 4.40b for lower values of Kfs both SVM and ANFIS overestimated the Kfs, whereas for higher values of Kfs the both these methods have underestimated the values of Kfs.

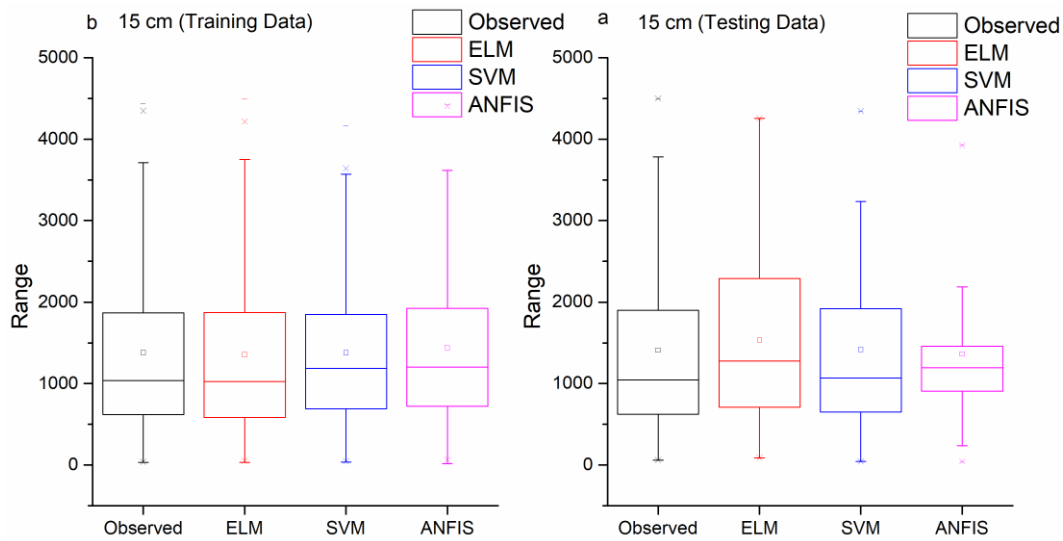


Fig 4.41 Box plot of Kfs, for observed and predicted values by ELM, SVM and ANFIS a) during training and b) during testing at 15cm depth.

Range of data values for measured and predicted Kfs during (Fig 4.41) training was found identical at 15cm depth. Median value of observed Kfs and that estimated by ELM is almost same. However, Median values of Kfs estimated by SVM and ANFIS is slightly more. During testing Kfs predicted values are densely arranged as compared to that predicted by other two methods.

e) 30cm depth model:

Table 4.23 Performance comparison of models for 30cm depth (75% training and 25% testing)

Model	Training			Testing		
	ELM	SVM	ANFIS	ELM	SVM	ANFIS
R	0.90	0.82	0.90	0.87	0.78	0.77
MRE	0.79	0.20	0.69	0.89	1.19	0.51
RMSE (myr^{-1})	329.33	456.65	451.67	426.36	515.87	569.81
NRMSE	0.07	0.10	0.10	0.10	0.12	0.13
NSE	0.81	0.64	0.65	0.73	0.61	0.52

Correlation coefficient of SVM during training (0.82) was lower than that for ANFIS (0.90) however, for testing the performance of SVM was found slightly better. Correlation coefficient of SVM during training (0.82) was lower than that for

ANFIS (0.90), however for testing the performance of SVM was found slightly better than ANFIS in terms of R. Both during and training the correlation coefficient (Table 4.23) for ELM was found better than other two methods. NRMSE of ELM better than ANFIS in terms of R. Both during and training the correlation coefficient

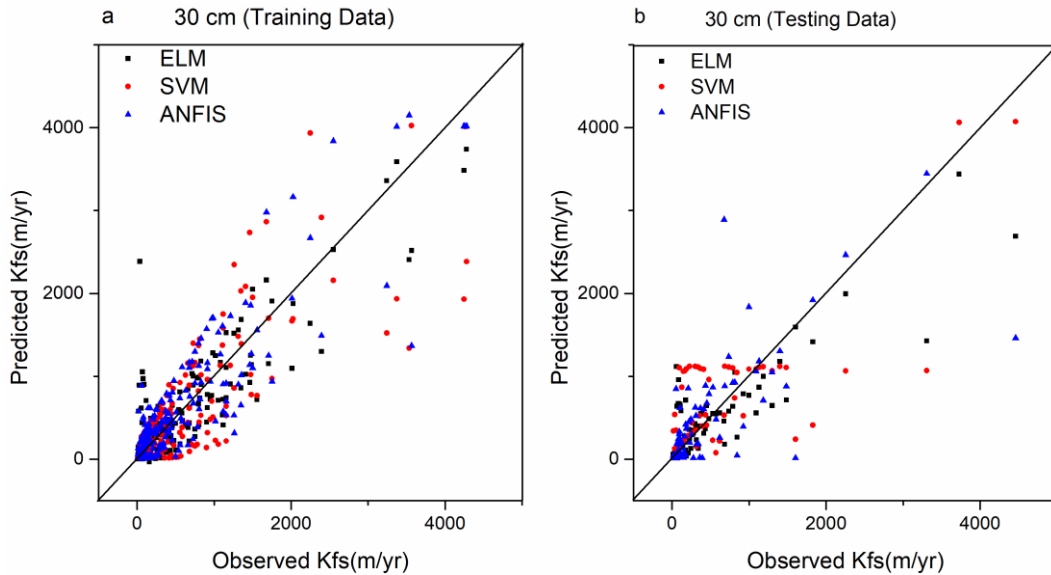


Fig 4.42 Scatter plot of predicted Kfs V/S observed Kfs for 30cm depth during training (a) and testing (b)

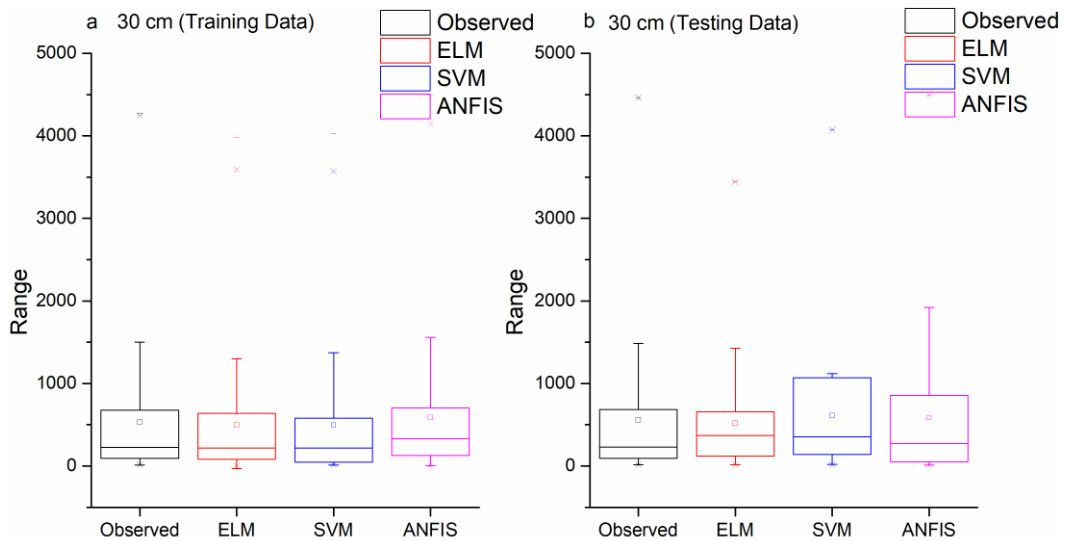


Fig 4.43 Box plot of Kfs, for observed and predicted values by ELM, SVM and ANFIS a) during training and b) during testing at 30cm depth.

Correlation coefficient of SVM during training (0.82) was lower than that for ANFIS (0.90) however, for testing the performance of SVM was found slightly

better than ANFIS in terms of R. Both during and training the correlation coefficient (Table 4.23) for ELM was found better than other two methods. NRMSE of ELM during training was found 0.07, which is smaller than that of SVM (0.10) and ANFIS (0.10). Scatter plot of the predicted V/S observed Kfs at 30cm depth is shown in Fig 4.43. Prediction of all three methods is good for smaller values of Kfs, however for higher values of Kfs. Prediction of all these methods deviate from observed values either on higher side or on lower side. Box plot of observed Kfs , and Kfs predicted by ELM, SVM and ANFIS is shown in Fig 4.43. Variation of Kfs between 25% and 50% values is least during training by all methods, but during testing this variation is more by all three methods. Distribution of data estimated by SVM during training is spread large as compared to other methods.

f) 45cm depth model:

Table 4.24 Performance comparison of models for 45cm depth (80% training data and 20% testing data)

Model	Training			Testing		
	ELM	SVM	ANFIS	ELM	SVM	ANFIS
R	0.99	0.80	0.97	0.94	0.70	0.87
MRE	0.33	3.39	1.55	1.48	0.70	6.72
RMSE (myr ⁻¹)	34.74	288.73	114.21	164.65	475.73	360.42
NRMSE	0.008	0.06	0.03	0.04	0.11	0.08
NSE	0.99	0.67	0.94	0.94	0.50	0.71

ANFIS performance (Table 4.24) was at par with that of ELM model during training (R = 0.97) but SVM performance was relatively inferior with R = 0.80, and during testing (R = 0.87) also, performance of SVM was poor compared to other two models. MRE of ELM (0.33) during training is far below as compared to other two models. However, during testing MRE of SVM (0.70) is lower than that of ELM (1.48). Predictive capability of ELM was good both in training and testing as depicted in Fig 4.43, ANFIS and SVM predicted good during training barring few outliers , but during testing their performance is not satisfactory as it is deviating away from observed value (either higher side or lower side).

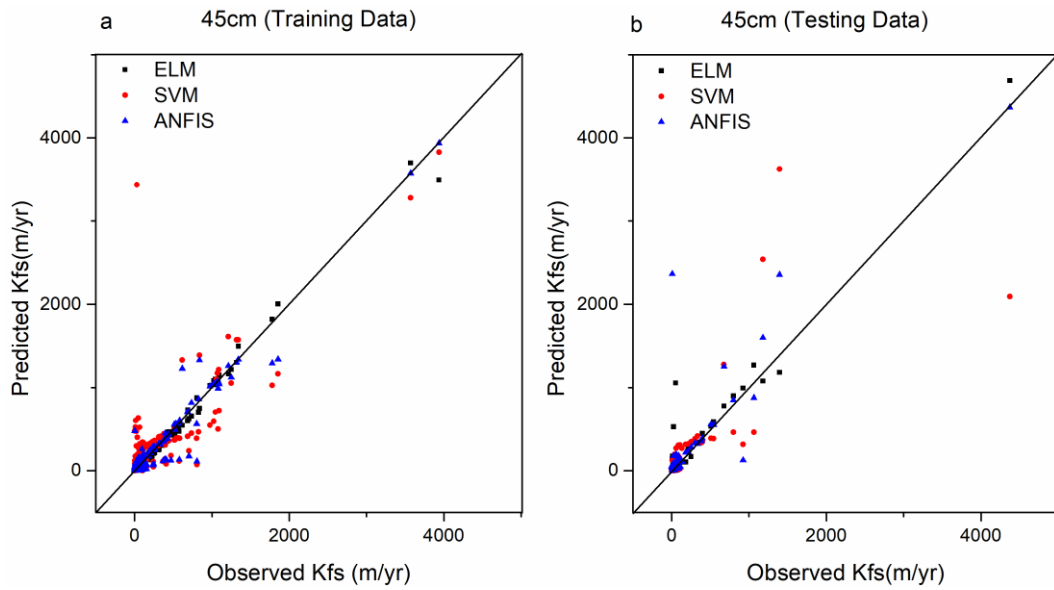


Fig 4.44 Scatter plot of predicted Kfs V/S observed Kfs for 45cm depth during training (a) and testing (b)

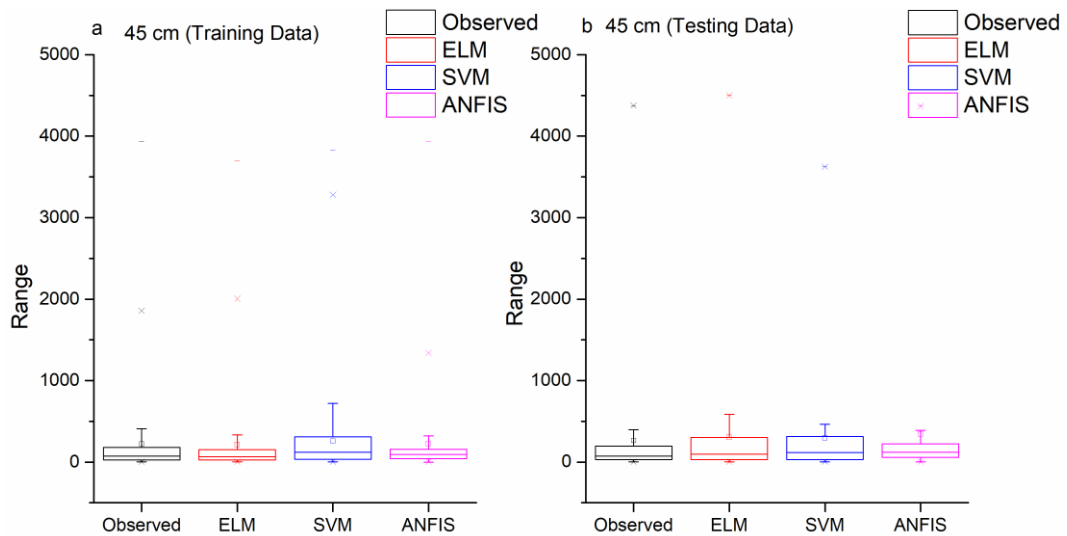


Fig 4.45 Box plot of Kfs, for observed and predicted values by ELM, SVM and ANFIS a) during training and b) during testing at 30cm depth.

Predicted value of Kfs by ANFIS during training (Fig 4.45) as well as during testing is more concise (less spread) as compared to other methods. Spread in Kfs by SVM. Lower whisker for observed and predicted values of Kfs, during training and testing is similar. This indicates that prediction by all methods is good for lower values of Kfs.

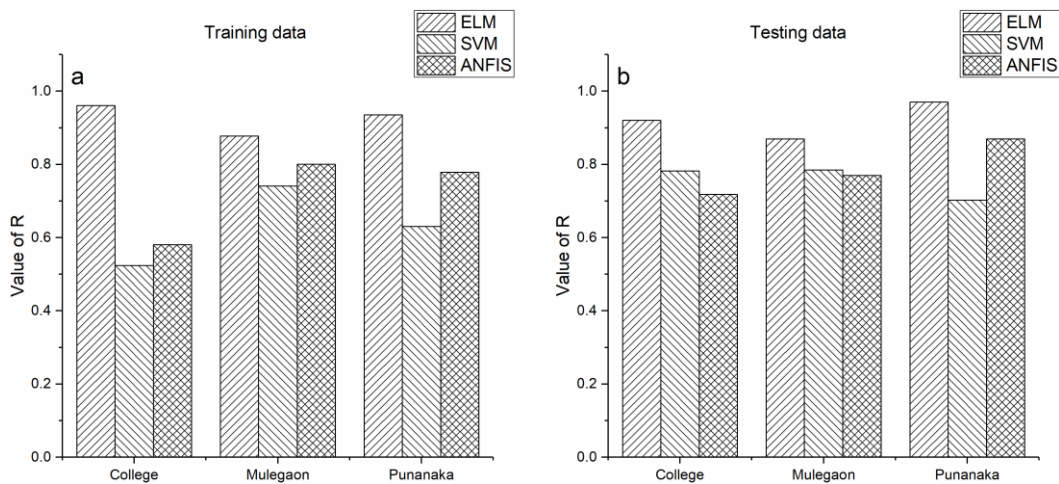


Fig 4.46 Bar chart showing the variation of R at various sampling station a) during training and b) during testing

To have an overall variation of R for all sites and all depths, bar charts are presented in Fig 4.45 and Fig 4.46. Performance of various models at various sampling stations is shown in fig 4.38. The value of R was found more than 0.9 during training at all sampling location. R-value for SVM in college model is relatively poor during testing.

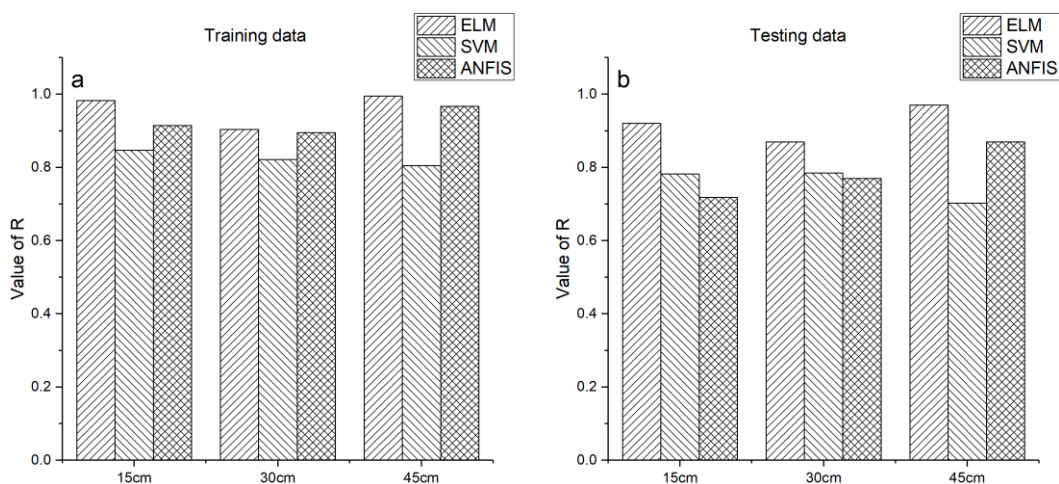


Fig 4.47 Bar chart showing the variation of R at various sampling depth a) during training and b) during testing

Predictive capability of ELM model and ANFIS model in terms of R is more or less same during training but during testing, ELM capability is superior to that of ANFIS. (Fig 4.46).

5.1 SUMMARY

This study aims to develop various soft computing models to estimate saturated hydraulic conductivity from index properties of the soil. The process involved in doing it is explained here briefly. The site where measurements are to taken is divided into small grids of size 10m X 10m. An in situ measurement of Kfs of soil is carried out at the corner points of all such grids at three depths (15cm, 30cm and 45cm) by using Guelph permeameter. Soil samples were collected from 15cm depth, 30cm depth and 45cm depth at all three sampling stations by using cylindrical container, immediately after field measurement at one depth is over. The samples were taken to the laboratory and then tested to estimate index properties of it. Statistical analysis of the measured data (Laboratory and field) was carried out to check the distribution of the data and its variability. Normality of the data was checked by using QQ plot and it was found that data's are not showing normal distribution. Data are log transformed to ensure the normal distribution. Before modeling data's were normalized between 0.05 and 0.95 by using min – max normalization. Total dataset is segregated into six sub dataset (college, Mulegaon, Punanaka, 15cm, 30cm and 45cm). Each subset is further split into two parts in six different ways (90% + 10%, 85% + 15%, 80% +20%, 75% + 25%, 70% + 30%, and 67% + 33%) to train the models and validate it, the combination which gives good results during training and validation is selected. For checking performance of model various statistical parameters such as correlation coefficient (R), mean relative error (MRE), root mean square error (RMSE), normalized root mean square error (NRMSE) and Nash Sutcliffe efficiency (NSE). Scatter plots were used to evaluate the accuracies of the models. For deciding best model these checks are used, Value of R ~ 1, value and NSE ~ 1, MRE close to zero, and NRMSE is close to zero. Scatter plot point distribution should be around and close to 1:1 line.

5.2 CONCLUSIONS

Based on the study carried out following conclusion were drawn

5.2.1 Main finding of the work

- a) Saturated hydraulic conductivity found to vary in vertical direction (along the depth) as well as horizontal direction (lateral / longitudinal)
- b) In general Kfs was found decreasing with the depth of soil
- c) Land use land cover has significant influence on Kfs.
- d) Kfs found decreasing down the slope
- e) ELM model outperformed other two models such as ANFIS and SVM in modeling Saturated Hydraulic Conductivity for the site considered.

5.2.2 Conclusion drawn from the study

- a) Variability in Kfs was found more at College site as compared to other two sites
- b) Variability of Kfs was found more at 45cm depth at college site as compared to other two depths (15cm and 30cm)
- c) Variability of porosity, bulk density and specific gravity of soil was insignificant in logarithmic scale as compared to other soil parameters at all depth and all sampling stations.
- d) Soil texture was found declining from coarser to finer with depth at majority of sampling locations.
- e) Blend of all nine textural class of soil was found distributed in all sampling location and depth, sand % dominated at 15cm depth, at 30cm and 45cm blend of fine texture (clay,silt and loam was observed)
- f) Mean value of Kfs at puna naka site (15cm depth) was found relatively more in logarithmic scale as compare to that at other two sites.
- g) Mean value of Kfs was found least at 45cm depth in college site.
- h) Maximum Standard deviation (0.804 myr^{-1}) was found at College and minimum standard deviation (0.296 myr^{-1}) was found at Punanaka 15cm depth
- i) Pearson correlation coefficient of porosity (positive) was found dominant at all depths and all locations. Maximum correlation of porosity was found at 15cm depth (0.9) in college site.

- j) Pearson correlation coefficient of bulk density (negative) was dominating at all location and depth, its maximum value (-0.9) was found at Mulegaon.
- k) Performance of ELM model was excellent at all six sub classes of data (College, Mulegaon, Punanaka, 15cm, 30cm, and 45cm) in terms of all statistical performance criteria's both during training and testing .
- l) The performance of SVM and ANFIS are almost at par in modeling modeling Saturated Hydraulic Conductivity for the site considered

5.2.3 Limitation of study:

- a) Though Guelph permeameter has lot many advantages but it also has limitations. It will reflect the Kfs value of soil within the zone of wetted zone of soil around the well. In order to get representative value of Kfs more number of observations needs to be taken along depth as well as horizontally. Presence of local heterogeneity within the zone of influence may give wrong results.
- b) To detect spatial variability of saturated hydraulic conductivity more closer spaced points need to be taken as well as observations need to be taken at more depths which is costly in terms of time.
- c) Only three methods were explored to develop the model, though performance of ELM model is good in training but its performance in testing is not satisfactory as reflected by the values of R, NSE, MRE, and NRMSE.

5.2.4 Suggested direction for future work

- a) Looking at the limitation of the instrument used, we need to explore latest digital equipment having data acquisition facility for measurement of Kfs.
- b) Model results for testing were not satisfactory. So we need to explore other technique or some kind of hybridization of the model to improve predictability during testing
- c) Only soil physical properties were taken as input, other properties of the soil (chemical) need to be explored particularly in case of fine grained soil which may have influence on hydraulic conductivity.

5.2.5 Contribution from the thesis:

The result of thesis can be useful to various hydrological models that will be developed in semiarid area as it is an important input parameter for the model and thus following agencies will get benefitted from the work such as agriculture, waste management, irrigation, environment and ecology and water resource management.

REFERENCES

- Aimrun, W., & Amin, M. S. M. (2009). "Pedo-transfer function for saturated hydraulic conductivity of lowland paddy soils." *Paddy and Water Environment*, 7(3), 217–225.
- Alagna, V., Bagarello, V., Di Prima, S., Giordano, G., & Iovino, M. (2016). "Testing infiltration run effects on the estimated water transmission properties of a sandy-loam soil." *Geoderma*, 267, 24–33.
- Alletto, L., & Coquet, Y. (2009). "Temporal and spatial variability of soil bulk density and near-saturated hydraulic conductivity under two contrasted tillage management systems." *Geoderma*, 152(1–2), 85–94.
- Amoozegar, A. (1989). "A Compact Constant-Head Permeameter for Measuring Saturated Hydraulic Conductivity of the Vadose Zone." *Soil Science Society of America Journal*, 53(5), 1356.
- Anderson, J. L., & Bouma, J. (1973). "Relationships between hydraulic conductivity and morphometric data of an argillic horizon." *Soil Sci. Soc. Am. Proc.* 37, 408–413.
- Archer, N. A. L., Bonell, M., MacDonald, A. M., & Coles, N. (2014). "A constant head well permeameter formula comparison: its significance in the estimation of field-saturated hydraulic conductivity in heterogeneous shallow soils." *Hydrology Research*, 45(6), 788–805.
- Ashagrie, Y., Zech, W., Guggenberger, G., & Mamo, T. (2007). "Soil aggregation, and total and particulate organic matter following conversion of native forests to continuous cultivation in Ethiopia." *Soil and Tillage Research*, 94(1), 101–108.
- Atiquzzaman, M., & Kandasamy, J. (2016). "Prediction of hydrological time-series using extreme learning machine." *Journal of Hydroinformatics*, 18(2), 345–353.
- Bagarello, V. (1997). "Influence of well preparation on field-saturated hydraulic conductivity measured with the Guelph Permeameter." *Geoderma*, 80(1–2), 169–180.
- Bagarello, V., & Giordano, G. (1999). "Comparison of Procedures to estimate Steady Flow Rate in Field Measurement of Saturated Hydraulic Conductivity by the Guelph Permeameter Method." *Journal of Agricultural Engineering Research*, 74(1), 63–71.

- Bagarello, V., Iovino, M., & Lai, J. Bin. (2013). 'Field and Numerical Tests of the Two-Ponding Depth Procedure for Analysis of Single-Ring Pressure Infiltrometer Data." *Pedosphere*, 23(6), 779–789.
- Bagarello, V., Sferlazza, S., & Sgroi, A. (2009). "Comparing two methods of analysis of single-ring infiltrometer data for a sandy-loam soil." *Geoderma*, 149(3–4), 415–420.
- Bagarello, V., & Sgroi, A. (2004). "Using the single-ring infiltrometer method to detect temporal changes in surface soil field-saturated hydraulic conductivity." *Soil and Tillage Research*, 76(1), 13–24.
- Balland, V., Pollacco, J. A. P., & Arp, P. A. (2008). "Modeling soil hydraulic properties for a wide range of soil conditions." *Ecological Modelling*, 219(3–4), 300–316.
- Benson, C. H. (1995). "Hydraulic Conductivity of Thirteen Compacted Clays." *Clays and Clay Minerals*, 43(6), 669–681.
- Bezdek, J. C., Coray, C., Gunderson, R., & Watson, J. (1981). "Detection and Characterization of Cluster Substructure I. Linear Structure: Fuzzy c -Lines." *SIAM Journal on Applied Mathematics*, 40(2), 339–357.
- Bhattacharyya, R., Prakash, V., Kundu, S., & Gupta, H. S. (2006). "Effect of tillage and crop rotations on pore size distribution and soil hydraulic conductivity in sandy clay loam soil of the Indian Himalayas." *Soil and Tillage Research*, 86(2), 129–140.
- Bouma, J., Jongmans, A. G., Stein, A., & Peek, G. (1989). "Characterizing spatially variable hydraulic properties of a boulder clay deposit in the Netherlands." *Geoderma*, 45(1), 19–29.
- Bouteldja, F., Breul, P., & Boissier, D. (2011). "Experimental Validation of an Method for In Situ Estimation of Hydraulic Conductivity of Water Treatment Granular Materials." *Geotechnical and Geological Engineering*, 29(6), 1009–1021.
- Bouwer, H. (2010). "Measuring Horizontal and Vertical Hydraulic Conductivity of Soil With the Double-Tube Method1." *Soil Science Society of America Journal*, 28(1), 19.
- Bowles, J. E.(1992). "Engineering properties of soils and their measurement", *McGraw-Hill, New York*.

- Braud, I., Dantas, C., Vauclin, M., & Thony, L. (1995). "A simple soil-plant-atmosphere transfer model (SiSPAT) development and field verification." *Journal of Hydrology*, 169(4), 213–250.
- Campbell, G.S., and S. Shiozawa. (1992). "Prediction of hydraulic properties of soils using particle-size distribution and bulk density data". p. 317–328. *In M.Th . van Genuchten et al. (ed.) Indirect methods for estimating the hydraulic properties of unsaturated soils*. Univ. of California, Riverside.
- Campbell, C. M., & Fritton, D. D. (1994). "Factors Affecting Field-Saturated Hydraulic Conductivity Measured by the Borehole Permeameter Technique." *Soil Science Society of America Journal*, 58(5), 1354.
- Candemir, F., & Gülser, C. (2012). "Influencing Factors and Prediction of Hydraulic Conductivity in Fine-Textured Alkaline Soils." *Arid Land Research and Management*, 26(1), 15–31.
- C.C. Chang and C.J. Lin, (2002) "LIBSVM: a Library for Support Vector Machines" (Version 2.33), <http://www.csie.ntu.edu.tw/~cjlin/libsvm/>,
- Chen, H., Liu, J., Zhang, W., & Wang, K. (2011). "Soil hydraulic properties on the steep karst hillslopes in northwest Guangxi, China." *Environmental Earth Sciences*, 66(1), 371–379.
- Chen, X., Zhang, Z., Chen, X., & Shi, P. (2009). "The impact of land use and land cover changes on soil moisture and hydraulic conductivity along the karst hillslopes of southwest China." *Environmental Earth Sciences*, 59(4), 811–820.
- Chih-Wei Hsu, Chih-Chung Chang, and C.-J. L. (2004). "A Practical Guide to Support Vector Classification." *Middle East Journal of Anesthesiology*, 17(5), 819–832.
- Cosby, B. J., Hornberger, G. M., Clapp, R. B., & Ginn, T. R. (1984). "A Statistical Exploration of the Relationships of Soil Moisture Characteristics to the Physical Properties of Soils." *Water Resources Research*, 20(6), 682–690.
- C.-W. Hsu, C.-C. Chang, C.-J. Lin, (2003) "A Practical Guide to Support Vector Classification." *Tech. Rep., Taipei*,
- Das, B. M. (2002). "Soil Mechanics Laboratory Manual". Sixth Edition, *Oxford University Press*.
- Das, S. K., & Basudhar, P. K. (2007). "Prediction of hydraulic conductivity of clay liners using artificial neural network." *Lowland Technology International*.

International Association of Lowland Technology (IALT), 9(1), 50–58.

Das, S. K., Samui, P., & Sabat, A. K. (2012). "Prediction of Field Hydraulic Conductivity of Clay Liners Using an Artificial Neural Network and Support Vector Machine." *International Journal of Geomechanics*, 12(5), 606–611.

Deo, R. C., & Şahin, M. (2015). "Application of the extreme learning machine algorithm for the prediction of monthly Effective Drought Index in eastern Australia." *Atmospheric Research*, 153, 512–525.

Di Prima, S., Lassabatere, L., Bagarello, V., Iovino, M., & Angulo-Jaramillo, R. (2016). "Testing a new automated single ring infiltrometer for Beerkan infiltration experiments." *Geoderma*, 262, 20–34.

Dirksen C. (1999). "Soil physics measurement" *Yokendo, Tokyo*,

Dörner, J., Dec, D., Peng, X., & Horn, R. (2010). "Effect of land use change on the dynamic behaviour of structural properties of an Andisol in southern Chile under saturated and unsaturated hydraulic conditions." *Geoderma*, 159(1–2), 189–197.

Dunn, J. C. (1973). "A Fuzzy Relative of the ISODATA Process and Its Use in Detecting Compact Well-Separated Clusters." *Journal of Cybernetics*, 3(3), 32–57.

Edoga RN. (2010) "Comparison of saturated hydraulic conductivity measurement methods for Samaru-Nigeria Soils." *Lib Agric Res Center J Int.*;1(4):269-273

Elbisy, M. S. (2015). "Support Vector Machine and regression analysis to predict the field hydraulic conductivity of sandy soil." *KSCE Journal of Civil Engineering*, 19(7), 2307–2316.

Elrick, D.E., W.D. Reynolds, and K. A. T. (1989). "Hydraulic conductivity measurements in the unsaturated zone using improved well analyses." *Ground Water Monit.Rev.*, 9, 184–193.

Elrick, D. E., & Reynolds, W. D. (1992). "Methods for analyzing constant- head well permeameter data." *Soil Science Society of America Journal*, 56, 320–323.

Fernuik, N., & Haug, M. (1990). "Evaluation of In Situ Permeability Testing Methods." *Journal of Geotechnical Engineering*, 116(2), 297–311.

Fu, T., Chen, H., Zhang, W., Nie, Y., Gao, P., & Wang, K. (2015). "Spatial variability of surface soil saturated hydraulic conductivity in a small karst catchment of

- southwest China." *Environmental Earth Sciences*, 74(3), 2381–2391.
- Gallichand, J., Madramootoo, C. A., Emight, P., & Barrington, S. F. (1990). "An Evaluation of The Guelph Permeameter For Measuring Saturated Hydraulic Conductivity." *American Society of Agricultural Engineers*, 33(August), 1179–1184.
- Ghanbarian-Alavijeh, B., Liaghat, A., Huang, G.-H., & Van Genuchten, M. T. (2010). "Estimation of the van Genuchten Soil Water Retention Properties from Soil Textural Data." *Pedosphere*, 20(4), 456–465.
- Guang-Bin Huang, & Chee-Kheong Siew. (2004). "Extreme learning machine: RBF network case." *ICARCV 2004 8th Control, Automation, Robotics and Vision Conference, 2004.*, 2(Icarcv), 1029–1036.
- Gunn, S. R. (1998). "Support Vector Machines for Classification and Regression." In *Faculty of Engineering, Science and Mathematics School of Electronics and Computer Science. University of Southampton.*
- Han, G.-Z., Zhang, G.-L., Gong, Z.-T., & Wang, G.-F. (2012). "Pedotransfer Functions for Estimating Soil Bulk Density in China." *Soil Science*, 177(3), 158–164.
- Hausmann MR.(2012) "Engineering principles of ground modification." *McGraw-Hill Education (India) Private Limited; New Delhi:*
- Haynes, R. J., Swift, R. S., & Stephen, R. C. (1991). "Influence of mixed cropping rotations (pasture-arable) on organic matter content, water stable aggregation and clod porosity in a group of soils." *Soil and Tillage Research*, 19(1), 77–87.
- Hillel D (1980) "Fundamentals of soil physics." *Academic press, NewYork*
- Hu, R., Chen, Y.-F., Liu, H.-H., & Zhou, C.-B. (2013). "A water retention curve and unsaturated hydraulic conductivity model for deformable soils: consideration of the change in pore-size distribution." *Géotechnique*, 63(16), 1389–1405.
- Hu, W., Shao, M. A., Wang, Q. J., Fan, J., & Reichardt, K. (2008). "Spatial variability of soil hydraulic properties on a steep slope in the loess plateau of China." *Scientia Agricola*, 65(3), 268–276.
- Hu, W., Shao, M., Wang, Q., & She, D. (2013). "Effects of Measurement Method, Scale, and Landscape Features on Variability of Saturated Hydraulic Conductivity." *Journal of Hydrologic Engineering*, 18(4), 378–386.

- Huang, G.-B., Zhu, Q., & Siew, C. (2006). "Extreme learning machine: Theory and applications." *Neurocomputing*, 70(1–3), 489–501.
- Iovino, M., Castellini, M., Bagarello, V., & Giordano, G. (2016). "Using Static and Dynamic Indicators to Evaluate Soil Physical Quality in a Sicilian Area." *Land Degradation & Development*, 27(2), 200–210.
- IS: 2720 - Part 4, "Grain size analysis." BIS, 1975
- IS 2720 – Part 29, "Determination of dry density of soil, In – place by the core cutter method." BIS, 1975.
- IS 2720 – Part 3/sec.1, Determination of specific gravity – Fine grained soil, BIS 1980
- IS 2720 – Part 3/sec.2, Determination of specific gravity – Fine, medium and coarse grained soil, BIS 1981
- IS: 2720 Part17, Laboratory determination of Permeability, BIS 1986
- J.-P. Fuentes, & M. Flury. (2005). "HYDRAULIC CONDUCTIVITY OF A SILT LOAM SOIL AS AFFECTED BY SAMPLE LENGTH." *Transactions of the ASAE*, 48(1), 191–196.
- Jabro, J. D. (1992). "Estimation of saturated hydraulic conductivity of soils from particle-size distribution and bulk-density data." *Transactions of the Asae*, 35(2), 557–560.
- Jabro, J. D., & Evans, R. G. (2006). "Discrepancies Between Analytical Solutions Of Two Borehole Permeameters For Estimating Field-Saturated Hydraulic Conductivity." *Applied Engineering in Agriculture*, 22(4), 549–554.
- Jadczyzyn, J., & Niedźwiecki, J. (2005). "Relation of saturated hydraulic conductivity to soil losses." *Polish Journal of Environmental Studies*, 14(4), 431–435.
- Jana, R. B., Mohanty, B. P., & Springer, E. P. (2007). "Multiscale Pedotransfer Functions for Soil Water Retention." *Vadose Zone Journal*, 6(4), 868.
- Jang, J.-S. R. (1993). "ANFIS: adaptive-network-based fuzzy inference system." *IEEE Transactions on Systems, Man, and Cybernetics*, 23(3), 665–685.
- Jarvis, N., Koestel, J., Messing, I., Moeys, J., & Lindahl, A. (2013). "Influence of soil, land use and climatic factors on the hydraulic conductivity of soil." *Hydrology and Earth System Sciences*, 17(12), 5185–5195.

- Jauhiainen, M. (2004). "Relationships of particle size distribution curve, soil water retention curve and unsaturated hydraulic conductivity and their implications on water balance of forested and agricultural hillslopes." Dissertation, Helsinki University of Technology, Finland
- Jiang, Y., & Shao, M. (2014)." Effects of soil structural properties on saturated hydraulic conductivity under different land-use types." *Soil Research*, 52(4), 340.
- Jirků, V., Kodešová, R., Nikodem, A., Mühlhanselová, M., & Žigová, A. (2013). "Temporal variability of structure and hydraulic properties of topsoil of three soil types." *Geoderma*, 204–205, 43–58.
- J.Kacprzyk and W. Pedrycz (2015). "Springer Handbook of Computational Intelligence". Berlin- Heidelberg: Springer-Verlag,.
- John, B., Yamashita, T., Ludwig, B., & Flessa, H. (2005). "Storage of organic carbon in aggregate and density fractions of silty soils under different types of land use." *Geoderma*, 128(1–2), 63–79.
- Kargas, G., & Londra, P. A. (2015)." Effect of tillage practices on the hydraulic properties of a loamy soil." *Desalination and Water Treatment*, 54(8), 2138–2146.
- Khaledian, Y., Kiani, F., Weindorf, D. C., & Ebrahimi, S. (2013)." Relationship of Potentially Labile Soil Organic Carbon with Soil Quality Indicators in Deforested Areas of Iran." *Soil Horizons*, 54(4), 0.
- Khodaverdiloo, H., Homae, M., van Genuchten, M. T., & Dashtaki, S. G. (2011). "Deriving and validating pedotransfer functions for some calcareous soils." *Journal of Hydrology*, 399(1–2), 93–99.
- Khodaverdiloo, H., Khani Cheraghabdal, H., Bagarello, V., Iovino, M., Asgarzadeh, H., & Ghorbani Dashtaki, S. (2017)." Ring diameter effects on determination of field-saturated hydraulic conductivity of different loam soils." *Geoderma*, 303(January), 60–69.
- Klir, G.J., Yuan, B., (1995). "Fuzzy Sets and Fuzzy Logic: Theory and Applications." Prentice-Hall Inc., USA.
- Klute, A. & Dirksen, C. (1986). "Hydraulic conductivity of saturated soils." In: Methods of Soil Analysis (ed. A. Klute), pp. 694–700. ASA and SSSA, Madison, WI.
- Köhne, J. M., Alves Júnior, J., Köhne, S., Tiemeyer, B., Lennartz, B., & Kruse, J.

- (2011)." Double-Ring And Tension Infiltrometer Measurements Of Hydraulic Conductivity And Mobile Soil Regions." *Pesquisa Agropecuária Tropical*, 41(3), 336–347.
- Lai, J., & Ren, L. (2007). "Assessing the Size Dependency of Measured Hydraulic Conductivity Using Double-Ring Infiltrometers and Numerical Simulation." *Soil Science Society of America Journal*, 71(6), 1667.
- Lamorski, K., Pachepsky, Y., Sławiński, C., & Walczak, R. T. (2008). "Using Support Vector Machines to Develop Pedotransfer Functions for Water Retention of Soils in Poland." *Soil Science Society of America Journal*, 72(5), 1243.
- Lee, D. M., Elrick, D. E., Reynolds, W. D., & Clothier, B. E. (1985). "A Comparison Of Three Field Methods For Measuring Saturated Hydraulic Conductivity." *Canadian Journal of Soil Science*, 65(3), 563–573.
- Lee, D. M., Reynolds, W. D., Elrick, D. E., & Clothier, B. E. (1985). "A Comparison Of Three Field Methods For Measuring Saturated Hydraulic Conductivity." *Can. J. Soil Sci.*, 65, 563–573.
- Lee, J., Shackelford, C. D., Benson, C. H., Jo, H., & Edil, T. B. (2006). "Correlating Index Properties and Hydraulic Conductivity of GCLs.pdf." *Journal of Geotechnical and Geoenvironmental Engineering*, 131(11), 1319–1329.
- Lehrsch, G. A., Sojka, R. E., & Koehn, A. C. (2012). "Surfactant effects on soil aggregate tensile strength." *Geoderma*, 189–190, 199–206.
- Li, Y., Wallach, R., & Cohen, Y. (2002). "The role of soil hydraulic conductivity on the spatial and temporal variation of root water uptake in drip-irrigated corn." *Plant and Soil*, 243(2), 131–142.
- Li Zhang, Yuan Li, & Nevatia, R. (2008). "Global data association for multi-object tracking using network flows." *2008 IEEE Conference on Computer Vision and Pattern Recognition*, 1–8.
- Lilly, A. (1994). "The determination of field-saturated hydraulic conductivity in some Scottish soils using the Guelph permeameter." *Soil Use and Management*, 10, 72–78.
- Luk, S.H., Cai, Q.G. and Wang, G.P., (1993). "Effects of surface cresting and slope gradient on soil and water losses in the hilly loess region, North China." *Catena Suppl.*, 24: 29--45.

- Mahler, R.L., D.F. Bezdicek, and R.E. Witters. (1979). "Influence of slope position on nitrogen fixation and yield of dry peas." *Agron. J.* 71:348–354
- Malaya, C., & Sreedeeep, S. (2013). "A study on unsaturated hydraulic conductivity of hill soil of north-east India." *ISH Journal of Hydraulic Engineering*, 19(3), 276–281.
- Mallants, D., Mohanty, B. P., Vervoort, A., & Feyen, J. (1997). "Spatial analysis of saturated hydraulic conductivity in a soil with macropores." *Soil Technology*, 10(2), 115–131.
- Mamdani, E. H. (1974)." Application of fuzzy algorithms for control of simple dynamic plant." *Proceedings of the Institution of Electrical Engineers*, 121(12), 1585.
- Mapa, R. B., Green, R. E., & Santo, L. (1986). "Temporal Variability of Soil Hydraulic Properties with Wetting and Drying Subsequent to Tillage1." *Soil Science Society of America Journal*, 50(5), 1133–1138.
- Mbonimpa, M., Aubertin, M., Chapuis, R. P., & Bussi re, B. (2002). "Practical pedotransfer functions for estimating the saturated hydraulic conductivity." *Geotechnical and Geological Engineering*, 20(3), 235–259.
- Merdun, H. (2010)." Alternative methods in the development of pedotransfer functions for soil hydraulic characteristics." *Eurasian Soil Science*, 43(1), 62–71.
- Merdun, H.,  ınar,  ., Meral, R., & Apan, M. (2006). "Comparison of artificial neural network and regression pedotransfer functions for prediction of soil water retention and saturated hydraulic conductivity." *Soil and Tillage Research*, 90(1–2), 108–116.
- Minasny, B., McBratney, A. B., & Bristow, K. L. (1999). " Comparison of different approaches to the development of pedotransfer functions for water-retention curves." *Geoderma*, 93(3–4), 225–253.
- M. Mukaidono, (2001) "Fuzzy Logic for Beginners", *World Scientific*,
- Mohanty, B. P., Kanwar, R. S., & Everts, C. J. (1994)." Comparison of Saturated Hydraulic Conductivity Measurement Methods for a Glacial-Till Soil." *Soil Science Society of America Journal*, 58(3), 672–677.
- Mohanty, B. P., & Mousli, Z. (2000)." Saturated hydraulic conductivity and soil water retention properties across a soil-slope transition." *Water Resources Research*, 36(11), 3311–3324.

- Mukerji, A., Chatterjee, C., & Raghuvanshi, N. S. (2009). "Flood Forecasting Using ANN, Neuro-Fuzzy, and Neuro-GA Models." *Journal of Hydrologic Engineering*, 14(June), 647–652.
- Nemes, A., Schaap, M. G., & Wösten, J. H. M. (2003). "Functional Evaluation of Pedotransfer Functions Derived from Different Scales of Data Collection." *Soil Science Society of America Journal*, 67(4), 1093.
- O’Callaghan, J.O., (1996). “Land use: the interaction of economics, ecology and hydrology.” *London*.
- Öztekin, T., & Erşahin, S. (2006). "Saturated hydraulic conductivity variation in cultivated and virgin soils." *Turkish Journal of Agriculture and Forestry*, 30(1), 1–10.
- Parasuraman, K., Elshorbagy, A., & Si, B. C. (2006)." Estimating Saturated Hydraulic Conductivity In Spatially Variable Fields Using Neural Network Ensembles." *Soil Science Society of America Journal*, 70(6), 1851.
- Parasuraman, K., Elshorbagy, A., & Si, B. C. (2007)." Estimating Saturated Hydraulic Conductivity Using Genetic Programming." *Soil Science Society of America Journal*, 71(6), 1676.
- Patil, A. P., & Deka, P. C. (2016)." An extreme learning machine approach for modeling evapotranspiration using extrinsic inputs." *Computers and Electronics in Agriculture*, 121, 385–392.
- Punmia B.C. et al. (2005) “Soil Mechanics and Foundations.” *Laxmi Publications (P) Limited New Delhi*:
- Quinton, W. L., Hayashi, M., & Carey, S. K. (2008). "Peat hydraulic conductivity in cold regions and its relation to pore size and geometry." *Hydrological Processes*, 22(15), 2829–2837.
- Raj P. Purushothama (2001) “Soil Mechanics and Foundation Engineering.” *Pearson Education. New Delhi*
- Raouf, M., Nazemi, A.M., Sadraddini, A.A., and Marofi, S. (2011). “Measuring and estimating saturated and unsaturated hydraulic conductivity in steady and transient states on sloping lands.” *World Applied Sciences Journal*, 13(4): 747 – 755.

- Rawls, W.J. and Brakensick, D.L., (1985) "Prediction of soil water properties for hydrologic modeling". *Proceedings of Symposium on Watershed Management*, American Society of Civil Engineers, New York, p. 293–299.
- Rawls, W. J., Brakensiek, D. L., & Logsdon, S. D. (1993)." Predicting Saturated Hydraulic Conductivity Utilizing Fractal Principles." *Soil Science Society of America Journal*, 57(5), 1193.
- Regalado, C. M., & Muñoz-Carpena, R. (2004). "Estimating the saturated hydraulic conductivity in a spatially variable soil with different permeameters: a stochastic Kozeny–Carman relation." *Soil and Tillage Research*, 77(2), 189–202.
- Reynolds, W.D., Elrick, D.E., Topp, G.C., (1983). "A re-examination of the constant head well permeameter method for measuring saturated hydraulic conductivity above the water." *Soil Science* 136, 250–268.
- Reynolds, W. D. and D. E. Elrick. (1985). "In-situ measurement of field-saturated hydraulic conductivity, sorptivity and a parameter using the Guelph Permeameter." *Soil Science* 140(4):292-302.
- Reynolds W.D., Elrick D.E., and Clothier, B.E. (1985). "The constant head well permeameter: effect of unsaturated flow." *Soil Sci.* 139: 172 – 180
- Reynolds, W. D., Bowman, B. T., Brunke, R. R., Drury, C. F., & Tan, C. S. (2000)." Comparison of Tension Infiltrometer, Pressure Infiltrometer, and Soil Core Estimates of Saturated Hydraulic Conductivity." *Soil Science Society of America Journal*, 64(2), 478.
- Reynolds, W. D., Vieira, S. R., & Topp, G. C. (1992). "An assessment of the single-head analysis for the constant head well permeameter." *Can. J. Soil Sci.*, 72, 489–501.
- Riebsame, W. E., Meyer, W. B., & Turner, B. L. (1994)." Modeling land use and cover as part of global environmental change." *Climatic Change*, 28(1–2), 45–64.
- Rong Chang, B. (2006)." Applying nonlinear generalized autoregressive conditional heteroscedasticity to compensate ANFIS outputs tuned by adaptive support vector regression." *Fuzzy Sets and Systems*, 157(13), 1832–1850.
- R.R. Yager, L.A. Zadeh (Eds.), (1992) "An Introduction to Fuzzy Logic Applications in Intelligent Systems." *Kluwer Academic Publishers*,
- S, Hamedi. (2015). "Estimating Saturated Hydraulic Conductivity Using Fuzzy Set

- Theory." *Indian Journal of Fundamental and Applied Life Sciences*, 5, 2850–2860.
- Salchow, E., Lal, R., Fausey, N. R., & Ward, A. (1996). "Pedotransfer functions for variable alluvial soils in southern Ohio." *Geoderma*, 73(3–4), 165–181.
- Salverda, A. P., & Dane, J. H. (1993). "An examination of the Guelph permeameter for measuring the soil 's hydraulic properties." *Geoderma*, 57(3), 405–421.
- Sanjit K. Deb and Manoj K. Shukla. (2012). "Variability Of Hydraulic Conductivity Due To Multiple Factors." *American Journal of Environmental Sciences*, 8(5), 489–502. <https://doi.org/10.3844/ajessp.2012.489.502>
- Sarmadian, F., & Taghizadeh-Mehrjardi, R. (2010). "Development of Pedotransfer Functions to Predict Soil Hydraulic Properties in Golestan Province, Iran." *19th World Congress of Soil Science, Soil Solutions for a Changing World*, (August), 2008–2011.
- Sayed, T., & Razavi, A. (2000). "Comparison of Neural and Conventional Approaches to Mode Choice Analysis." *Journal of Computing in Civil Engineering*, 14(1), 23–30.
- Saxton, K.E., W.J. Rawls, J.S. Romberger, and R.I. Papendick. (1986). "Estimating generalized soil water characteristics from texture." *Trans. ASAE* 50:1031–1035.
- Schaap, M. G., Leij, F. J., & van Genuchten, M. T. (2001). "ROSETTA : A computer program for estimating soil hydraulic parameters with hierarchical pedotransfer functions." *Journal of Hydrology*, 251(3–4), 163–176.
- Schulze-Makuch, D., Carlson, D. A., Cherkauer, D. S., & Malik, P. (1999). "Scale Dependency of Hydraulic Conductivity in Heterogeneous Media." *Ground Water*, 37(6), 904–919.
- Sepaskhah, A. R., & Karizi, A. (2011). "Effects of alternate use of wastewater and fresh water on soil saturated hydraulic conductivity." *Archives of Agronomy and Soil Science*, 57(2), 149–158.
- Seyfried, M. S. and Wilcox B. P. (1995). "Scale and the Nature of Spatial Variability." *Water Resource Research*, 31(1), 173–184.
- Shiri, J., & Kişi, Ö. (2011). "Comparison of genetic programming with neuro-fuzzy systems for predicting short-term water table depth fluctuations." *Computers & Geosciences*, 37(10), 1692–1701.

- Shukla, M.K., (2013) "Soil Physics an Introduction." *CRC Press Boca Raton, FL, USA*, pp.478.
- Soilmoisture Equipment Corporation (2010). "Operating instructions – Guelph Peremeameter". *Soilmoisture Equipment Corp., Santa Barbara, CA*
- Stephens, D. B., & Heermann, S. (1988). "Dependence of Anisotropy on Saturation in a Stratified Sand." *Water Resources Research*, 24(5), 770–778.
- Stumpp, C., Engelhardt, S., Hofmann, M., & Huwe, B. (2009)." Evaluation of pedotransfer functions for estimating soil hydraulic properties of prevalent soils in a catchment of the Bavarian Alps." *European Journal of Forest Research*, 128(6), 609–620.
- Sugeno, M. (1985)." An Introductory Survey of Fuzzy Control." *INFORMATION SCIENCES*, 36, 59–83.
- Suriya, S., & Mudgal, B. V. (2012)." Impact of urbanization on flooding: The Thirusoolam sub watershed – A case study." *Journal of Hydrology*, 412–413, 210–219.
- Talsma, T. (1987). "Re-evaluation of the Well Permeameter as a Field Method for Measuring Hydraulic Conductivity." *Aust.J.Soil Res.*, 25, 361–368.
- Tamura, S., & Tateishi, M. (1997)." Capabilities of a four-layered feedforward neural network: four layers versus three." *IEEE Transactions on Neural Networks*, 8(2), 251–255.
- Terzi, Ö., Erol Keskin, M., & Dilek Taylan, E. (2006)." Estimating Evaporation Using ANFIS." *Journal of Irrigation and Drainage Engineering*, 132(5), 503–507.
- Tian, Y., Ma, J., Lu, C., & Wang, Z. (2015). "Rolling bearing fault diagnosis under variable conditions using LMD-SVD and extreme learning machine." *Mechanism and Machine Theory*, 90, 175–186.
- Trillas, E., Eciolaza, L. (2015), "Fuzzy Logic: An Introductory Course for Engineering Students." *Springer*.
- Twarakavi, N. K. C., Šimůnek, J., & Schaap, M. G. (2009). "Development of Pedotransfer Functions for Estimation of Soil Hydraulic Parameters using Support Vector Machines." *Soil Science Society of America Journal*, 73(5), 1443.

- Vereecken H, Maes J, Feyen J.(1990) “*Estimating unsaturated hydraulic conductivity from easily measured soil properties.*” *Soil Science*. 149:1-12.
- V. Vapnik, (1993) “The Nature of Statistical Learning Theory,” *Springer-Verlag, New York*,
- Vapnik, V. N. (1996). “The nature of statistical learning theory.” *New York: Wiley*.
- Vapnik, V. (1998). “Statistical learning theory.” *New York: Wiley*
- Wang, T., Zlotnik, V. A., Wedin, D., & Wally, K. D. (2008)." Spatial trends in saturated hydraulic conductivity of vegetated dunes in the Nebraska Sand Hills: Effects of depth and topography." *Journal of Hydrology*, 349(1–2), 88–97.
- Wang, W.-C., Chau, K.-W., Cheng, C.-T., & Qiu, L. (2009). "A comparison of performance of several artificial intelligence methods for forecasting monthly discharge time series." *Journal of Hydrology*, 374(3–4), 294–306.
- Wang, Y., Shao, M., Liu, Z., & Horton, R. (2013). "Regional-scale variation and distribution patterns of soil saturated hydraulic conductivities in surface and subsurface layers in the loessial soils of China." *Journal of Hydrology*, 487, 13–23.
- Wösten, J. H. ., Lilly, A., Nemes, A., & Le Bas, C. (1999). "Development and use of a database of hydraulic properties of European soils." *Geoderma*, 90(3–4), 169–185.
- Wu, L., Pan, L., Mitchell, J., & Sanden, B. (1999). "Measuring Saturated Hydraulic Conductivity using a Generalized Solution for Single-Ring Infiltrimeters." *Soil Science Society of America Journal*, 63(4), 788.
- Yao, S., Zhang, T., Zhao, C., & Liu, X. (2013)." Saturated hydraulic conductivity of soils in the Horqin Sand Land of Inner Mongolia, northern China." *Environmental Monitoring and Assessment*, 185(7), 6013–6021.
- Yaseen, Z. M., Jaafar, O., Deo, R. C., Kisi, O., Adamowski, J., Quilty, J., & El-Shafie, A. (2016)." Stream-flow forecasting using extreme learning machines: A case study in a semi-arid region in Iraq." *Journal of Hydrology*, 542, 603–614.
- Yusef Kianpoor Kalkhajeh , Ruhollah Rezaie Arshad, Hadi Amerikhah, M. S. (2012). "Multiple Linear Rgression, Artificial Neural Network (Mlp, Rbf) Models For Modeling The Saturated Hydraulic Conductivity (A Case Study :Khuzestan Province, Southwest Iran)." *International Journal of Agriculture: Research and Review*, 2(3), 255–265.

- Zacharias, S., & Wessolek, G. (2007). "Excluding Organic Matter Content from Pedotransfer Predictors of Soil Water Retention." *Soil Science Society of America Journal*, 71(1), 43.
- Zelege, T. B., & Si, B. C. (2005). "Parameter estimation using the falling head infiltration model: Simulation and field experiment." *Water Resources Research*, 41(2), 1–7.
- Zhang, R. (1997). "Determination of Soil Sorptivity and Hydraulic Conductivity from the Disk Infiltrometer." *Soil Science Society of America Journal*, 61, 1024–1030.
- Zhao, C., Shao, M., Jia, X., Nasir, M., & Zhang, C. (2016). "Using pedotransfer functions to estimate soil hydraulic conductivity in the Loess Plateau of China." *CATENA*, 143, 1–6.
- Zimmermann, B., Elsenbeer, H., & De Moraes, J. M. (2006). "The influence of land-use changes on soil hydraulic properties: Implications for runoff generation." *Forest Ecology and Management*, 222(1–3), 29–38.

LIST OF PUBLICATIONS

Journals

- Satish Bhaurao More and Paresh Chandra Deka. “Estimation Of Saturated Hydraulic Conductivity Using Fuzzy Neural Network In A Semi-Arid Basin Scale For Murum Soils Of India.” ISH journal of Hydraulic Engineering (online) DOI - 10.1080/09715010.2017.1400408.

Conferences

- Satish Bhaurao More and Paresh Chandra Deka. “Field Scale Variability of Saturated Hydraulic Conductivity On Sloping Ground.” Hydro 2017 Ahmedabad
- Satish Bhaurao More and Paresh Chandra Deka. “Spatial Variability Of Saturated Hydraulic Conductivity Of Soil Up To Root Zone In Solapur.” National Symposium (west zone) Plant health management for sustainable agriculture, Udgir 2016
- Satish Bhaurao More and Paresh Chandra Deka. “Determination of Saturated hydraulic conductivity of soil – Review” National Symposium (west zone) Plant health management for sustainable agriculture, Udgir 2016.

BIO-DATA

Name: Mr. Satish Bhaurao More

D.O.B: 02 – 02 – 1967

Address: Bhaurao Jawalgekar
Teen Dukan Galli, Bhalki
At post Bhalki, Dist Bidar
Karnataka, Pin: 585328

Email: moresb23@gmail.com

Qualification: M. E. (Geotechnical)

Area of Specialization: Soil hydraulic properties